

FUNCTIONAL IDENTIFICATION OF REGULATORY ELEMENTS IN THE HUMAN GENOME

Li Li

李礼



Functional identification of regulatory elements in the human genome

Li Li

The research described in this thesis was supported by the grants from China Scholarship Council (CSC); ERC-AdG enhReg; ERC-ITN RNA TRAIN; The Dutch Organization for Research NWO-TOP

Layout and Print by Proefschriftmaken.nl, with financial support from the Netherlands Cancer Institute, Amsterdam, The Netherlands

Cover design: Zeng Ji Ling, Wu Hong, Li Li

Copyright © 2018 by Li Li. All rights reserved.

Functional identification of regulatory elements in the human genome

Functionele identificatie van regulerende elementen in het menselijk genoom

Thesis

to obtain the degree of Doctor from the
Erasmus University Rotterdam
by command of the
rector magnificus

Prof.dr. R.C.M.E. Engels

and in accordance with the decision of the Doctorate Board.
The public defence shall be held on

09-01-2019 at 11:30

by

Li Li

born in Hunan, China, 9th of February, 1988

Doctoral Committee

Promotor: Prof.dr. R. Agami

Other members: Prof.dr. E. Van Rooij
Prof.dr.ir. G. Jenster
Prof.dr. W. Zwart

Table of contents

Chapter 1	Introduction	7
Chapter 2	LncRNA-OIS1 regulates DPP4 activation to modulate senescence induced by RAS <i>Nucleic Acids Res.</i> 2018	27
Chapter 3	Functional CRISPR screen identifies AP1-associated enhancer regulating FOXF1 to modulate oncogene-induced senescence <i>Genome Biology.</i> 2018	69
Chapter 4	A functional genetic screen identifies TRAM2 as a key target of YAP-mediated proliferation and oncogenesis <i>Manuscript in preparation.</i> 2018	101
Chapter 5	Discussion	121
Addendum	English summary	130
	Nederlandse samenvatting	132
	Portfolio	134
	Curriculum vitae	135
	Publication list	136
	Acknowledgement	137



Chapter I

Introduction



The scope of the thesis

An adult human body is made up of different types of cells that exert a variety of functions but share nearly identical genomic DNA. What gives the different cells their morphologies, phenotypes, behaviours and functions? It is gene expression that determines the cell “fate”. Consequently, gene expression is an extremely important biological “business” in the cells that requires precise regulation. Indeed, the human genome is tightly and orderly packed, with genetic information in a genome held within genes. However, protein-coding genes only account for less than 2% of the human genome, so that more than 98% of regions are non-coding. Are these non-coding regions just garbage or very important? To answer this question, we need to explore the “dark matters” in our genome to better understand the functions of the non-coding regions.

The key to understand gene regulation is comprehensive identification of the regulatory elements in the non-coding regions which determine where and when the protein-coding genes are switched on and off in the life cycle of cells. It is worth noting that over half of the human disease-associated genetic variants reside in non-coding regions. Adequate understanding of the “language of gene regulation” is particularly relevant to understand human diseases, especially cancer.

The focus of this thesis is on the senescence (oncogene-induced senescence)-associated regulatory elements in non-coding regions. Senescence serves as a suppressive barrier to tumorigenesis. A full understanding of the gene regulation in the process of cellular senescence will empower us to know more about tumorigenesis.

In summary, the general goal of my research is to understand how the functional regulatory elements control gene expression.

Cancer

Cancer is a complex collection of distinct genetic diseases with a common characteristic of uncontrolled cell proliferation. In general, cancer cells can be distinguished from normal cells through six essential alterations, also called the hallmarks of cancer (1):

- (1) Cancer cells must self-sustain proliferative signalling to support their growth.
- (2) Cancer cells are insensitive to anti-growth signals.
- (3) Cancer cells develop resistance mechanisms to apoptosis, a form of intrinsic cell death.
- (4) Cancer cells acquire unlimited proliferation potential.
- (5) Cancer cells can attract new blood vessels, by a process called angiogenesis, to gain the extra oxygen and nutrients they need.

- (6) Lastly, cancer cells may obtain the ability to invade adjacent tissues, escaping from the mass of the primary tumours and travel to distant locations where they colonise foreign locations in the body.

Cancer cells achieve the above-mentioned phenotypes partly by modifying and re-activating some cellular programmes that control cell proliferation, migration, apoptosis and differentiation. Mostly, these phenotypic traits can be explained by genetic alterations, such as gain-of-function mutations, overexpression or amplification of some key oncogenes as well as loss-of-function mutations, silencing or deletions of some key tumour suppressor genes (2).

Senescence: a mechanism to suppress tumorigenesis

Senescence

Cellular senescence is a state of irreversible growth arrest which can be induced by different stimuli, including telomere shortening, DNA damage, oxidative stress and oncogenic stress (Figure 1) (3). Cellular senescence was initially discovered by Hayflick in 1965 as the limited lifespan of primary human fibroblasts in culture (4). This was defined as replicative stress-induced senescence caused by telomere shortening (5, 6). When telomeres lose protective structures and reach a critical minimal length, the DNA damage response and cell cycle arrest will be triggered. It is possible to artificially reconstitute telomerase activity by ectopic expression of telomerase reverse transcriptase (hTERT) in normal human cells. This leads to the elongation of telomeres, therefore extends the replicative lifespan allowing cellular immortalisation (6, 7). The activation of a telomere maintenance mechanism (TMM) is essential for cellular immortalisation, the hallmark of human cancers. Interestingly, many tumours possess activating mutations in the hTERT promoter that result in higher telomerase activity (8, 9). Alternatively, some tumours elongate their telomeres by a DNA recombination mechanism known as ALT (an alternative lengthening of telomeres)(10), thereby maintaining their telomeres at the length necessary for sustained proliferation.

Oncogene-induced senescence

Another form of cellular senescence caused by excessive mitogenic signalling was discovered in 1997 by Serrano and colleagues (11). They found that transduction of the oncogenic HRAS^{V12} gene into human embryonal fibroblasts resulted in an irreversible cell cycle arrest. This kind of proliferative arrest phenotypically resembled the replicative senescence, therefore was termed “premature senescence” or oncogene-induced senescence (OIS). Subsequently, it was found that hyper-expression of RAS in mammary epithelial cells can also activate tumour suppression pathways, triggering irreversible growth arrest (12). OIS can also be induced by other oncogene activation,

such as AKT (13), BRAF (14) and E2F1 (15). Importantly, inactivation of some tumour suppressor genes, such as PTEN and NF1, can induce senescence (16, 17). Initially, DNA damage response and OIS were thought to be different cellular stress responses, but more recent investigations suggested that OIS was caused by the accumulation of DNA damage. One model showed that the oncogene-driven accumulation of reactive oxygen species (ROS) can induce DNA damage resulting in cell cycle arrest (18), while another model proposed that excessive DNA replication caused by oncogene activation can trigger DNA replication stress, leading to activation of the DNA damage response (DDR), ultimately resulting in senescence (19, 20). In line with this, OIS was reported to play a crucial role in protecting normal tissues from tumorigenesis (16, 21, 22).

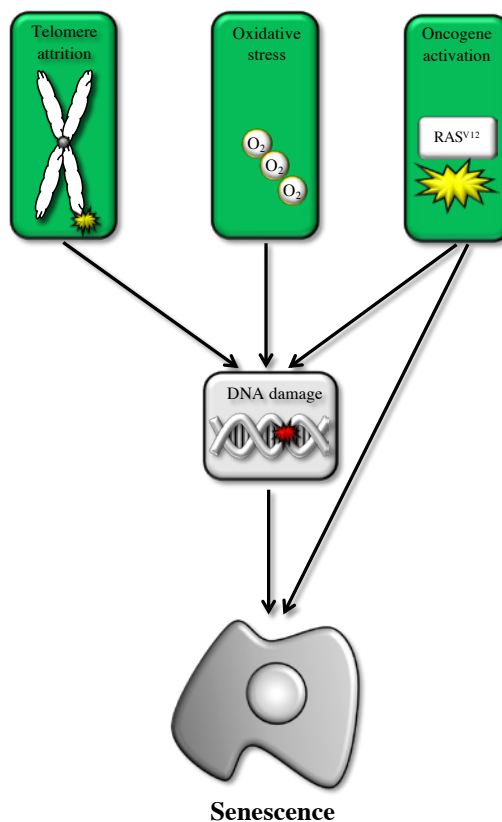
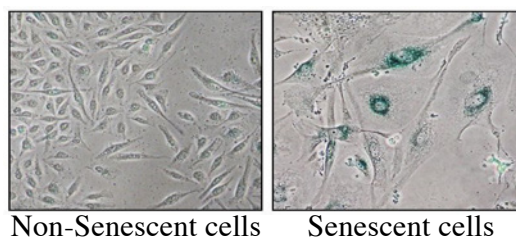


Figure I. Senescence can be induced by different stimuli

Senescence markers

In light of the importance of senescence, identifying senescent cells *in vivo* can have important diagnostic and therapeutic potential. However, the molecular pathways involved in triggering and/or maintaining the senescent phenotype are still not fully

characterised. Consequently, the identification of senescence markers is vital. Indeed, increasing numbers of potential markers for senescence identification have been reported in recent years (Figure 2). The first and the most important marker of senescence is the typically flat and enlarged morphology of the senescent cells. Secondly, the detection of senescence-associated β -galactosidase (SA- β -Gal) activity is the most widely utilised assay for senescence (23). The β -Gal activity is derived from the increased lysosomal content of senescent cells, which enables the detection of lysosomal β -galactosidase both in vitro and in vivo (24). Thirdly, genomic DNA is highly packed and well-organised with the combination of histone proteins in chromatin, which serves as another level for gene regulation. Chromatin-density can be visualised by DAPI staining. Heterochromatin is a tightly packed form of chromatin which encompasses transcriptionally inactive regions in the genome, whereas euchromatin is a lightly packed form of chromatin with active transcription. Active and inactive chromatin regions are usually marked by different and specific histone modifications. It has been reported that heterochromatin is critical in different nuclear functions including nuclear organisation, chromosome segregation and gene silencing (25, 26). The DNA foci of senescent cells do not contain active transcription sites but, in contrast, have the heterochromatin features known as senescence-associated heterochromatic foci (SAHF) (27). SAHFs constitute the typically morphological nuclear feature of senescent cells widely exploited to identify senescence. Fourth, the senescent cells do not proliferate, exhibiting expression of genes related to repressed cell cycle. There are two main signalling pathways involved in the initiation and establishment of senescence, RB (retinoblastoma)-p16^{INK4a} and p53-p21. High levels of p16^{INK4a} and p21 expression can be detected in senescent cells (28–30), and it is well established that these two pathways have a central role in tumour suppression.



- Large flattened morphology
 - Senescence-associated β -galactosidase activity (SA- β -Gal)
 - Senescence-associated heterochromatic foci (SAHF)
 - senescence-associated secretory phenotype (SASP): IL6, IL8
 - Irreversible proliferation arrest, changes in gene expression
- cell cycle gene ↓ p16^{INK4a} or p21 ↑

Figure 2. Features of senescent cells

Importantly, mutations in these two pathways are frequently found in tumours (31–33). Fifth, senescent cells secrete cytokines, such as IL6 and IL8, which reinforce the senescence (34). In fact, none of the above-mentioned markers solely represent senescence, so it is good practice to use a combination of different markers to identify senescent cells.

Gene regulatory elements

Genetic alterations of the human genome, such as mutations, deletions, and amplifications are the main causes of diseases. Interestingly, the human genome consists of only around 2% of protein-coding genes, with the majority of our genome (98%) being non-coding, which was previously considered as “junk DNA”. However, the so-called non-coding junk regions contain functional elements, such as microRNAs, long-non-coding RNAs (lncRNA), promoters, enhancers, insulators, silencer, and chromatin structure moieties.

The human body is made up of numerous cell types having a wide variety of specialised roles with the nearly identical genome. In its essence, this diversity of functions can be explained by regulating the transcriptional output of different genes in specific cell types, conditions, and developmental stages through numerous regulatory elements. Obviously, gene expression is a crucial biological process that requires precise and careful regulation. Uncovering the interplay between gene coding regions and regulatory regions is therefore essential to understand the mechanisms governing gene regulation in health and disease (35). Interestingly, it seems that mutations in functional regulatory regions are one of the major causes of gene expression deregulation in diseases. However, we have a very incomplete understanding of how many regulatory elements exist in the human genome and what their functions are in gene regulation. Therefore, it is very important, though quite challenging, to identify and functionally characterise regulatory elements in the human genome.

Identification of regulatory elements

The first step in understanding the biological function of regulatory elements is their identification. The development of high-throughput DNA sequencing methods enabled the identification of gene regulatory elements on a genome-wide scale. Some of the most popular techniques for this purpose include (A) DNase sequencing (DNase-seq) and the assay for transposase-accessible chromatin using sequencing (ATAC-seq), (B) chromosome conformation capture assays, and (C) chromatin immunoprecipitation followed by sequencing (ChIP-seq) (Figure 3).

The DNase-seq(36) and ATAC-seq(37) allow us to identify the regulatory elements by taking advantage of open and accessible nucleosome regions. Unfortunately, they cannot determine the functional roles of the identified elements.

The DNase-seq (36) and ATAC-seq (37) allow the identification of regulatory elements by taking advantage of open and accessible nucleosome regions. Unfortunately, they cannot determine the functional roles of the identified elements.

ChIP-seq can detect the specific regulatory elements depending on the antibody (against transcription factors (TFs), cofactors, or histone markers) used. ChIP-seq was commonly used to detect specific TF binding regions through the genome. Usually, TF binding regions are promoters or enhancers. For histone markers, three methyl groups on the lysine in position 4 of histone H3 (H3K4me3) are used as a marker to detect active promoters (38), whereas a single methyl group on the lysine in position 4 of histone H3 (H3K4me1) is a marker for enhancers (39). An acetyl group on the lysine in position 27 of histone H3 (H3K27ac) is another marker used to detect active enhancers (40, 41). More histone marks such as trimethylation of histone H3 on lysine 27 (H3K27me3) and di- or trimethylation of histone H3 on lysine 9 (H3K9me2/3) are commonly utilised to identify silenced regions(42).

Chromatin conformation capture assays identify the interactions between genomic loci, such as promoter-enhancer interactions, by fixing the interactions followed by ligation and sequencing or PCR. The advantage of this technique is that it detects not only the regulatory elements but also can identify target genes.

A large research consortia used the methodologies detailed above to explore the functions of the non-coding genome, leading to increased annotation of the regulatory genome landscape. For example, the Encyclopedia of DNA Elements (ENCODE) project (43, 44) identified and mapped histone modification marks, TF binding sites, DNase I hypersensitive sites, chromosome interaction maps, DNA methylation patterns, and the binding sites of RNA-binding proteins. The Functional Annotation of Mammalian Genome (FANTOM) project has mapped the TFs, sets of transcripts, enhancers, and promoters in several major primary mammalian cells by using the cap analysis of gene expression (CAGE) (45, 46). The Epigenome Roadmap project has mapped histone modifications, DNA methylation, small RNA transcripts and chromatin accessibility in stem cells (47, 48). All these projects provided a comprehensive insight into the regulatory elements landscape in the human genome. However, functional annotation of regulatory DNA elements lags behind. Consequently, large-scale and robust functional assays are required to elucidate the role of regulatory elements during normal development and in disease.

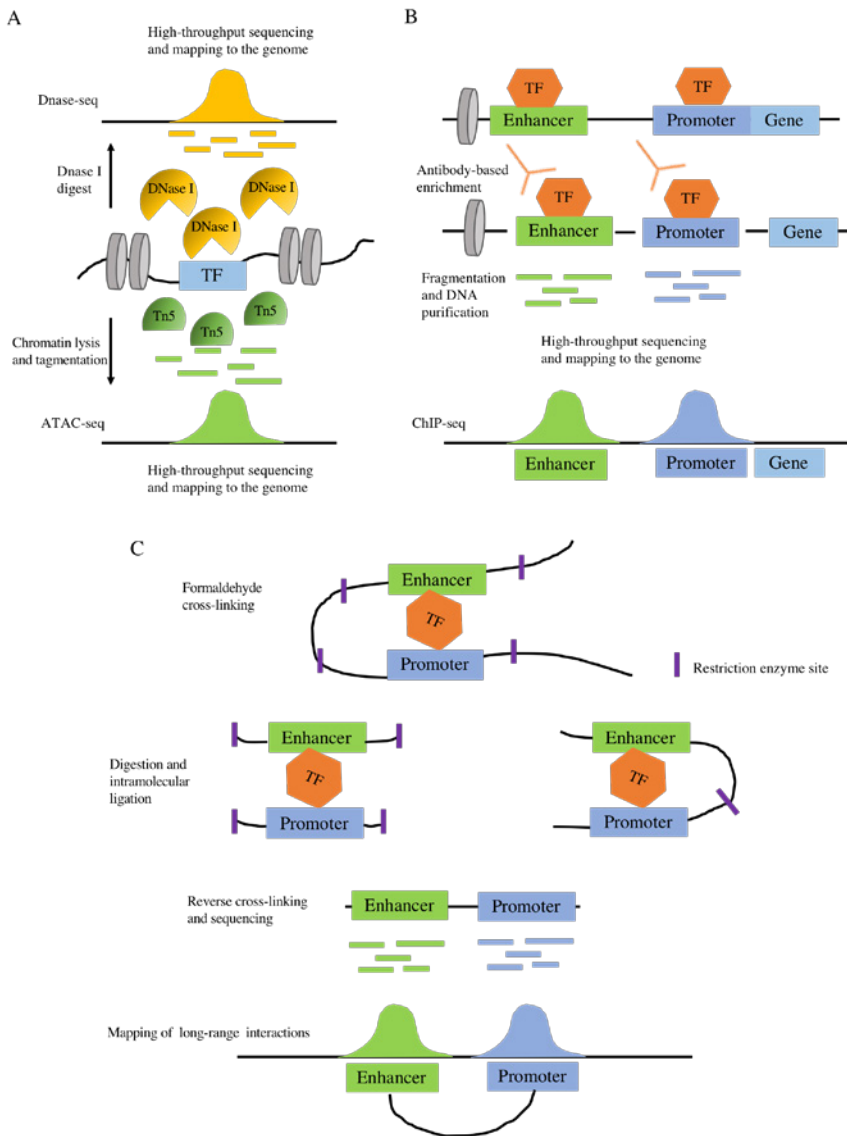


Figure 3. Genome-wide methods to identify gene regulatory elements.

(A) Gene regulatory elements are usually located in active regions of the genome where there are open chromatin regions and can be digested by enzymes, such as DNase I or modified Tn5 transposons, followed by massively parallel sequencing to identify them (DNase-seq or ATAC-seq). (B) Gene regulatory elements can be identified using the antibody against a specific TF, followed by immunoprecipitation and deep sequencing to identify the regions bound by specific TF (ChIP-seq). (C) Gene regulatory elements can be identified by proximity ligation methods (e.g., 3C, 4C, 5C, and Hi-C), which require cross-linking distal interacting DNA (such as enhancer and promoter) followed by sequencing to map the interactions. Abbreviations: ATAC-seq, assay for transposase-accessible chromatin using sequencing; 3C, chromosome conformation capture; 4C, circularised chromosome conformation capture; 5C, carbon copy chromosome conformation capture; ChIP-seq, chromatin immunoprecipitation followed by massively parallel sequencing; DNase-seq, DNase sequencing; TF, transcription factor.

LncRNAs: RNA regulatory element

RNA was considered as a messenger operating between DNA and protein. However, only 2% of the human genome contains protein-coding genes which can be transcribed into messenger RNA (mRNA). Over the last decades, the development of high-throughput technologies, such as next-generation sequencing, have allowed the in depth exploration of the non-coding genome. Notably, it has been increasingly and well demonstrated that the genome of many species, including human, is pervasively transcribed, resulting in the production of a huge amount of non-coding transcripts which were previously considered as “transcription noise”. Especially, some large-scale RNA profiling studies have shown that the majority of the human genome (>75%) is actively transcribed, forming a highly complicated network of non-coding transcripts (ncRNAs) and protein-coding transcripts (or mRNAs) (49, 50).

Long-non-coding RNAs (LncRNAs) are defined as RNAs that are larger than 200 bp without protein-coding potential (51). There is increasing evidence indicating that lncRNAs are involved in numerous biological processes including cell differentiation and development (52), antiviral response (53), and gene imprinting (54). It has been reported that deregulation (overexpression, deficiency or mutation) of lncRNAs is related to different diseases including cancers (55, 56, 57). While the majority of the lncRNAs are not characterised and their functions are unknown, some lncRNAs were well investigated. Generally, the mechanisms of lncRNAs function can be broadly divided into cis-regulating expression and/or chromatin state of nearby locus/gene or trans-functions throughout the cells (58–60). The key point to distinguish cis and trans regulation is whether the lncRNAs activities are found where they come from and neighbouring loci (cis) or somewhere else (trans). A well-characterised example of cis-function lncRNA is the X inactive specific transcript (XIST) in X chromosome inactivation (61). More studies have effectively demonstrated the sequence-specific requirements of XIST during the X inactivation (62, 63). In some cases, lncRNAs production is important for local gene regulation and this regulation is independent of its sequence. A classic example of this kind of regulation is the antisense lncRNA-Airn (antisense Igfr2 RNA non-coding), which overlaps with the Igfr2 gene body and promoter; moreover, it is important to silence the paternal allele. It has been demonstrated that Airn silencing regulation depends on the antisense transcription and importantly, is independent of the Airn sequence (64). In addition, it should also be considered that the lncRNA cis-regulatory activity is due to the DNA elements within the locus that functions independently of the sequences or production of the lncRNAs. LincRNA-P21 was initially reported to function as a P53-dependent trans-acting lncRNA by repressing a gene network in the P53 signalling pathway during DNA damage and apoptosis (65). Later investigation of the lincRNA-P21 locus revealed that actually, lincRNA-P21 regulates CDKN1A (P21) in cis (66), which was further confirmed by its short half-life and low copy number (66). These findings indicated the role of lincRNA-P21 as cis-acting lncRNA, which is in line

with another report that lincRNA-P21 acts as an enhancer RNA to regulate CDKN1A (67). In addition to these cis-regulatory lncRNAs, there is an increasing number of reports of lncRNAs that can leave the site of transcription and operate in trans. Such lncRNAs can be categorised into at least three major subgroups. First, lncRNAs can regulate gene expression and/or chromatin states far away from the transcription site, such as HOTAIR (68). Second, lncRNAs can regulate the nuclear architecture, the most-well investigated example being MALAT1 (69, 70). Third, lncRNAs can influence the interacted proteins and/or other RNAs, for instance, lncRNA NORAD acts as the decoy for RNA-binding proteins PUMILIO1 and PUMILIO2 (71, 72).

In summary, the discovery of lncRNAs as crucial RNA regulatory elements has revealed a new layer of genome regulation.

Enhancers: DNA regulatory element

Gene transcription is an important process during cellular development and the generation of different cell types within an organism. Thus, gene expression needs precise, accurate and robust regulation, strictly controlled by the interplay of various regulatory events. The promoter is a critical DNA regulatory element that can initiate the transcription of a gene. Besides promoters, enhancers have also been identified as key regulators of gene transcription. In 1981, the first enhancer was identified and characterised as a 72 bp DNA sequence of the SV40 virus (73, 74). Soon thereafter, many enhancers were discovered, and their functional properties have been extensively studied. Enhancers are defined as DNA sequences that activate gene transcription in cis, but independent of their relative location, distance, and orientation to their target promoters.

Genes are often controlled by multiple enhancers, each of which can provide diverse transcriptional regulation and modulate the level of gene expression under different biological circumstances. Thus, enhancers are extremely critical players in the response to the changes and demands of different environmental, developmental, and physiological conditions. It is worth noting that deregulation of enhancers is closely related to human diseases including cancers (75–79).

Enhancers are usually 100–1000 bp long and contain short DNA motifs that function as binding sites for TFs. TFs can recruit co-activators or co-repressors and determine the activity of the enhancer based on the combined regulatory cues of all bound factors. Generally, activation of enhancers requires multiple TFs binding, usually including lineage-specific factors and sequence-dependent factors which maintain the integration of intrinsic and extrinsic cues at enhancers (80). Mutations or alterations in the TFs binding motifs can abolish enhancer activities, leading to the deregulation of their target gene expression (81). The consensus TFs binding motifs on enhancers are often used for identification of putative enhancers (82). In addition, active enhancers are typically

devoid of nucleosomes. These regions are “open” and sensitive to DNA nucleases like DNase I, thus their chromatin is more accessible to be bound by TFs (82, 83). This “open”-chromatin accessibility is also used for the prediction of enhancers. Furthermore, a genome-wide effort to map histone modification on chromatin has revealed specific patterns with different marks that are enriched at promoters, active enhancers, and transcriptionally silent or repressed regions. These marks allow the prediction of enhancers on a genome-wide scale (39, 41, 84–86). It has been shown that active enhancers are typically marked by a high level of histone H3 lysine 4 monomethylation (H3K4me1) and H3K27 acetylation (H3K27ac) (41, 87). The combination of the above described “enhancer features” is frequently used for genome-wide prediction of enhancers. Recently, it has been shown that active enhancers produce RNAs, so-called enhancer-associated RNAs (or eRNAs) (45). The expression of eRNAs is highly correlated with enhancer activities and their target gene expression (88, 89), therefore can be utilised as a marker of active enhancers for systematic annotation of enhancers across the genome (45). Nevertheless, our knowledge about enhancers is rudimentary. Functional identification and characterisation of enhancers is currently an area of great interest and a major genomic challenge.

CRISPR-Cas system

Clustered regularly interspaced short palindromic repeats (CRISPR)/CRISPR-associated (Cas) system was found as RNA mediated adaptive defence system in bacteria and archaea that protects them from invading viruses and plasmids (90, 91). This defence system can detect and silence “foreign” nucleic acids in a sequence-specific manner, relying only on small RNAs. In response to the viral infection and plasmid challenges, the short fragments of foreign DNA from virus or plasmid (known as the protospacer) are integrated into the host chromosome in a repeat-spacer-repeat manner at the CRISPR array (92, 93). The “CRISPR repeat-spacer” loci are then transcribed and processed into short CRISPR-derived RNAs (crRNAs), which contain the sequence complementary to protospacer sequences from the invading nucleic acid (94–96). After that, the crRNAs direct the detection and silencing of the target foreign DNA with Cas proteins by packing them together into a surveillance complex (93, 97–99).

Type-II CRISPR from *S. pyogenes* was the first engineered system for genome editing (100), opening the gate for the manipulation of the human genome in a very effective and efficient manner. The most widely used version of this system is CRISPR-Cas9 which requires Cas9 nuclease and single guide RNA (sgRNA). The sgRNA is a fusion of crRNA and trans-activating CRISPR RNA (tracrRNA), which pairs with crRNA and guides the CRISPR-associated protein Cas9 to cleave the target DNA. The site-specific cleavage requires a short protospacer adjacent motif (PAM) in the target DNA (NGG in *S. pyogenes*). This Cas9 system is currently widely and successfully used to edit and target endogenous genes in human cells and even organisms (101–104).

Traditionally, the manipulation of non-coding regions in the genome was mainly dependent on homologous recombination techniques (105–107). Genome engineering technologies, such as synthetic zinc finger (ZF) proteins and transcription activator-like effectors (TALEs), facilitated the development of genome research, however, they were unsuitable for large-scale high-throughput functional analyses of regulatory DNA elements (for review see 108). The development of the CRISPR-Cas9 system overcame this, allowing functional screens to annotate regulatory DNA elements using functional genetic screening approaches (109).

References

1. Hanahan,D. and Weinberg,R.A. (2011) Hallmarks of cancer: The next generation. *Cell*, 10.1016/j.cell.2011.02.013.
2. Hahn,W.C. and Weinberg,R.A. (2002) Modelling the molecular circuitry of cancer. *Nat. Rev. Cancer*, 10.1038/nrc795.
3. Kuilman,T., Michaloglou,C., Mooi,W.J. and Peeper,D.S. (2010) The essence of senescence. *Genes Dev.*, 10.1101/gad.1971610.
4. Hayflick,L. (1965) The limited in vitro lifetime of human diploid cell strains. *Exp. Cell Res.*, 10.1016/0014-4827(65)90211-9.
5. Harley,C.B., Futcher,A.B. and Greider,C.W. (1990) Telomeres shorten during ageing of human fibroblasts. *Nature*, 10.1038/345458a0.
6. Bodnar,A.G., Ouellette,M., Frolkis,M., Holt,S.E., Chiu,C.P., Morin,G.B., Harley,C.B., Shay,J.W., Lichtsteiner,S. and Wright,W.E. (1998) Extension of life-span by introduction of telomerase into normal human cells. *Science (80-)*, 10.1126/science.279.5349.349.
7. Vaziri,H. and Benchimol,S. (1998) Reconstitution of telomerase activity in normal human cells leads to elongation of telomeres and extended replicative life span. *Curr. Biol.*, 10.1016/S0960-9822(98)70109-5.
8. Huang,F.W., Hodis,E., Xu,M.J., Kryukov,G. V., Chin,L. and Garraway,L.A. (2013) Highly recurrent TERT promoter mutations in human melanoma. *Science (80-)*, 10.1126/science.1229259.
9. Horn,S., Figl,A., Rachakonda,P.S., Fischer,C., Sucker,A., Gast,A., Kadel,S., Moll,I., Nagore,E., Hemminki,K., *et al.* (2013) TERT promoter mutations in familial and sporadic melanoma. *Science (80-)*, 10.1126/science.1230062.
10. Muntoni,A. and Reddel,R.R. (2005) The first molecular details of ALT in human tumor cells. *Hum. Mol. Genet.*, 10.1093/hmg/ddi266.
11. Serrano,M., Lin,A.W., McCurrach,M.E., Beach,D. and Lowe,S.W. (1997) Oncogenic ras provokes premature cell senescence associated with accumulation of p53 and p16(INK4a). *Cell*, 10.1016/S0092-8674(00)81902-9.
12. Sarkisian,C.J., Keister,B.A., Stairs,D.B., Boxer,R.B., Moody,S.E. and Chodosh,L.A. (2007) Dose-dependent oncogene-induced senescence in vivo and its evasion during mammary tumorigenesis. *Nat. Cell Biol.*, 10.1038/ncb1567.
13. Miyauchi,H., Minamino,T., Tateno,K., Kunieda,T., Toko,H. and Komuro,I. (2004) Akt negatively regulates the in vitro lifespan of human endothelial cells via a p53/p21-dependent pathway. *EMBO J.*, 10.1038/sj.emboj.7600045.
14. Michaloglou,C., Vredeveld,L.C.W., Soengas,M.S., Denoyelle,C., Kuilman,T., Van Der Horst,C.M.A.M., Majoro,D.M., Shay,J.W., Mooi,W.J. and Peeper,D.S. (2005) BRAFE600-associated senescence-like cell cycle arrest of human naevi. *Nature*, 10.1038/nature03890.
15. Dimri,G.P., Itahana,K., Acosta,M. and Campisi,J. (2000) Regulation of a senescence checkpoint response by the E2F1 transcription factor and p14(ARF) tumor suppressor. *Mol Cell Biol.*, 10.1128/MCB.20.1.273-285.2000.
16. Chen,Z., Trotman,L.C., Shaffer,D., Lin,H.K., Dotan,Z.A., Niki,M., Koutcher,J.A., Scher,H.I., Ludwig,T., Gerald,W., *et al.* (2005) Crucial role of p53-dependent cellular senescence in suppression of Pten-deficient tumorigenesis. *Nature*, 10.1038/nature03918.

17. Courtois-Cox,S., Genter Williams,S.M., Reczek,E.E., Johnson,B.W., McGillicuddy,L.T., Johannessen,C.M., Hollstein,P.E., MacCollin,M. and Cichowski,K. (2006) A negative feedback signaling network underlies oncogene-induced senescence. *Cancer Cell*, 10.1016/j.ccr.2006.10.003.
18. Lee,A.C., Fenster,B.E., Ito,H., Takeda,K., Bae,N.S., Hirai,T., Yu,Z.X., Ferrans,V.J., Howard,B.H. and Finkel,T. (1999) Ras proteins induce senescence by altering the intracellular levels of reactive oxygen species. *J. Biol. Chem.*, 10.1074/jbc.274.12.7936.
19. Bartkova,J., Rezaei,N., Liontos,M., Karakaidos,P., Kletsas,D., Issaeva,N., Vassiliou,L.V.F., Kolettas,E., Niforou,K., Zoumpourlis,V.C., *et al.* (2006) Oncogene-induced senescence is part of the tumorigenesis barrier imposed by DNA damage checkpoints. *Nature*, 10.1038/nature05268.
20. Di Micco,R., Fumagalli,M., Cicalese,A., Piccinin,S., Gasparini,P., Luise,C., Schurra,C., Garré,M., Giovanni Nuciforo,P., Bensimon,A., *et al.* (2006) Oncogene-induced senescence is a DNA damage response triggered by DNA hyper-replication. *Nature*, 10.1038/nature05327.
21. Braig,M. and Schmitt,C.A. (2006) Oncogene-induced senescence: Putting the brakes on tumor development. *Cancer Res.*, 10.1158/0008-5472.CAN-05-4006.
22. Braig,M., Lee,S., Loddenkemper,C., Rudolph,C., Peters,A.H.F.M., Schlegelberger,B., Stein,H., Dörken,B., Jenuwein,T. and Schmitt,C.A. (2005) Oncogene-induced senescence as an initial barrier in lymphoma development. *Nature*, 10.1038/nature03841.
23. Dimri,G.P., Lee,X., Basile,G., Acosta,M., Scott,G., Roskelley,C., Medrano,E.E., Linskens,M., Rubelj,I. and Pereira-Smith,O. (1995) A biomarker that identifies senescent human cells in culture and in aging skin in vivo. *Proc. Natl. Acad. Sci. U. S. A.*, DOI 10.1073/pnas.92.20.9363.
24. Kurz,D.J., Decary,S., Hong,Y. and Erusalimsky,J.D. (2000) Senescence-associated (beta)-galactosidase reflects an increase in lysosomal mass during replicative ageing of human endothelial cells. *J. Cell Sci.*
25. Henikoff,S. (2000) Heterochromatin function in complex genomes. *Biochim. Biophys. Acta - Rev. Cancer*, 10.1016/S0304-419X(99)00034-7.
26. Jenuwein,T. (2001) Re-SET-ting heterochromatin by histone methyltransferases. *Trends Cell Biol.*, 10.1016/S0962-8924(01)02001-3.
27. Narita,M., Nunez,S., Heard,E., Narita,M., Lin,A.W., Hearn,S.A., Spector,D.L., Hannon,G.J. and Lowe,S.W. (2003) Rb-mediated heterochromatin formation and silencing of E2F target genes during cellular senescence. *Cell*, 10.1016/S0092-8674(03)00401-X.
28. Tahara,H., Sato,E., Noda,A. and Ide,T. (1995) Increase in expression level of p21sdi1/cip1/waf1 with increasing division age in both normal and SV40-transformed human fibroblasts. *Oncogene*.
29. Alcorta,D.A., Xiong,Y., Phelps,D., Hannon,G., Beach,D. and Barrett,J.C. (1996) Involvement of the cyclin-dependent kinase inhibitor p16 (INK4a) in replicative senescence of normal human fibroblasts. *Proc. Natl. Acad. Sci. U. S. A.*, 10.1073/pnas.93.24.13742.
30. Collado,M. and Serrano,M. (2006) The power and the promise of oncogene-induced senescence markers. *Nat. Rev. Cancer*, 10.1038/nrc1884.
31. Hollstein,M., Sidransky,D., Vogelstein,B. and Harris,C.C. (1991) P53 Mutations in Human Cancers. *Science (80-)*, 10.1126/science.1905840.
32. Ruas,M. and Peters,G. (1998) The p16(INK4a)/CDKN2A tumor suppressor and its relatives. *Biochim. Biophys. Acta - Rev. Cancer*, 10.1016/S0304-419X(98)00017-1.

33. Sharpless,N.E. and Depinho,R.A. (1999) The INK4A/ARF locus and its two gene products. *Curr. Opin. Genet. Dev.*, 10.1016/S0959-437X(99)80004-5.
34. Salama,R., Sadaie,M., Hoare,M. and Narita,M. (2014) Cellular senescence and its effector programs. *Genes Dev.*, 10.1101/gad.235184.113.
35. Maston,G.A., Evans,S.K. and Green,M.R. (2006) Transcriptional Regulatory Elements in the Human Genome. *Annu. Rev. Genomics Hum. Genet.*, 10.1146/annurev.genom.7.080505.115623.
36. Song,L. and Crawford,G.E. (2010) DNase-seq: A high-resolution technique for mapping active gene regulatory elements across the genome from mammalian cells. *Cold Spring Harb. Protoc.*, 10.1101/pdb.prot5384.
37. Buenrostro,J.D., Giresi,P.G., Zaba,L.C., Chang,H.Y. and Greenleaf,W.J. (2013) Transposition of native chromatin for fast and sensitive epigenomic profiling of open chromatin, DNA-binding proteins and nucleosome position. *Nat. Methods*, 10.1038/nmeth.2688.
38. Bernstein,B.E., Kamal,M., Lindblad-Toh,K., Bekiranov,S., Bailey,D.K., Huebert,D.J., McMahon,S., Karlsson,E.K., Kulbokas,E.J., Gingeras,T.R., *et al.* (2005) Genomic maps and comparative analysis of histone modifications in human and mouse. *Cell*, 10.1016/j.cell.2005.01.001.
39. Heintzman,N.D., Stuart,R.K., Hon,G., Fu,Y., Ching,C.W., Hawkins,R.D., Barrera,L.O., Van Calcar,S., Qu,C., Ching,K.A., *et al.* (2007) Distinct and predictive chromatin signatures of transcriptional promoters and enhancers in the human genome. *Nat. Genet.*, 10.1038/ng1966.
40. Creyghton,M.P., Cheng,A.W., Welstead,G.G., Kooistra,T., Carey,B.W., Steine,E.J., Hanna,J., Lodato,M.A., Frampton,G.M., Sharp,P.A., *et al.* (2010) Histone H3K27ac separates active from poised enhancers and predicts developmental state. *Proc. Natl. Acad. Sci.*, 10.1073/pnas.10160711107.
41. Rada-Iglesias,A., Bajpai,R., Swigut,T., Brugmann,S.A., Flynn,R.A. and Wysocka,J. (2011) A unique chromatin signature uncovers early developmental enhancers in humans. *Nature*, 10.1038/nature09692.
42. Barski,A., Cuddapah,S., Cui,K., Roh,T.Y., Schones,D.E., Wang,Z., Wei,G., Chepelev,I. and Zhao,K. (2007) High-Resolution Profiling of Histone Methylations in the Human Genome. *Cell*, 10.1016/j.cell.2007.05.009.
43. Birney,E., Stamatoyannopoulos,J.A., Dutta,A., Guigó,R., Gingeras,T.R., Margulies,E.H., Weng,Z., Snyder,M., Dermitzakis,E.T., Thurman,R.E., *et al.* (2007) Identification and analysis of functional elements in 1% of the human genome by the ENCODE pilot project. *Nature*, 10.1038/nature05874.
44. Kellis,M., Wold,B., Snyder,M.P., Bernstein,B.E., Kundaje,A., Marinov,G.K., Ward,L.D., Birney,E., Crawford,G.E., Dekker,J., *et al.* (2014) Defining functional DNA elements in the human genome. *Proc. Natl. Acad. Sci. U. S. A.*, 10.1073/pnas.1318948111.
45. Andersson,R., Gebhard,C., Miguel-Escalada,I., Hoof,I., Bornholdt,J., Boyd,M., Chen,Y., Zhao,X., Schmidl,C., Suzuki,T., *et al.* (2014) An atlas of active enhancers across human cell types and tissues. *Nature*, 10.1038/nature12787.
46. Forrest,A.R.R., Kawaji,H., Rehli,M., Kenneth Baillie,J., de Hoon,M.J.L., Haberle,V., Lassmann,T., Kulakovskiy,I. V., Lizio,M., Itoh,M., *et al.* (2014) A promoter-level mammalian expression atlas. *Nature*, 10.1038/nature13182.
47. Bernstein,B.E., Stamatoyannopoulos,J.A., Costello,J.F., Ren,B., Milosavljevic,A., Meissner,A., Kellis,M., Marra,M.A., Beaudet,A.L., Ecker,J.R., *et al.* (2010) The NIH roadmap epigenomics mapping consortium. *Nat. Biotechnol.*, 10.1038/nbt1010-1045.

48. Roadmap Epigenomics Consortium, Kundaje,A., Meuleman,W., Ernst,J., Bilenky,M., Yen,A., Heravi-Moussavi,A., Kheradpour,P., Zhang,Z., Wang,J., *et al.* (2015) Integrative analysis of 111 reference human epigenomes. *Nature*, 10.1038/nature14248.
49. Djebali,S., Davis,C.A., Merkel,A., Dobin,A., Lassmann,T., Mortazavi,A., Tanzer,A., Lagarde,J., Lin,W., Schlesinger,F., *et al.* (2012) Landscape of transcription in human cells. *Nature*, 10.1038/nature11233.
50. Hangauer,M.J., Vaughn,I.W. and McManus,M.T. (2013) Pervasive Transcription of the Human Genome Produces Thousands of Previously Unidentified Long Intergenic Noncoding RNAs. *PLoS Genet.*, 10.1371/journal.pgen.1003569.
51. Derrien,T., Johnson,R., Bussotti,G., Tanzer,A., Djebali,S., Tilgner,H., Guernec,G., Martin,D., Merkel,A., Knowles,D.G., *et al.* (2012) The GENCODE v7 catalog of human long noncoding RNAs: Analysis of their gene structure, evolution, and expression. *Genome Res.*, 10.1101/gr.132159.111.
52. Fatica,A. and Bozzoni,I. (2014) Long non-coding RNAs: New players in cell differentiation and development. *Nat. Rev. Genet.*, 10.1038/nrg3606.
53. Fortes,P. and Morris,K. V. (2016) Long noncoding RNAs in viral infections. *Virus Res.*, 10.1016/j.virusres.2015.10.002.
54. Kanduri,C. (2016) Long noncoding RNAs: Lessons from genomic imprinting. *Biochim. Biophys. Acta - Gene Regul. Mech.*, 10.1016/j.bbarm.2015.05.006.
55. Esteller,M. (2011) Non-coding RNAs in human disease. *Nat Rev Genet*, 10.1038/nrg3074.
56. Wapinski,O. and Chang,H.Y. (2011) Long noncoding RNAs and human disease. *Trends Cell Biol.*, 10.1016/j.tcb.2011.04.001.
57. Huarte,M. (2015) The emerging role of lncRNAs in cancer. *Nat. Med.*, 10.1038/nm.3981.
58. Ulitsky,I. and Bartel,D.P. (2013) LincRNAs: Genomics, evolution, and mechanisms. *Cell*, 10.1016/j.cell.2013.06.020.
59. Geisler,S. and Collier,J. (2013) RNA in unexpected places: Long non-coding RNA functions in diverse cellular contexts. *Nat. Rev. Mol. Cell Biol.*, 10.1038/nrm3679.
60. Kornienko,A.E., Guenzl,P.M., Barlow,D.P. and Pauler,F.M. (2013) Gene regulation by the act of long non-coding RNA transcription. *BMC Biol.*, 10.1186/1741-7007-11-59.
61. Brown,C.J., Hendrich,B.D., Rupert,J.L., Lafrenière,R.G., Xing,Y., Lawrence,J. and Willard,H.F. (1992) The human XIST gene: Analysis of a 17 kb inactive X-specific RNA that contains conserved repeats and is highly localized within the nucleus. *Cell*, 10.1016/0092-8674(92)90520-M.
62. Cerase,A., Pintacuda,G., Tattermusch,A. and Avner,P. (2015) Xist localization and function: New insights from multiple levels. *Genome Biol.*, 10.1186/s13059-015-0733-y.
63. Da Rocha,S.T. and Heard,E. (2017) Novel players in X inactivation: Insights into Xist-mediated gene silencing and chromosome conformation. *Nat. Struct. Mol. Biol.*, 10.1038/nsmb.3370.
64. Latos,P.A., Pauler,F.M., Koerner,M. V., Şenergin,H.B., Hudson,Q.J., Stocsits,R.R., Allhoff,W., Stricker,S.H., Klement,R.M., Warczok,K.E., *et al.* (2012) Airn transcriptional overlap, but not its lncRNA products, induces imprinted Igf2r silencing. *Science (80-.)*, 10.1126/science.1228110.
65. Huarte,M., Guttman,M., Feldser,D., Garber,M., Koziol,M.J., Kenzelmann-Broz,D., Khalil,A.M., Zuk,O., Amit,I., Rabani,M., *et al.* (2010) A large intergenic noncoding RNA induced by p53 mediates global gene repression in the p53 response. *Cell*, 10.1016/j.cell.2010.06.040.

66. Dimitrova,N., Zamudio,J.R., Jong,R.M., Soukup,D., Resnick,R., Sarma,K., Ward,A.J., Raj,A., Lee,J.T., Sharp,P.A., *et al.* (2014) LincRNA-p21 Activates p21 In cis to Promote Polycomb Target Gene Expression and to Enforce the G1/S Checkpoint. *Mol. Cell*, 10.1016/j.molcel.2014.04.025.
67. Allen,M.A., Andrysik,Z., Dengler,V.L., Mellert,H.S., Guarnieri,A., Freeman,J.A., Sullivan,K.D., Galbraith,M.D., Luo,X., Lee Kraus,W., *et al.* (2014) Global analysis of p53-regulated transcription identifies its direct targets and unexpected regulatory mechanisms. *Elife*, 10.7554/eLife.02200.001.
68. Rinn,J.L., Kertesz,M., Wang,J.K., Squazzo,S.L., Xu,X., Bruggmann,S.A., Goodnough,L.H., Helms,J.A., Farnham,P.J., Segal,E., *et al.* (2007) Functional Demarcation of Active and Silent Chromatin Domains in Human HOX Loci by Noncoding RNAs. *Cell*, 10.1016/j.cell.2007.05.022.
69. Hutchinson,J.N., Ensminger,A.W., Clemson,C.M., Lynch,C.R., Lawrence,J.B. and Chess,A. (2007) A screen for nuclear transcripts identifies two linked noncoding RNAs associated with SC35 splicing domains. *BMC Genomics*, 10.1186/1471-2164-8-39.
70. Bernard,D., Prasanth,K. V., Tripathi,V., Colasse,S., Nakamura,T., Xuan,Z., Zhang,M.Q., Sedel,F., Jourden,L., Couplier,F., *et al.* (2010) A long nuclear-retained non-coding RNA regulates synaptogenesis by modulating gene expression. *EMBO J.*, 10.1038/emboj.2010.199.
71. Lee,S., Kopp,F., Chang,T.C., Sataluri,A., Chen,B., Sivakumar,S., Yu,H., Xie,Y. and Mendell,J.T. (2016) Noncoding RNA NORAD Regulates Genomic Stability by Sequestering PUMILIO Proteins. *Cell*, 10.1016/j.cell.2015.12.017.
72. Tichon,A., Gil,N., Lubelsky,Y., Solomon,T.H., Lemze,D., Itzkovitz,S., Stern-Ginossar,N. and Ulitsky,I. (2016) A conserved abundant cytoplasmic long noncoding RNA modulates repression by Pumilio proteins in human cells. *Nat. Commun.*, 10.1038/ncomms12209.
73. Banerji,J., Rusconi,S. and Schaffner,W. (1981) Expression of a β -globin gene is enhanced by remote SV40 DNA sequences. *Cell*, 10.1016/0092-8674(81)90413-X.
74. Moreau,P., Hen,R., Wasylyk,B., Everett,R., Gaub,M.P. and Chambon,P. (1981) The SV40 72 base repair repeat has a striking effect on gene expression both in SV40 and other chimeric recombinants. *Nucleic Acids Res.*, 10.1093/nar/9.22.6047.
75. Herz,H.M. (2016) Enhancer deregulation in cancer and other diseases. *BioEssays*, 10.1002/bies.201600106.
76. Hindorf,L.A., Sethupathy,P., Junkins,H.A., Ramos,E.M., Mehta,J.P., Collins,F.S. and Manolio,T.A. (2009) Potential etiologic and functional implications of genome-wide association loci for human diseases and traits. *Proc. Natl. Acad. Sci.*, 10.1073/pnas.0903103106.
77. Maurano,M.T., Humbert,R., Rynes,E., Thurman,R.E., Haugen,E., Wang,H., Reynolds,A.P., Sandstrom,R., Qu,H., Brody,J., *et al.* (2012) Systematic localization of common disease-associated variation in regulatory DNA. *Science (80-.)*, 10.1126/science.1222794.
78. Weinhold,N., Jacobsen,A., Schultz,N., Sander,C. and Lee,W. (2014) Genome-wide analysis of noncoding regulatory mutations in cancer. *Nat. Genet.*, 10.1038/ng.3101.
79. Hnisz,D., Abraham,B.J., Lee,T.I., Lau,A., Saint-André,V., Sigova,A.A., Hoke,H.A. and Young,R.A. (2013) Super-enhancers in the control of cell identity and disease. *Cell*, 10.1016/j.cell.2013.09.053.
80. Buecker,C. and Wysocka,J. (2012) Enhancers as information integration hubs in development: Lessons from genomics. *Trends Genet.*, 10.1016/j.tig.2012.02.008.

81. Grossman,S.R., Zhang,X., Wang,L., Engreitz,J., Melnikov,A., Rogov,P., Tewhey,R., Isakova,A., Deplancke,B., Bernstein,B.E., *et al.* (2017) Systematic dissection of genomic features determining transcription factor binding and enhancer function. *Proc. Natl. Acad. Sci.*, 10.1073/pnas.1621150114.
82. Shlyueva,D., Stampfel,G. and Stark,A. (2014) Transcriptional enhancers: From properties to genome-wide predictions. *Nat. Rev. Genet.*, 10.1038/nrg3682.
83. Gross,D. (1988) Nuclease Hypersensitive Sites In Chromatin. *Annu. Rev. Biochem.*, 10.1146/annurev.biochem.57.1.159.
84. Heintzman,N.D., Hon,G.C., Hawkins,R.D., Kheradpour,P., Stark,A., Harp,L.F., Ye,Z., Lee,L.K., Stuart,R.K., Ching,C.W., *et al.* (2009) Histone modifications at human enhancers reflect global cell-type-specific gene expression. *Nature*, 10.1038/nature07829.
85. Roh,T.Y., Cuddapah,S. and Zhao,K. (2005) Active chromatin domains are defined by acetylation islands revealed by genome-wide mapping. *Genes Dev.*, 10.1101/gad.1272505.
86. Bonn,S., Zinzen,R.P., Girardot,C., Gustafson,E.H., Perez-Gonzalez,A., Delhomme,N., Ghavi-Helm,Y., Wilczyński,B., Riddell,A. and Furlong,E.E.M. (2012) Tissue-specific analysis of chromatin state identifies temporal signatures of enhancer activity during embryonic development. *Nat. Genet.*, 10.1038/ng.1064.
87. Arnold,C.D., Gerlach,D., Stelzer,C., Boryń,L.M., Rath,M. and Stark,A. (2013) Genome-wide quantitative enhancer activity maps identified by STARR-seq. *Science (80-.)*, 10.1126/science.1232542.
88. de Santa,F., Barozzi,I., Muetton,F., Ghisletti,S., Polletti,S., Tusi,B.K., Muller,H., Ragoussis,J., Wei,C.L. and Natoli,G. (2010) A large fraction of extragenic RNA Pol II transcription sites overlap enhancers. *PLoS Biol.*, 10.1371/journal.pbio.1000384.
89. Li,W., Notani,D., Ma,Q., Tanasa,B., Nunez,E., Chen,A.Y., Merkurjev,D., Zhang,J., Ohgi,K., Song,X., *et al.* (2013) Functional roles of enhancer RNAs for oestrogen-dependent transcriptional activation. *Nature*, 10.1038/nature12210.
90. Horvath,P. and Barrangou,R. (2010) CRISPR/Cas, the immune system of Bacteria and Archaea. *Science (80-.)*, 10.1126/science.1179555.
91. Wiedenheft,B., Sternberg,S.H. and Doudna,J.A. (2012) RNA-guided genetic silencing systems in bacteria and archaea. *Nature*, 10.1038/nature10886.
92. Barrangou,R., Fremaux,C., Deveau,H., Richards,M., Boyaval,P., Moineau,S., Romero,D.A. and Horvath,P. (2007) CRISPR provides acquired resistance against viruses in prokaryotes. *Science (80-.)*, 10.1126/science.1138140.
93. Garneau,J.E., Dupuis,M.È., Villion,M., Romero,D.A., Barrangou,R., Boyaval,P., Fremaux,C., Horvath,P., Magadán,A.H. and Moineau,S. (2010) The CRISPR/cas bacterial immune system cleaves bacteriophage and plasmid DNA. *Nature*, 10.1038/nature09523.
94. Carte,J., Wang,R., Li,H., Terns,R.M. and Terns,M.P. (2008) Cas6 is an endoribonuclease that generates guide RNAs for invader defense in prokaryotes. *Genes Dev.*, 10.1101/gad.1742908.
95. Deltcheva,E., Chylinski,K., Sharma,C.M., Gonzales,K., Chao,Y., Pirzada,Z.A., Eckert,M.R., Vogel,J. and Charpentier,E. (2011) CRISPR RNA maturation by trans-encoded small RNA and host factor RNase III. *Nature*, 10.1038/nature09886.
96. Gesner,E.M., Schellenberg,M.J., Garside,E.L., George,M.M. and MacMillan,A.M. (2011) Recognition and maturation of effector RNAs in a CRISPR interference pathway. *Nat. Struct. Mol. Biol.*, 10.1038/nsmb.2042.

97. Brouns,S.J.J., Jore,M.M., Lundgren,M., Westra,E.R., Slijkhuis,R.J.H., Snijders,A.P.L., Dickman,M.J., Makarova,K.S., Koonin,E. V. and Van Der Oost,J. (1993) Small Crispr Rnas Guide Antiviral Defense in Prokaryotes. *Cancer Epidemiol. Biomarkers Prev.*, 10.1126/science.1159689.
98. Wiedenheft,B., Lander,G.C., Zhou,K., Jore,M.M., Brouns,S.J.J., Van Der Oost,J., Doudna,J.A. and Nogales,E. (2011) Structures of the RNA-guided surveillance complex from a bacterial immune system. *Nature*, 10.1038/nature10402.
99. Wiedenheft,B., van Duijn,E., Bultema,J.B., Waghmare,S.P., Zhou,K., Barendregt,A., Westphal,W., Heck,A.J.R., Boekema,E.J., Dickman,M.J., *et al.* (2011) RNA-guided complex from a bacterial immune system enhances target recognition through seed sequence interactions. *Proc. Natl. Acad. Sci.*, 10.1073/pnas.1102716108.
100. Jinek,M., Chylinski,K., Fonfara,I., Hauer,M., Doudna,J.A. and Charpentier,E. (2012) A programmable dual-RNA-guided DNA endonuclease in adaptive bacterial immunity. *Science (80-)*, 10.1126/science.1225829.
101. Mali,P., Yang,L., Esvelt,K.M., Aach,J., Guell,M., DiCarlo,J.E., Norville,J.E. and Church,G.M. (2013) RNA-guided human genome engineering via Cas9. *Science (80-)*, 10.1126/science.1232033.
102. Cong,L., Ran,F.A., Cox,D., Lin,S., Barretto,R., Habib,N., Hsu,P.D., Wu,X., Jiang,W., Marraffini,L.A., *et al.* (2013) Multiplex genome engineering using CRISPR/Cas systems. *Science (80-)*, 10.1126/science.1231143.
103. Jinek,M., East,A., Cheng,A., Lin,S., Ma,E. and Doudna,J. (2013) RNA-programmed genome editing in human cells. *Elife*, 10.7554/eLife.00471.
104. Hwang,W.Y., Fu,Y., Reyon,D., Maeder,M.L., Tsai,S.Q., Sander,J.D., Peterson,R.T., Yeh,J.R. and Joung,J.K. (2013) Efficient genome editing in zebrafish using a CRISPR-Cas system. *Nat Biotechnol*, 10.1038/nbt.2501.
105. Smithies,O., Gregg,R.G., Boggs,S.S., Koralewski,M.A. and Kucherlapati,R.S. (1985) Insertion of DNA sequences into the human chromosomal beta-globin locus by homologous recombination. *Nature*, 10.1038/317230a0.
106. Bender,M. a, Reik, a, Close,J., Telling, a, Epner,E., Fiering,S., Hardison,R. and Groudine,M. (1998) Description and targeted deletion of 5' hypersensitive site 5 and 6 of the mouse beta-globin locus control region. *Blood*.
107. Reik,A., Telling,A., Zitnik,G., Cimbor,D., Epner,E. and Groudine,M. (1998) The Locus Control Region Is Necessary for Gene Expression in the Human beta -Globin Locus but Not the Maintenance of an Open Chromatin Structure in Erythroid Cells. *Mol. Cell. Biol*.
108. Hilton,I.B. and Gersbach,C.A. (2015) Enabling functional genomics with genome engineering. *Genome Res.*, 10.1101/gr.190124.115.
109. Korkmaz,G., Lopes,R., Ugalde,A.P., Nevedomskaya,E., Han,R., Myacheva,K., Zwart,W., Elkon,R. and Agami,R. (2016) Functional genetic screens for enhancer elements in the human genome using CRISPR-Cas9. *Nat. Biotechnol.*, 10.1038/nbt.3450.

2



Chapter 2

LncRNA-OIS1 regulates DPP4 activation to modulate senescence induced by RAS

Li Li¹, Pieter C. van Breugel¹, Fabricio Loayza-Puch¹, Alejandro P Ugalde¹, Gozde Korkmaz¹, Naama Messika-Gold⁶, Ruiqi Han¹, Rui Lopes¹, Eric Pintó Barbera², Hans Teunissen³, Elzo de Wit³, Ricardo J. Soares⁴, Boye S. Nielsen⁴, Kim Holmstrøm⁴, Dannys Jorge Martínez-Herrera⁵, Maite Huarte⁵, Annita Louloup¹, Jarno Drost¹, Ran Elkon^{6,*} & Reuven Agami^{1,7,8,*}

¹Division of Oncogenomics, Netherlands Cancer Institute, Plesmanlaan 121, 1066CX, Amsterdam, the Netherlands

²Division of Molecular Genetics, Netherlands Cancer Institute, Plesmanlaan 121, 1066CX, Amsterdam, the Netherlands

³Division of Gene Regulation, Netherlands Cancer Institute, Plesmanlaan 121, 1066CX, Amsterdam, the Netherlands

⁴Bioneer A/S, Kogle Allé 2, DK-2970 Hørsholm, Denmark

⁵Institute of Health Research of Navarra (IdiSNA), 31008 Pamplona, Spain

⁶Department of Human Molecular Genetics and Biochemistry, Sackler School of Medicine, Tel Aviv University, Tel Aviv, Israel

⁷Erasmus MC, Rotterdam University, Rotterdam, the Netherlands

⁸Onco institute, Netherlands Cancer Institute, Plesmanlaan 121, 1066CX, Amsterdam, the Netherlands

* To whom correspondence should be addressed. Tel: +20512199; Email: r.agami@nki.nl

Correspondence may also be addressed to Ran ElkonTel; Email: ranel@tauex.tau.ac.il

ABSTRACT

Oncogene-induced senescence (OIS), provoked in response to oncogenic activation, is considered an important tumour suppressor mechanism. Long-noncoding RNAs (lncRNAs) are transcripts longer than 200 nucleotides without a protein-coding capacity. Functional studies showed that deregulated lncRNA expression promote tumorigenesis and metastasis and that lncRNAs may exhibit tumor-suppressive and oncogenic. Here, we first identified lncRNAs that were differentially expressed between senescent and non-senescent human fibroblast cells. Using RNA interference, we performed a loss-function screen targeting the differentially expressed lncRNAs, and identified lncRNA-OIS1 (lncRNA#32, AC008063.3 or ENSG00000233397) as a lncRNA required for OIS. Knockdown of lncRNA-OIS1 triggered bypass of senescence, higher proliferation rate, lower abundance of the cell cycle inhibitor CDKN1A, and high expression of cell cycle associated genes. Subcellular inspection of lncRNA-OIS1 indicated nuclear and cytosolic localization in both normal culture conditions as well as following oncogene induction. Interestingly, silencing lncRNA-OIS1 diminished the senescent-associated induction of a nearby gene (Dipeptidyl Peptidase 4, DPP4) with established role in tumor suppression. Intriguingly, similar to lncRNA-OIS1, silencing DPP4 caused senescence bypass, and ectopic expression of DPP4 in lncRNA-OIS1 knockdown cells restored the senescent phenotype. Thus, our data indicate that lncRNA-OIS1 links oncogenic induction and senescence with the activation of the tumor suppressor DPP4.

INTRODUCTION

Next-generation sequencing and microarray technologies uncovered thousands of long non-coding RNAs (lncRNAs) encoded in the human genome(1, 2). The majority of those lncRNAs are transcribed and processed in a similar manner to mRNAs, however, lack protein-coding potential(3, 4). Although it is still unclear how many of those lncRNAs have a significant biological function, some of them have been found to be crucial players in the regulation of cellular processes such as proliferation, differentiation or development, as well as in a progression of a variety of human diseases including cancer(5–10). It has been shown that lncRNAs are key determinants of epigenetic regulation, modulation of chromatin structure, scaffolding or decoy function of mRNAs, and post-transcriptional mRNA regulation(11–15). Gene regulation by lncRNAs can be a result of cis-action on nearby genes, or in trans by modulating mRNA stability, mRNA translation, or microRNA and RNA-binding-protein function(16–23).

Cellular senescence was initially defined by Hayflick in 1965 as the limited lifespan of primary human fibroblasts in culture(24). It is a state of irreversible growth arrest which can be induced by different stimuli such as telomere shortening, DNA damage, oxidative stress or oncogene activation(25). Serrano et al., were the first to observe that primary human and mouse fibroblasts enter senescence following the induction of oncogenic RAS, a process termed oncogene induced senescence (OIS)(26). Cellular senescence has been studied most extensively as a strong tumor suppressive mechanism against the emergence of oncogenes(27). Moreover, there is evidence indicating for a role of senescence in age-related conditions and diseases, including cancer, cardiovascular diseases, neurodegeneration, diabetes, sarcopenia, and declining immune function in the elderly(28–32). In contrast, senescent cells can also contribute to tumorigenesis by secreting interleukins (e.g., IL-6, IL-8, and IL-1 α), metalloproteases (e.g., MMP-1, and MMP-3) and other cytokines (e.g., granulocyte-macrophage colony-stimulating factor (GM-CSF)), as part of the senescence associated secretory phenotype(SASP)(25, 30, 33–37). Therefore, senescence may either suppress or promote tumour progression depending on the context where it occurs(38, 39). Given the impact of senescence on human physiology and pathology, it is of interest to understand the molecular mechanisms underlying senescence in order to utilize it for diagnosis and therapy.

A number of factors have been implicated in regulating senescence, including transcription factors, RNA binding proteins, and microRNAs, such as p53, Ets(40), HuR(41), AUF1(42) and TTP(43), and miR-377(44), miR-22(45). In contrast, despite increasing interest in the expression and function of lncRNAs, their possible implication in senescence remains largely unexplored. Recent works indicated a role of MIR31HG and SALNR in senescence(46)(47), but a focused functional genetic screen was not described before. We therefore sought to identify senescence-associated lncRNAs

using our established cellular system that induces senescence in primary human BJ fibroblasts(48). Using transcriptomic profiling we identified a number of differentially-expressed lncRNAs following oncogene induction. Next, using functional screen, we discovered that one of lncRNAs whose expression was induced upon oncogenic stress -lncRNA-OIS1- is required for OIS. We demonstrate that lncRNA-OIS1 is required for senescence by controlling a nearby DPP4 gene with a tumor suppressive activity. Collectively, our results provide a new lncRNA-mediated regulatory pathway for controlling DPP4 during OIS. Our findings support the role of lncRNAs as transcriptional regulators in critical processes such as cellular senescence and a potential role in cancer.

Material and methods

cell culture, transfection, retroviral and lentiviral transduction

BJ/ET/Ras^{V12}, TIG3/ET/RAS^{V12}, Ecopack 2 and HEK293-T cells were cultured in DMEM medium (Gibco), supplemented with 10% FCS (fetal calf serum) (Hyclone), and 1% penicillin/streptomycin (Gibco). Senescence was induced by treatment with 100 nM 4-OHT (Sigma) for 14days. Retroviruses were made by calcium phosphate transfection of Ecopack 2 cells and harvest at 40 and 64 h later. Lentiviruses were made by PEI (polyethylenimine) transfection of HEK293T. Medium was refreshed after 16h and collect the lentivirus by filtering through a 0.45 µm membrane (Milipore Steriflip HV/PVDF) 40 h post-transfection and stored at -80 °C. Cells were selected with the proper selection medium 48 h after transduction for at least 4 days until no surviving cells remained in the no-transduction control plate.

RNA-seq and analysis

RNA-seq samples were processed with TruSeq RNA library prep kit v2 (Illumina) and sequenced in a HiSeq 2500 (Illumina). Sequenced reads were aligned to the human genome (hg19) using TopHat2(49) and gene expression levels were counted using HTseq(50) and normalized using quantile normalization. To avoid inflation of lowly-expressed genes among the genes called as differentially expressed, we applied a dynamic cut-off which takes into account that technical variation varies with expression level. Specifically, in the comparison between two conditions, we divided the genes into 20 bins according to their average expression level, and calculated the standard deviation (SD) of fold-change within each bin. Genes whose expression was changed by at least 1.75-fold and this fold-change was above the bin's 1.75 SD (dashed curve in Fig 1B and 3B) were called as differentially expressed. To further avoid false positive calls among lowly expressed genes we set a floor level of 5 counts (that is, any level below 5 was set to 5). Functional enrichment analysis was done using DAVID(51). Global characterization of pathways that were de-regulated upon knockdown of lncRNA-OIS1 was done using Gene Set Enrichment Analysis (GSEA)(52).

In situ hybridization

In situ hybridization was performed using double-FAM labeled LNA (locked nucleic acid) probes (Exiqon) as described previously(53). Briefly, cells were fixed, permeabilized and pre-hybridized in hybridization buffer and then hybridized at 55°C for 1 h with LNA probes for lncRNA-OIS1: 5-TTGAAAACCCATCACTCCT-3, or with a scramble probe 5-TGTAACACGTCTATACGCCCA-3 as negative control, all at 25 nM. Cells were subsequently incubated with 3% hydrogen peroxide to block potential endogenous peroxidase, and then probes were detected with peroxidase-conjugated anti-fluorescein-Ab (Roche applied Sciences) diluted 1:400 followed by addition of Cy3-labeled TSA substrate for 10 minutes (Perkin Elmer). All cells were mounted with ProLong®GoldAntifade Mountant containing DAPI nuclear stain (ThermoFisher Scientific). Images were acquired using a Zeiss Axio Imager Z1 epi-fluorescence microscope equipped with an AxioCamMRm CCD camera and a Plan-APOCHROMAT 63x/1.4 objective (Zeiss). Within the same experiment, images were acquired at the same exposure conditions.

BrdU proliferation assay

BJ and TIG3 Cells were pulsed for 3 h with 30 μ M bromodeoxyuridine (BrdU, Sigma), washed two times with PBS and then fixed with 4% formaldehyde, wash two times with PBS and treated with 5M HCl/0.5% Triton to denature DNA and neutralized with 0.1M $\text{Na}_2\text{B}_4\text{O}_7$, incubated with anti-BrdU (Dako) for 2 hours in RT after half hour blocking with 3% BSA in 0.5% Tween PBS, washed in blocking buffer (PBS, Tween 0.5%, 3% BSA) three times, and finally incubated with FITC-conjugated anti-mouse Alexa FLOUR 488 secondary antibody (Dako) for 1 hour, washed three times, stained with propidium iodide for half hour. BrdU incorporation was measured by immunofluorescence (at least 300 cells were scored for each condition).

Senescence-associated β -galactosidase assay

BJ and TIG3 cells were transduced with different shRNAs constructs, plated in triplicate and treated with 100 nM 4-OHT for 14 days. β -galactosidase activity was determined by using the kit (Cell Signaling), and at least 300 cells were analyzed for each condition.

Ribosome profiling (Ribo-seq)

BJ Cells were treated with cycloheximide (100 μ g/ml) for 5 minutes, and lysed 20 mM Tris-HCl, pH 7.8, 100 mM KCl, 10 mM MgCl_2 , 1% Triton X-100, 2 mM DTT (dithiothreitol), 100 μ g/ml cycloheximide, 1X complete protease inhibitor. Lysates were centrifuged at 1,300g and the supernatant was treated with 2 U/ μ l of RNase I (Invitrogen) for 45 min at room temperature. Lysates were fractionated on a linear sucrose gradient (7% to 47%) using the SW-41Ti rotor at 36,000 rpm for 2h. Fractions enriched in monosomes were pooled and treated with proteinase K (Roche, Mannheim, Germany) in a 1% SDS solution. Released RNA fragments were purified using Trizol reagent

and precipitated in the presence of glycogen. For libraries preparation, RNA was gel-purified on a denaturing 10% polyacrylamide urea (7 M) gel. A section corresponding to 30 to 33 nucleotides, the region where most of the ribosome-protected fragments are comprised, was excised, eluted and ethanol precipitated. The resulting fragments were 3'-dephosphorylated using T4 polynucleotide kinase (New England Biolabs Inc. Beverly, MA, USA) for 6 h at 37°C in 2-(N-morpholino) ethanesulfonic acid (MES) buffer (100 mM MES-NaOH, pH 5.5, 10 mM MgCl₂, 10 mM β-mercaptoethanol, 300 mM NaCl). 3' adaptor was added with T4 RNA ligase 1 (New England Biolabs Inc. Beverly, MA, USA) for 2.5 h at 37°C. Ligation products were 5'-phosphorylated with T4 polynucleotide kinase for 30 min at 37°C. 5' adaptor was added with T4 RNA ligase 1 for 18 h at 22°C. The library was sequenced in illumina HiSeq2000 machine. The data was analysed as described(54).

GRO-seq

Briefly, 5×10^6 nuclei were isolated and incubated 5 min at 30 °C with equal volume of reaction buffer (10 mM Tris-Cl pH 8.0, 5 mM MgCl₂, 1 mM DTT, 300 mM KCL, 20 units of SUPERase In, 1% sarkosyl, 500 μM adenosine triphosphate (ATP), (Guanosine triphosphate) GTP and Br-Uridine triphosphate (UTP), 0.2 μM CTP+32P Cytidine triphosphate (CTP) for the nuclear run-on. The reaction was stopped and total RNA was extracted with Trizol LS (Invitrogen) according to the manufacturer's instructions. RNA was fragmented using fragmentation reagents (Ambion) and the reaction was purified through p-30 RNase free spin column (BioRad). BrU-labeled RNA was immunoprecipitated with anti-BrdU agarose beads (Santa Cruz), washed one time in binding buffer, one time in low salt buffer (0.2× SSPE, 1 mM EDTA, 0.05% Tween-20), one time high-salt buffer (0.25× SSPE, 1 mM EDTA, 0.05% Tween-20, 137.5 mM NaCl) and two times in TET buffer (TE with 0.05% Tween-20). RNA was eluted with elution buffer (20 mM DTT, 300 mM NaCl, 5 mM Tris-Cl pH 7.5, 1 mM EDTA and 0.1% SDS) and isolated with Trizol LS. After the binding step, BrU-labeled RNA was treated with tobacco acid pyrophosphatase (TAP, Epicenter) to remove 5'-methyl guanosine cap, followed by T4 polynucleotide kinase (PNK; NEB) to remove 3'-phosphate group. BrU-containing RNA was treated with T4 PNK again at high pH in the presence of ATP to add 5'-phosphate group. The reaction was stopped and RNA was extracted with Trizol LS. Sequencing libraries were prepared using TruSeq Small RNA kit (Illumina) following manufacturer's instructions. Briefly, end-repaired RNA was ligated to RNA 3' and 5' adapters, followed by RT-PCR amplification. cDNA was purified using Agencourt AMPure XP (Beckman Coulter) and amplified by PCR for 12 cycles. Finally, amplicons were cleaned and size-selected using Agencourt AMPure XP (Beckman Coulter), quantified in a Bioanalyzer 2100 (Agilent), and sequenced in a HiSeq 2500 (Illumina). Sequenced reads were aligned to the human genome (hg19) using bowtie2(55).

RNA isolation, reverse-transcription and quantitative real-time PCR (qPCR)

Total RNA was extracted by using TRIsure (Bioline) reagent and following the manufacturer's protocol. cDNA was produced with SuperScript III (Invitrogen) using 4 µg of total RNA per reaction. qPCR reaction was performed with SYBR green I Master mix in a LightCycler 480 (Roche). Primers used in qPCR are listed in Supplementary Table S5.

Western blot analysis

Whole-cell lysates were prepared as previously described(56). Membranes were immunoblotted with the following antibodies: CDKN1A (Sc-397, Santa Cruz; 1: 1,000), HRAS (C-20, Santa Cruz; 1: 1,000), DPP4 (ab28340, abcam; 1: 2,000), GAPDH (Sc-47724, Santa Cruz; 1: 5,000). Protein bands were visualized using corresponding secondary antibodies (Dako) and ECL reagent (GE Healthcare).

Chromosome conformation capture combined with sequencing (4C-seq)

Briefly, BJ cells were treated with or without 4-OHT for 14 days and 10⁷ of cells for each condition were harvested and we performed 4C as previously described(57). An adapted two-step 4C-PCR was performed as previously described(58) to introduce template specific indexes. We had two viewpoints and used the following primers in the first PCR:

vp1_forward

AATGATACGGCGACCAACCGAGATCTACACTCTTTCCCTA-
CAGACGCTCTTCCGATCTCTTTGCTACTCTGTGAGATC

vp1_reverse

ACTGGAGTTCAGACGTGTGCTCTTCCGATCTATAGGGCTCTGGAGTCAG

vp2_forward

AATGATACGGCGACCAACCGAGATCTACACTCTTTCCCTA-
CAGACGCTCTTCCGATCTGTATTTCTCTAGCTGGGATC

vp2_reverse

ACTGGAGTTCAGACGTGTGCTCTTCCGATCAACCGTAAAGTCTTCGCTC

We used the forward primers from the first PCR and combined the following reverse primers for the second PCR:

BJ – 4-OHT rep1

CAAGCAGAAGACGGCATACGAGAT CGTGAT GTGACTGGAGTTCAGACGT-
GTGCT

BJ– 4-OHT rep2

CAAGCAGAAGACGGCATAACGAGAT GCCTAA GTGACTGGAGTTCAGACGT-
GTGCT

BJ + 4-OHT rep1

CAAGCAGAAGACGGCATAACGAGAT GGAACGT GTGACTGGAGTTCAGACGT-
GTGCT

BJ + 4-OHT rep2

CAAGCAGAAGACGGCATAACGAGAT GCGGAC GTGACTGGAGTTCAGACGT-
GTGCT

LncRNA-OIS1 expression analysis in tumors

Gene expression data was obtained from the TCGA Data Portal (<https://tcga-data.nci.nih.gov>). We selected those cancer types with transcriptome data available for at least five normal and five tumor samples, belonging to phenotypes “solid tissue normal” and “primary solid tumor”, respectively. Lowly expressed genes (genes with raw read counts in less than half the normal samples and half the tumor samples) were removed within each cancer type data. Differential expression analysis was carried out with R/Bioconductor package limma(59) using voom normalization(60). Pearson correlation calculation was carried out using normalized gene expression values, also in R/Bioconductor.

RESULTS

Genome-wide identification of lncRNAs responsive to OIS

To identify lncRNAs with a role in OIS, we used the model of primary human BJ fibroblasts expressing hTERT and 4-OH-tamoxifen (4-OHT)-inducible oncogenic H-Ras^{V12} (BJ/ET/Ras^{V12}ER cells) (48). RNA sequencing (RNA-seq) in senescent cells and non-senescent control cells revealed senescence-associated differentially expressed transcripts (Fig. 1B). Of those transcripts, we found 34 and 6 lncRNAs upregulated and downregulated respectively during OIS (Supplementary Table S1). Ribosome profiling confirmed the non-coding nature of these RNAs (Fig. 1C). We also confirmed by qRT-PCR the induction of some lncRNAs following H-Ras^{V12} induction (Supplementary Fig. S1A).

A focused loss-of-function screen for lncRNAs required for OIS identifies lncRNA-OIS1.

To examine possible causal roles for lncRNAs in OIS, we developed RNAi tools to target the 40 lncRNAs that were differentially expressed in OIS. We generated a pooled library consisting of 5 different shRNAs against each lncRNA, and included 4 non-

targeting shRNAs as negative controls, as well as two positive control shRNAs targeting BRD7— a gene identified as a tumour suppressor in OIS(48)(Supplementary Table S2). We transduced cells with three independent retroviral pools of the shRNAs library, and following puro selection harvested half of each cell population as control (T0, Time 0). We cultured the rest of the cells with 4-OHT treatment for 4 weeks, then harvested the cells (T4, Time 4weeks) and performed next-generation sequencing to identify shRNAs enriched in the final populations (T4) compared to the initial (T0) pool (Fig. 1D).

Our screen detected the positive control shRNAs against BRD7, as well as few shRNAs targeting different lncRNAs enriched in the RAS-induced cell populations, suggesting that the knockdown of these lncRNAs conferred a growth advantage in BJ/ ET cells expressing Ras^{V12} (Fig. 1E). For further validation, we selected two hits: lncRNA#32, which has one shRNA (shRNA3) at the top of the enrichment list in all three replicates, and another shRNA (shRNA2) giving minor enrichment; and lncRNA#30 with two shRNAs (shRNA5 and shRNA3) showing consistent enrichment in all three replicates (Fig. 1E and Supplementary Table S3). We validated the hits by repeating the OIS experiment using individual shRNAs. We used an shRNA targeting BRD7 (BRD7_shRNA4) as a positive control, and two non-targeting shRNA as negative controls. A proliferation assay (using BrdU labelling) indicated bypass of oncogene-induced cellular arrest by one shRNA (#30-5) targeting lncRNA#30 and two shRNAs (#32-2 and #32-3) targeting lncRNA#32 (Fig. 2A and Supplementary Fig. S2A). To further examine the effect of loss-of lncRNA#30 and #32 in OIS, we measured the induction of senescence-associated β -galactosidase (SA- β -Gal). In comparison with negative control cells, a marked decrease in SA- β -Gal was observed in Ras^{V12}-expressing BRD7-knockdown (BRD7 kd), lncRNA#30-5 and lncRNA#32-2 and #32-3 cells (Fig. 2B and supplementary Fig. S2B). In contrast, shRNA (#30-3) was not validated as expected from the screen outcome. Interestingly, RNA expression analysis indicated that only shRNAs #30-5, #32-2 and #32-3 were effective towards their lncRNA targets, suggesting on-target activity (Fig. 2C, 2D). To exclude off-target effects of the shRNAs, we designed additional vectors targeting lncRNA#30 and #32 (Supplementary Table S6), and repeated the proliferation and SA- β -Gal assays. This experiment identified more functional shRNAs (#32-8, #32-9) targeting lncRNA#32, but no additional shRNAs targeting lncRNA#30 (Fig. 2E, 2F and supplementary Fig. S3A, S3B). qRT-PCR confirmed loss-of expression of lncRNA#32 by all four active shRNA vectors (#32-2, 3, 8 and 9) (Fig. 2H). In contrast, two new shRNAs (#30-8, #30-9) showed efficient loss-of lncRNA#30 (Fig. 2G) but did not induce bypass of OIS (Fig. 2E, 2F and supplementary Fig. S3A, S3B), indicating that the bypass of OIS by shRNA#30-5 was not mediated by its targeted lncRNA. Altogether, these results demonstrate that lncRNA#32 is both induced by oncogenic RAS and is required for the establishment of the OIS phenotype.

To further solidify the role of lncRNA#32 in OIS we made use of a dual CRISPR-Cas9 system(61), and induced deletions of the lncRNA#32 locus. As BJ cells do not form single clones, generation of monoclonal population of deleted cells was not possible. Instead, we performed a functional genetic experiment to test whether the cells containing the lncRNA#32 deletion are enriched in cells undergoing OIS. Notably, supplementary Fig. S4A shows that control-transduced BJ cells completely senesced, p53 knockout BJ cells strongly bypassed OIS, and targeting lncRNA#32 attenuated senescence, albeit to a lesser extent than p53KO. To confirm that the dual CRISPR-Cas9 system triggered deletion of lncRNA#32, we isolated genomic DNA and performed semi-quantitative PCR to detect lncRNA#32 with oligos (FW: TGGAGGGCTGAATCATCAAGTT, REV: ACTTCAAAGGGCAATTGCTGAAC) surrounding the CRISPR-target region. While wild type and control-transduced cells produced only one band of about 1.8Kb, cells transduced with the lncRNA#32-targeting vector showed lncRNA#32 deleted bands (~ 350bp), indicating the functionality of the CRISPR vector (Supplementary Fig. S4B). Intriguingly, the PCR signal of the deletion band increased after 2 and 3 weeks following OIS induction, in line with a bypass of the OIS phenotype. In comparison, no enrichment of the deleted allele was noted following 3 weeks of culturing without induction of OIS (Supplementary Fig. S4B). This indicates that lncRNA#32 deletion gives growth advantage only under OIS conditions. As expected, we found by qRT-PCR that cells expressing sgRNAs targeting lncRNA#32 have reduced level of lncRNA#32 (Supplementary Fig. S4C). Sanger sequencing confirmed the correct deletion of lncRNA#32 (Supplementary Fig. S4D). For simplicity and in conjunction with its function, we hereafter refer to lncRNA#32 as lncRNA-OIS1.

To extend our finding on the role of lncRNA-OIS1 in OIS we employed a different cell system. We transduced all four functional shRNAs targeting lncRNA-OIS1 (#32-2, 3, 8 and 9, which we renamed KD1, 2, 3, and 4, respectively) into TIG3 cells expressing hTERT and 4-OH-tamoxifen (4-OHT)-inducible oncogenic H-Ras^{V12}, and repeated the BrdU labelling and SA- β -Gal experiments. First, q-RT-PCR and GRO-seq analysis indicated up-regulation of lncRNA-OIS1 following oncogenic RAS induction (Supplementary Fig. S5E, S9A). Second, as expected, the introduction of all four lncRNA-OIS1 shRNAs reduced lncRNA-OIS1 expression (Supplementary Fig. S5E). Last, and most profoundly, all four lncRNA-OIS1 shRNAs very effectively bypassed OIS as measured by the proliferation and senescent assays BrdU and SA- β -Gal, respectively (Supplementary Fig. S5A, S5B, S5C, S5D). Altogether, our results demonstrate that intact lncRNA-OIS1 is required for senescence induction following RAS^{V12} activation in primary human cells.

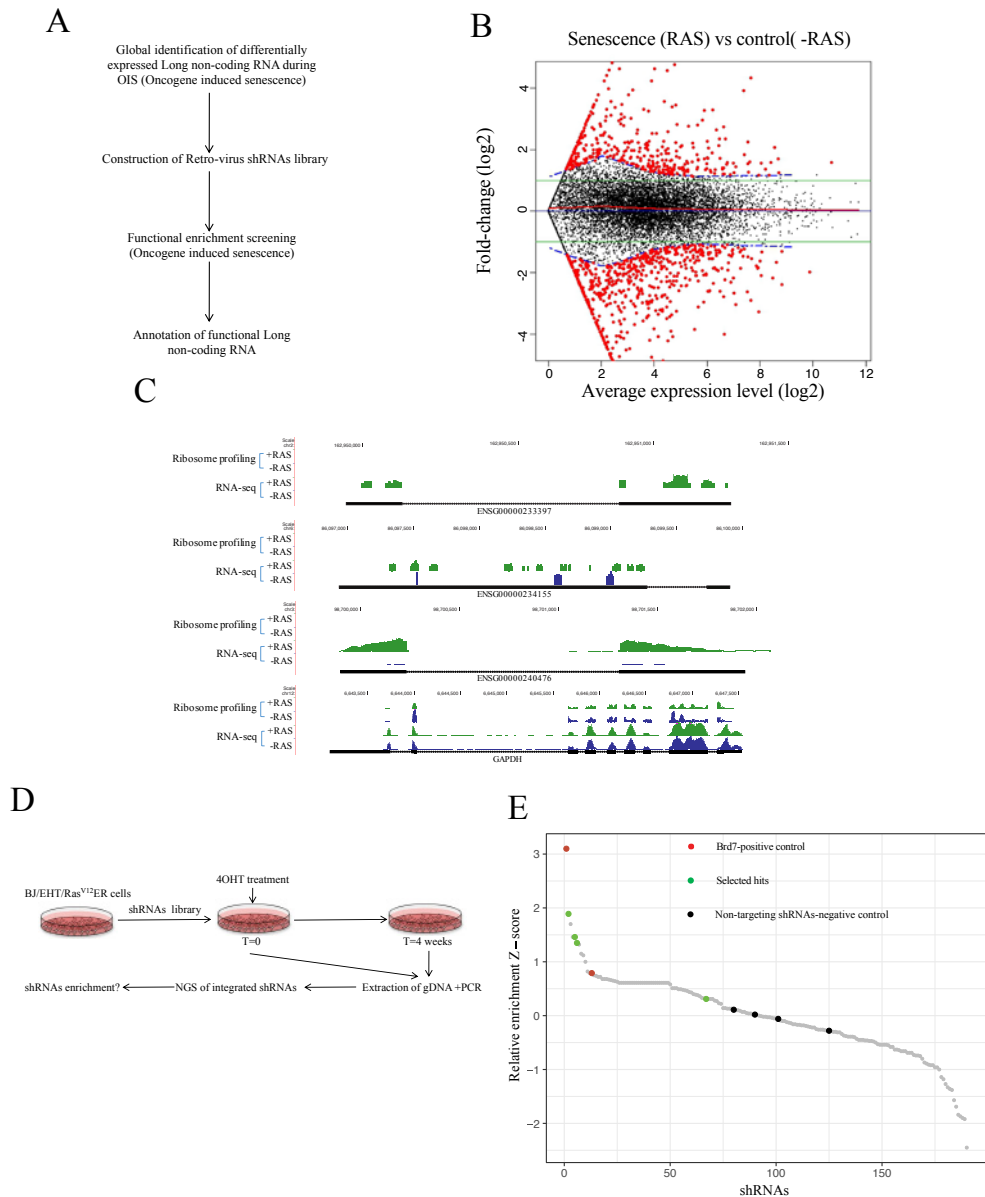


Figure I. shRNAs screen identifies a lncRNA required for OIS.

(A) A screening strategy of detecting functional lncRNAs. (B) RNA-seq comprehensively identified differentially expressed transcripts (mRNAs and long non-coding RNAs) in senescent cells (treated with 4-OHT for 14 days) compared to untreated cells. (C) Ribosome profiling confirmed that the identified OIS lncRNAs have no protein coding capacity. Shown are selected examples and GAPDH as control. (D) The functional genetic screen procedure. NGS, next-generation sequencing. (E) Enrichment score calculated for each shRNA vector based on its prevalence in the pool, harvested after 4 weeks of tamoxifen (4-OHT) treatment (RAS^{V12} induction), relative to its prevalence in the T0 pool. The plot shows the distribution of standardized enrichment scores (Z-scores) for the entire shRNA library.

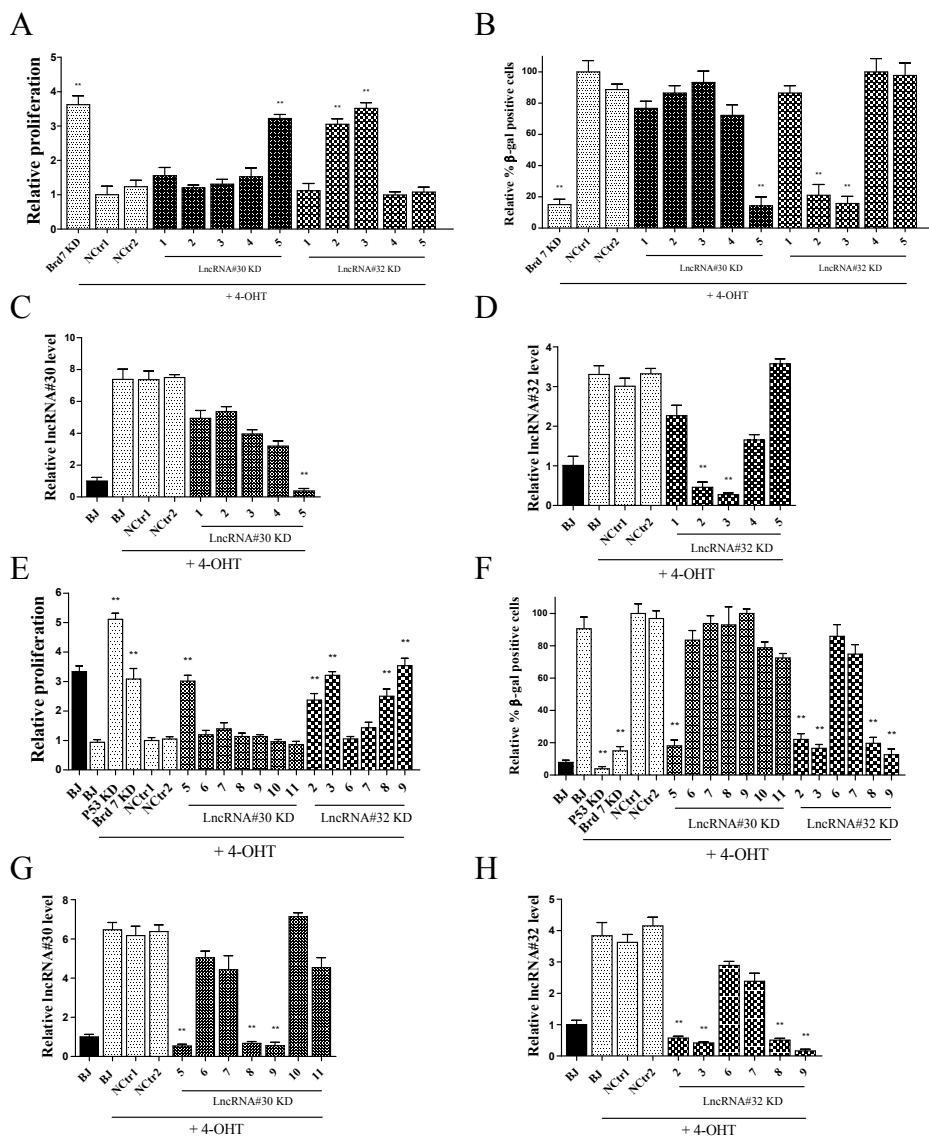


Figure 2. Functional validation of selected lncRNAs.

(A) The proliferation of the various shRNA-transduced BJ-RAS^{v12} cells was quantified using BrdU assay, $**P < 0.0005$, two-tailed Student's t-test. For every condition, the percentage of BrdU-positive cells was normalized to negative control cells. (B) Senescent cells were quantified using SA- β -gal assay, $**P < 0.0005$, two-tailed Student's t-test. For every condition, the percentage of β -gal-positive cells was normalized to negative control cells. (C, D) qRT-PCR analysis of lncRNA#30 and #32 in the various shRNA-transduced cells treated with 4-OHT relative to untreated cells. Data were normalized to a housekeeping gene and the levels in untreated cells set to 1, $**P < 0.0005$, two-tailed Student's t-test. (E, F) Validation of additional shRNA-transduced BJ-RAS^{v12} cells was performed as in panel A and B. BrdU ($**P < 0.001$) and SA- β -gal assay ($**P < 0.0005$) were quantified by two-tailed Student's t-test. (G, H) qRT-PCR analysis of lncRNA #30 and #32 in the shRNA-transduced cells presented in E and F. Data were normalized to a housekeeping gene and the levels in untreated cells set to 1, $**P < 0.0005$, two-tailed Student's t-test.

Knockdown of lncRNA-OIS1 abolishes OIS gene expression signature

Next, we sought to explore the mode of action of lncRNA-OIS1 in senescence. To this goal, we first performed RNA-seq of cells transduced with shRNAs against lncRNA-OIS1, the positive controls p53 and BRD7, and negative controls (Fig. 3A). Comparison of gene expression profiles in negative controls and p53kd cells upon activation of oncogenic RAS (the former enters senescence while the latter bypasses it) identified 885 differentially-expressed genes (386 up- and 499 down-regulated in senescent cells) (Fig. 3B). Functional enrichment analysis showed that the set of genes whose expression was significantly repressed in senescent cells (compared to the p53kd cells) was markedly enriched for cell-cycle related genes (Fig. 3C), reflecting the strong proliferation arrest that is imposed in negative control cells upon oncogenic stress. This sharp down-regulation of cell-cycle genes defines a molecular signature that characterizes the induction of the senescent physiological state. Remarkably, knocking-down lncRNA-OIS1 significantly abolished the repression of these genes (Fig. 3D). The effect observed for lncRNA-OIS1-kd was comparable to the effect obtained by BRD7-kd but weaker than the effect elicited by p53-kd (Fig. 3D). In accordance with the phenotypic effect of OIS-bypass, we observed that lncRNA-OIS1-kd resulted in attenuation of the induction of CDKN1A (p21), a prime target of p53 that is required for OIS in BJ cells (55)(Supplementary. S6A). We confirmed this result at the protein level using western blot analysis (Fig. 3E and supplementary Fig. S6B). We included one shRNA (#32-6) which did not give knockdown of lncRNA-OIS1 and showed no bypass of the senescence phenotype (Fig. 3E and supplementary Fig. S6B) to demonstrate specificity of the decreased expression of CDKN1A due to lncRNA-OIS1-kd.

To further characterize the effect of knocking-down lncRNA-OIS1 on the cellular transcriptome, we systematically compared, using GSEA analysis(52), gene expression profiles in cells induced for oncogenic RAS, and transduced either with shRNAs against lncRNA-OIS1 or with non-targeting shRNAs. As expected from the phenotypic effect and inline with the above analysis, the strongest gene sets that were up-regulated upon knocking-down lncRNA-OIS1 were related to proliferation and cell-cycle (Supplementary Fig. S6C). A set of genes that are induced in response to ionizing irradiation (IR) was the most significantly down-regulated gene set in the lncRNA-OIS1 kd cells. This set contains numerous p53 direct target genes, indicating that attenuated expression of lncRNA-OIS1 compromises the activation of the p53 network (Supplementary Fig. S6C). In addition, genes of the oxidative phosphorylation pathway are down-regulated too in the lncRNA-OIS1 kd cells. Notably, all these gene sets show the opposite response in cells that enter senescence in response to oncogenic stress (Supplementary Fig. S6C), demonstrating that loss of lncRNA-OIS1 abolishes OIS gene expression signature.

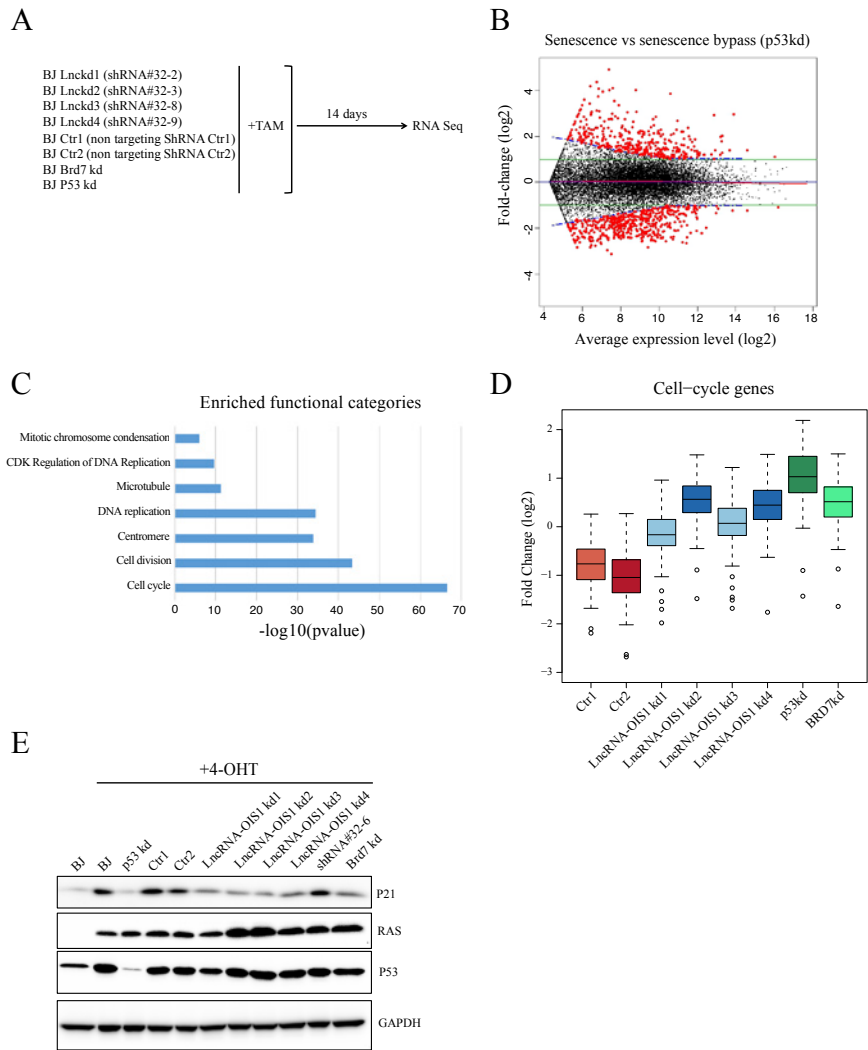


Figure 3. LncRNA-OIS1 knockdown shows a gene expression signature characteristic of senescence bypass.

(A) A scheme of the RNA-seq experiment. RNA was collected from positive and negative control cells, and the various LncRNA-OIS1kd cells treated with 4-OHT for 14 days. Cells knocked-down for p53 and BRD7 served as positive controls. (B) The comparison of gene expression profiles between p53kd and negative control cells, both treated with 4-OHT to induce oncogenic RAS, identified 885 differentially expressed genes. 386 and 499 genes were up- and down-regulated, respectively. (C) Enriched functional categories in the set of genes that were downregulated in the senescent cells. As expected, the enriched categories are related to cell proliferation and cell division. (D) For each of the conditions that we examined, we calculated the distribution of fold-change of expression for the set of 135 cell-cycle genes whose expression is down-regulated in senescence, relative to their expression in control untreated cells. In control cells, 4-OHT treatment resulted in strong suppression of this set of genes (Ctrl1, Ctrl2 samples). In contrast, in LncRNA-OIS1-kd cells, the expression of these cell-cycle genes was elevated compared to control cells. Notably, the effect observed in LncRNA-OIS1kds was similar to the effect of BRD7, but, as expected, weaker than that of the p53kd. (E) CDKN1A protein levels examined by western blotting.

Loss-of lncRNA-OIS1 compromises the induction of DPP4 by OIS

To investigate the mechanism(s) by which lncRNA-OIS1 affects OIS induction, we first examined its subcellular localization. In control BJ/ET/Ras^{V12}ER cells, lncRNA-OIS1 was located both in the nucleus and the cytosol. Following RAS^{V12} activation, lncRNA-OIS1 maintained a similar pattern in these two compartments (Fig. 4A). In situ hybridization (ISH) analysis confirmed lncRNA-OIS1 increased expression following RAS^{V12} induction, and its localization in the nucleus and cytosol. Loss-of lncRNA-OIS1 confirmed the specificity of the signal to lncRNA-OIS1 (Fig. 4B).

LncRNAs can impact the expression of nearby genes on the chromatin (Cis function), or affect gene expression in trans (for example by controlling mRNA transcription, splicing, and translation). We therefore firstly interrogated whether lncRNA-OIS1 functions in trans, and whether ectopic expression of lncRNA-OIS1 can drive cells into senescence without RAS induction. We over-expressed lncRNA-OIS1 in primary BJ cells (full length or exons; Supplementary Fig. S7A), but observed no induction of senescence as measured by BrdU labelling and SA- β -Gal assays (Supplementary Fig. S7B, S7C, S7D). Secondly, we overexpressed lncRNA-OIS1 (both full length and exons) in lncRNA-OIS1-kd cells to test whether ectopic expression of lncRNA-OIS1 can restore the senescence phenotype. However, despite the high expression of lncRNA-OIS1 (Supplementary Fig. S8A), OIS-bypass by lncRNA-OIS1-kd was maintained (Supplementary Fig. S8B, S8C, S8D). These data indicated that lncRNA-OIS1 does not function in trans, rather, a localized expression and effect on neighbouring genes is required (cis effect).

In general, lncRNAs can be physically linked to the locus from which they are encoded, and exert its function during transcription without the need for processing or shuttling. Well-studied examples of cis-acting lncRNAs are those that cause X-inactivation(62)(63). Examples of other cis-regulatory lncRNAs include ncRNA-a1-7, Hottip, and Mistral, the perturbation of which lead to decreased expression of nearby genes(64)(65)(66)(67), suggesting that gene regulation in cis is a very important mode of lncRNA action. To investigate whether lncRNA-OIS1 expression influences nearby genes, we analysed Global Run-On Sequencing data (GRO-Seq) of senescent and proliferation BJ cells(55). We observed that both lncRNA-OIS1 and its nearby gene DPP4 were increased in the BJ cells upon RAS induction (Fig. 4C). We also observed the same effect in TIG3 cells (Supplementary Fig. S9A). Additionally, loss-of lncRNA-OIS1 abolished the activation of DPP4 following oncogene induction based on BJ cells RNA-seq data (Supplementary Fig. S9B). We solidified these results by qRT-PCR (Fig. 4D and supplementary Fig. S9C) and chose the best two lncRNA-OIS1 knockdowns (KD2 and 4) for western blot analyses of DPP4 expression four days following RAS^{V12} induction, before the cell cycle is arrested and senescence is established (Fig. 4D, E). Indeed, attenuated activation of DPP4 protein expression was obtained in cells with lncRNA-OIS knockdown. A similar effect was also observed in TIG3 lncRNA-OIS1-kd cells 4

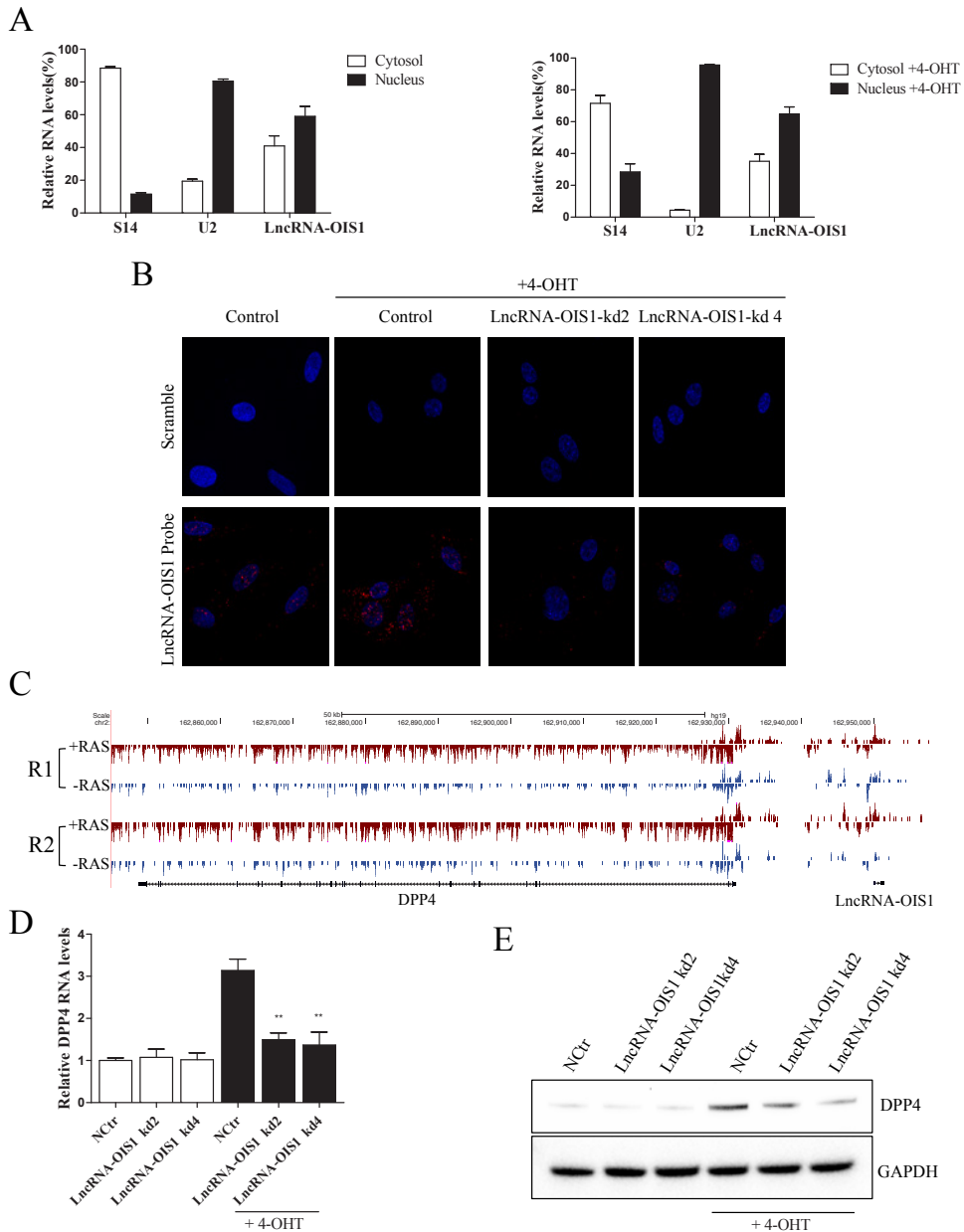


Figure 4. LncRNA-OISI expression is required for the activation of DPP4 in response to oncogenic stress.

(A) Subcellular localization of lncRNA-OIS1 in BJ cells treated with or without 4-OHT. U2 and S14 RNAs were used as controls for nucleus and cytosol fractions, respectively. (B) In situ hybridization of lncRNA-OIS1 in BJ cells treated with or without 4-OHT. (C) Screenshots of GRO-seq data of the lncRNA-OIS1 and DPP4 genomic locus. R1 and R2 are two biological replicates. (D) qRT-PCR analysis of DPP4 expression upon lncRNA-OIS1kd treated with or without 4-OHT, **P < 0.002, two-tailed Student's t-test. (E) DPP4 protein levels examined by western blotting.

days following RAS^{V12} induction (Supplementary Fig. S9D). Altogether, these data link lncRNA-OIS1 to regulation of DPP4 expression and to the senescent phenotype induced by oncogenic RAS.

Loss-of DPP4 bypasses OIS

Interestingly, it has been reported that DPP4 is a tumor suppressor in melanoma (68)(69), non-small cell lung cancer (70), ovarian cancer(71)(72)(73), endometrial carcinoma(74), prostate cancer(75), neuroblastoma(76), and glioma(77). We therefore hypothesized that the tumour suppressive role of DPP4 is linked to OIS. To examine this issue, we generated shRNAs (Supplementary Table S7) transduced DPP4 knockdown BJ cells. qRT-PCR and western blot analyses confirmed significant reduction of DPP4 mRNA and protein levels upon knockdown (Fig. 5A, B).

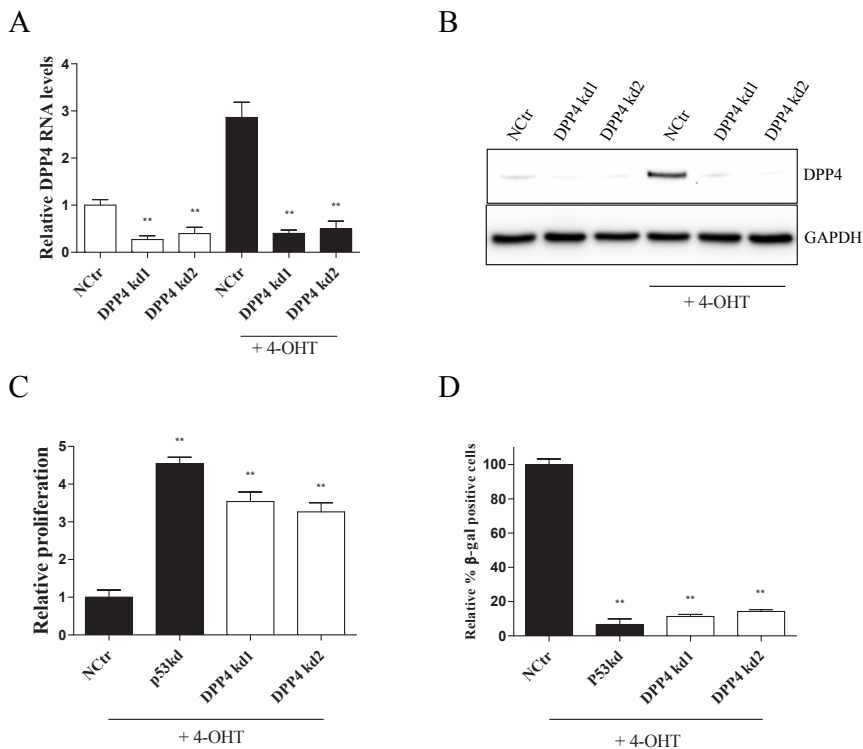


Figure 5. Induction of DPP4 is required for OIS.

(A) qRT-PCR analysis of DPP4 expression upon DPP4 kd (two different shRNAs) treated with or without 4-OHT, **P < 0.005, two-tailed Student's t-test. (B) Western blot analysis of DPP4 protein. (C) BrdU proliferation analysis of DPP4 kd BJ-RAS^{V12} cells, **P < 0.0005, two-tailed Student's t-test. The percentage of BrdU-positive cells was normalized to negative control cells. (D) Senescence SA-β-gal assay. **P < 0.0005, two-tailed Student's t-test. The percentage of β-gal-positive cells was normalized to negative control cells.

As predicted, loss-of DPP4 bypassed OIS, as determined by proliferation and SA- β -Gal assays (Fig. 5C, D and supplementary Fig. S9E). Next, we examined whether lncRNA-OIS1 regulates senescence through DPP4. We cloned DPP4 in a lentiviral vector, ectopically-expressed it in lncRNA-OIS1-kd cells, and induced OIS. Intriguingly, proliferation (BrdU labelling) and SA- β -Gal assays demonstrated that ectopic expression of DPP4 abolished the senescence bypass phenotype of lncRNA-OIS1-kd cells, while a control vector did not (Figure. 6A, 6B and supplementary Fig. S10A, S10B). We confirmed the overexpression of DPP4 by western blot (Figure. 6C and supplementary Fig. S10C). These experiments indicate that DPP4 is the relevant target gene of lncRNA-OIS1 during OIS, and that lncRNA-OIS1 is a major determinant of DPP4 function in OIS.

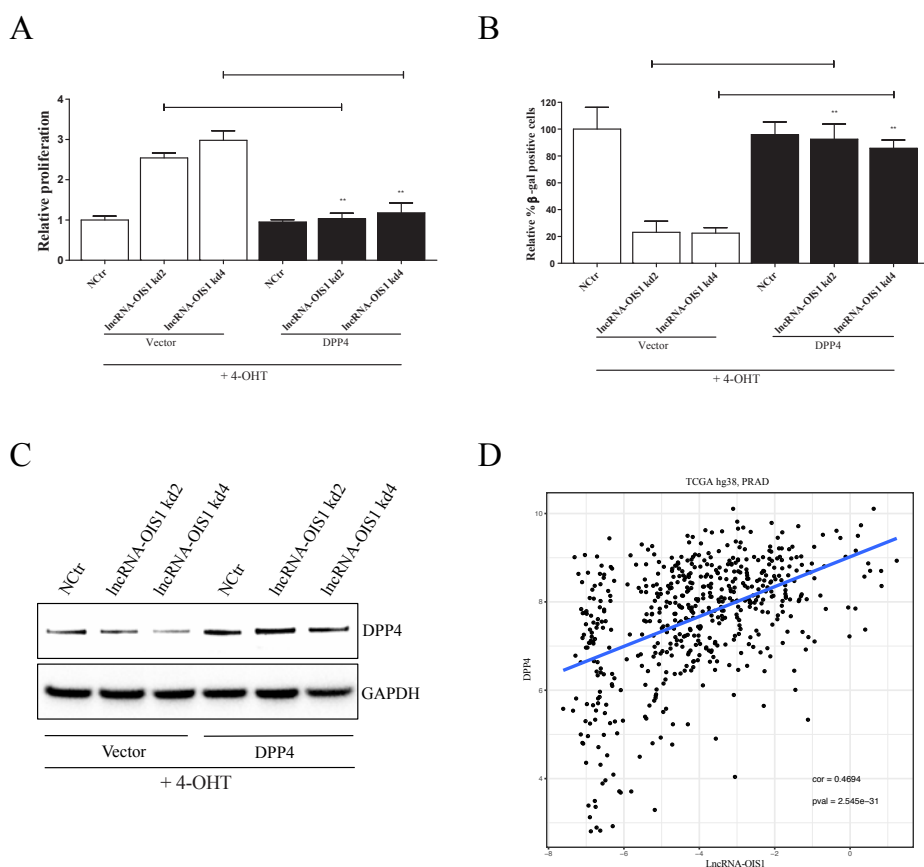


Figure 6. Ectopic expression of DPP4 induces senescence in lncRNA-OIS1 kd cells.

(A) BrdU proliferation assay of DPP4 or vector-transduced BJ-RAS^{v12}-lncRNA-OIS1kd cells. ** $P < 0.001$, two-tailed Student's t-test. The percentage of BrdU-positive cells was normalized to negative control cells. (B) SA- β -gal assay. ** $P < 0.001$, two-tailed Student's t-test. The percentage of β -gal-positive cells was normalized to negative control cells. (C) Western blot analysis of DPP4 protein. (D) TCGA data analysis of lncRNA-OIS1 and DPP4 expression in prostate adenocarcinoma (PRAD) samples ($r = 0.469$, $p\text{value} = 2.5e^{-31}$).

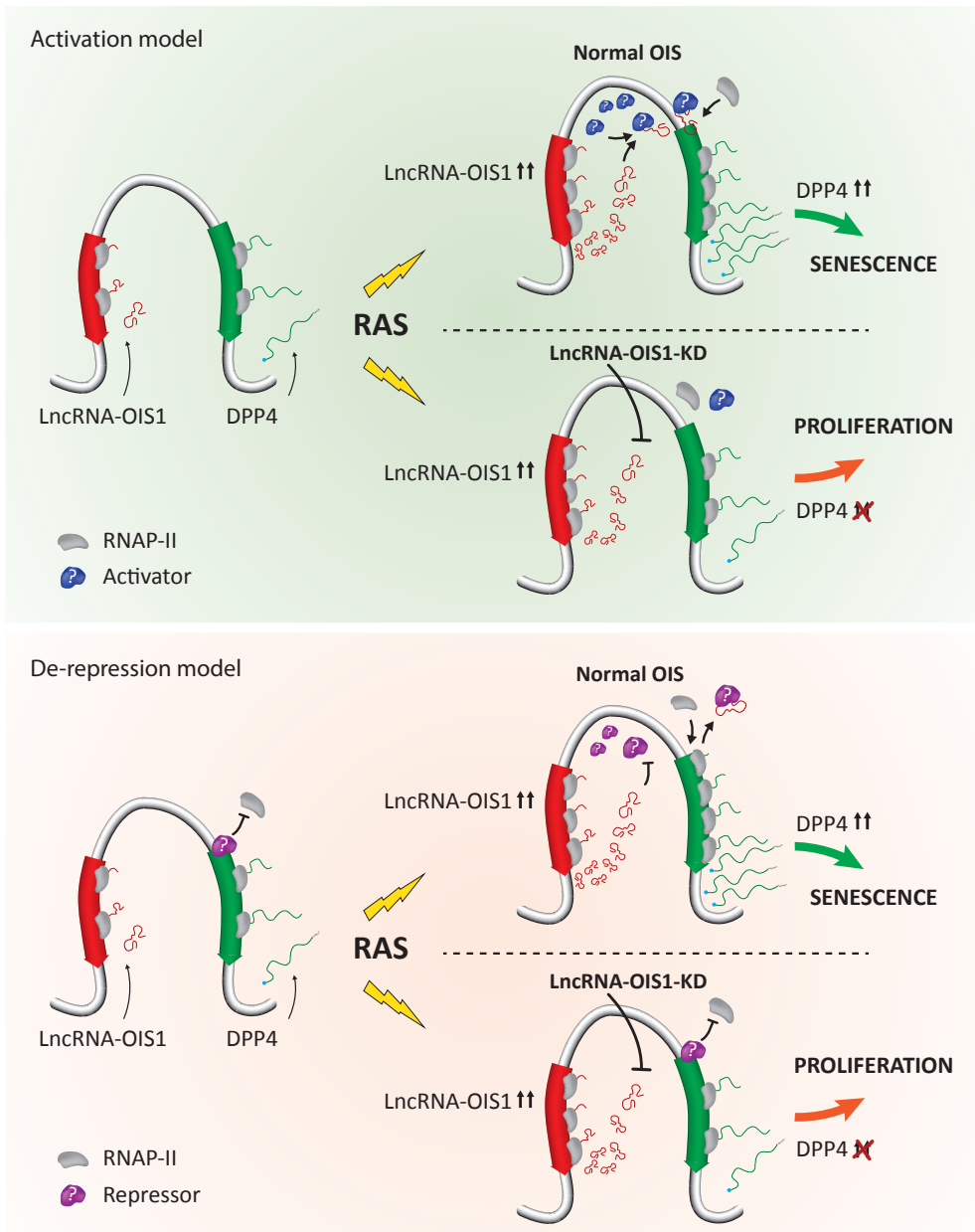


Figure 7. Schematic representation of LncRNA-OIS1 function in normal and senescence conditions.

Association of LncRNA-OIS1 and DPP4 in the tumors

Last, we interrogated LncRNA-OIS1 expression in tumors and its correlation with that of DPP4 by analysing TCGA data. LncRNA-OIS1 is very lowly expressed in most tumor types (Supplementary Fig. S11A). We plotted the read counts of the LncRNA-OIS1 among

normal and tumor samples, indicating in each type the number of samples with at least 1 read count for lncRNA-OIS1. Interestingly, prostate adenocarcinoma (PRAD) samples showed clear lncRNA-OIS1 expression. Using this dataset for differential expression analysis, we observed no change between tumor and normal samples (empirical Bayes test, $B = -5.79$, $p\text{value} = 0.28$) (Supplementary Table S4), but a significant positive correlation between lncRNA-OIS1 and DPP4 expression in the tumor samples ($r = 0.469$, $p\text{value} = 2.5e^{-31}$) (Figure. 6D), suggesting that at least in PRAD DPP4 expression is controlled by lncRNA-OIS1.

Discussion

Over the past few years, numerous lncRNAs have been discovered and characterized as critical factors in physiological and pathological processes. However, the role of lncRNAs in oncogene-induced senescence (OIS) remained unexplored. Here, we contribute to the understanding of the function of lncRNAs by describing a role of lncRNA-OIS1 in cellular senescence provoked by the expression of oncogenic RAS (OIS). Upregulation of lncRNA-OIS1 following OIS was required for the induction of DPP4, a well-described gene with tumour suppressive activity. Differential gene expression analyses of lncRNA-OIS1 knockdown cells indicated attenuated activation of CDKN1A following OIS induction, and confirmed changes in cell cycle regulatory genes favouring cellular proliferation. Gene complementation experiments indicated that DPP4, a lncRNA-OIS1 neighboring gene, is the downstream target of lncRNA-OIS1 in senescence. Exactly how DPP4 affects CDKN1A and cell cycle genes, and how lncRNA-OIS1 controls DPP4 expression, remains to be uncovered. Nevertheless, we describe here an important function of lncRNAs with potentially influential implications in cancer biology.

OIS is a major senescence type and it poses a critical barrier to cancer. A recent study shown that the lncRNA-MIR31HG was a senescence modulator during BRAF-V600 induced senescence in TIG3 cells(46). It has also been shown that loss-of MIR31HG reduces cell growth and promotes a strong senescence phenotype through the regulation of the tumor suppressor P16^{INK4A}. Here, we add to this knowledge by identifying and characterizing the role of lncRNA-OIS1 in regulating senescence through the control of a nearby gene DPP4.

Interestingly, we also overexpressed lncRNA-OIS1 in BJ cells to examine whether high levels of the lncRNA-OIS1 can drive cells into senescence. However, we neither observed senescence-induction nor DPP4 was activated (Supplementary Fig. S7). Additionally, also the ectopic expression of lncRNA-OIS1 was not able to revert the bypass of senescence and the reduced DPP4 activation induced by lncRNA-OIS1 knockdown under OIS

(Supplementary Fig. S8). This is indicative of a cis function of lncRNA-OIS1. Indeed, we identified DPP4, a nearby gene to lncRNA-OIS1, as a key component of OIS. First, loss-of DPP4, similar to lncRNA-OIS1 loss, resulted in bypass of senescence (Figure. 5). Second, ectopic expression of DPP4 reverted the bypass of senescence induced by the loss-of lncRNA-OIS1 (Figure. 6A, 6B, 6C and supplementary Fig. S10). Additionally, a recent research found that DPP4 can regulate senescence in WI-38 cells, strongly supporting our observations(78). However, although both lncRNA-OIS1 and DPP4 genes reside in the same topologically associating chromatin domain (TAD) through a CTCF (CCCTC-binding factor) loop (Supplementary Fig. S12A), and chromatin loops can be identified in various ChIA-PET and Hi-C chromatin conformation capture datasets (Supplementary Fig. S12B), we did not observe a clear direct interaction of lncRNA-OIS1 locus with the promoter of DPP4 using 4C, a chromatin capture analysis technique, through two distinct view point sites (Supplementary Fig. S13A). Thus, how exactly the expression of DPP4 depends on lncRNA-OIS1 remains unclear. We speculate that lncRNA-OIS1 expression may be required to allow high chromatin accessibility to senescence-associated DPP4-activating transcription factors by directly recruiting essential transcription factors, or alternatively by counteracting chromatin-repressive components of the chromatin (Figure. 7). Nevertheless, our findings here elucidate the importance of lncRNA-OIS1 for eliciting a proper cellular response to the emergence of oncogenic stress.

Data availability

rNA-seq, Ribosome profiling (Ribo-seq), GRO-seq data are deposited in GEO DB (accession number GSE42509, GSE106414, GSE109290).

Supplementary data

Supplementary Data are available at NAR online.

Acknowledgement

We thank the China Scholarship Council for support. RNA Train supports our research and provides a great platform for training, learning, calibration. We thank all the members of the Agami group for helpful discussions. We thank Andrea Ventura for kindly providing the plasmid PX333 and all the reagents for lncRNA-OIS1 deletion. We also want to thank Jing Li (Cnkingbio Company) for helpful suggestions.

Funding

This work was supported by the China Scholarship Council (CSC) (to L.L.); ERC-AdG enhReg [322493 to R.A.]; ERC-ITN RNA TRAIN [607720 to R.A.]; Edmond J. Safrá Center for Bioinformatics Fellowship (to R.E.). The Human Frontier Science Program [LT000640/2013 to Alejandro Pineiro Ugalde]. Funding for open access charge: CSC; ERC-AdG enhReg [322493]; RNATrain [607720].

Conflict of interest statement. None declared.

References

1. Cabili,M., Trapnell,C., Goff,L., Koziol,M., Tazon-Vega,B., Regev,A. and Rinn,J.L. (2011) Integrative annotation of human large intergenic noncoding RNAs reveals global properties and specific subclasses. *Genes Dev.*, **25**, 1915–1927.
2. Djebali,S., Davis,C.A., Merkel,A., Dobin,A., Lassmann,T., Mortazavi,A., Tanzer,A., Lagarde,J., Lin,W., Schlesinger,F., *et al.* (2012) Landscape of transcription in human cells. *Nature*, **489**, 101–108.
3. Guttman,M., Russell,P., Ingolia,N.T., Weissman,J.S. and Lander,E.S. (2013) Ribosome profiling provides evidence that large noncoding RNAs do not encode proteins. *Cell*, **154**, 240–251.
4. Guttman,M., Amit,I., Garber,M., French,C., Lin,M.F., Feldser,D., Huarte,M., Zuk,O., Carey,B.W., Cassady,J.P., *et al.* (2009) Chromatin signature reveals over a thousand highly conserved large non-coding RNAs in mammals. *Nature*, **458**, 223–227.
5. Guttman,M., Donaghey,J., Carey,B.W., Garber,M., Grenier,J.K., Munson,G., Young,G., Lucas,A.B., Ach,R., Bruhn,L., *et al.* (2011) lincRNAs act in the circuitry controlling pluripotency and differentiation. *Nature*, **477**, 295–300.
6. Wapinski,O. and Chang,H.Y. (2011) Long noncoding RNAs and human disease. *Trends Cell Biol.*, **21**, 354–361.
7. Tsai,M.C., Spitale,R.C. and Chang,H.Y. (2011) Long intergenic noncoding RNAs: New links in cancer progression. *Cancer Res.*, **71**, 3–7.
8. Batista,P.J. and Chang,H.Y. (2013) Long noncoding RNAs: Cellular address codes in development and disease. *Cell*, **152**, 1298–1307.
9. Qureshi,I.A. and Mehler,M.F. (2012) Emerging roles of non-coding RNAs in brain evolution, development, plasticity and disease. *Nat Rev Neurosci*, **13**, 528–541.
10. Ghosal,S., Das,S. and Chakrabarti,J. (2013) Long Noncoding RNAs: New Players in the Molecular Mechanism for Maintenance and Differentiation of Pluripotent Stem Cells. *Stem Cells Dev.*, **22**, 2240–2253.
11. Lee,J.T. (2012) Epigenetic Regulation by Long Noncoding RNAs. *Science (80-.)*, **338**, 1435–1439.
12. Gong,C. and Maquat,L.E. (2011) lncRNAs transactivate STAU1-mediated mRNA decay by duplexing with 3' UTRs via Alu elements. *Nature*, **470**, 284–288.
13. Yoon,J.-H., Abdelmohsen,K. and Gorospe,M. (2013) Posttranscriptional Gene Regulation by Long Noncoding RNA. *J. Mol. Biol.*, **425**, 3723–3730.
14. Cesana,M., Cacchiarelli,D., Legnini,I., Santini,T., Sthandier,O., Chinappi,M., Tramontano,A. and Bozzoni,I. (2011) A long noncoding RNA controls muscle differentiation by functioning as a competing endogenous RNA. *Cell*, **147**, 358–369.
15. Bergmann,J.H. and Spector,D.L. (2014) Long non-coding RNAs: Modulators of nuclear structure and function. *Curr. Opin. Cell Biol.*, **26**, 10–18.
16. Petruk,S., Sedkov,Y., Riley,K.M., Hodgson,J., Schweisguth,F., Hirose,S., Jaynes,J.B., Brock,H.W. and Mazo,A. (2006) Transcription of bxd Noncoding RNAs Promoted by Trithorax Represses Ubx in cis by Transcriptional Interference. *Cell*, **127**, 1209–1221.
17. Zhao,J., Sun,B.K., Erwin,J.A., Song,J.-J. and Lee,J.T. (2008) Polycomb Proteins Targeted by a Short Repeat RNA to the Mouse X Chromosome. *Science (80-.)*, **322**, 750–756.

18. Melo,C.A., Drost,J., Wijchers,P.J., van de Werken,H., de Wit,E., Vrieling,J.A.F.O., Elkon,R., Melo,S.A., Léveillé,N., Kalluri,R., *et al.* (2013) ERNAs Are Required for p53-Dependent Enhancer Activity and Gene Transcription. *Mol. Cell*, **49**, 524–535.
19. Gupta,R.A., Shah,N., Wang,K.C., Kim,J., Horlings,H.M., Wong,D.J., Tsai,M.-C., Hung,T., Argani,P., Rinn,J.L., *et al.* (2010) Long non-coding RNA HOTAIR reprograms chromatin state to promote cancer metastasis. *Nature*, **464**, 1071–1076.
20. Tsai,M.-C., Manor,O., Wan,Y., Mosammaparast,N., Wang,J.K., Lan,F., Shi,Y., Segal,E. and Chang,H.Y. (2010) Long Noncoding RNA as Modular Scaffold of Histone Modification Complexes. *Science* (80-), **329**, 689–693.
21. Huarte,M., Guttman,M., Feldser,D., Garber,M., Koziol,M.J., Kenzelmann-Broz,D., Khalil,A.M., Zuk,O., Amit,I., Rabani,M., *et al.* (2010) A large intergenic noncoding RNA induced by p53 mediates global gene repression in the p53 response. *Cell*, **142**, 409–419.
22. Ulitsky,I. and Bartel,D.P. (2013) XlincRNAs: Genomics, evolution, and mechanisms. *Cell*, **154**.
23. Kornienko,A.E., Guenzl,P.M., Barlow,D.P. and Pauler,F.M. (2013) Gene regulation by the act of long non-coding RNA transcription. *BMC Biol.*, **11**, 59.
24. Hayflick,L. (1965) The limited in vitro lifetime of human diploid cell strains. *Exp. Cell Res.*, **37**, 614–636.
25. Kuilman,T., Michaloglou,C., Mooi,W.J. and Peeper,D.S. (2010) The essence of senescence. *Genes Dev.*, **24**, 2463–2479.
26. Serrano,M., Lin,A.W., McCurrach,M.E., Beach,D. and Lowe,S.W. (1997) Oncogenic ras provokes premature cell senescence associated with accumulation of p53 and p16(INK4a). *Cell*, **88**, 593–602.
27. Campisi,J. (2005) Senescent cells, tumor suppression, and organismal aging: Good citizens, bad neighbors. *Cell*, **120**, 513–522.
28. Baker,D.J., Wijshake,T., Tchkonja,T., LeBrasseur,N.K., Childs,B.G., van de Sluis,B., Kirkland,J.L. and van Deursen,J.M. (2011) Clearance of p16Ink4a-positive senescent cells delays ageing-associated disorders. *Nature*, **479**, 232–236.
29. Kuilman,T., Michaloglou,C., Vredeveld,L.C.W., Douma,S., van Doorn,R., Desmet,C.J., Aarden,L.A., Mooi,W.J. and Peeper,D.S. (2008) Oncogene-Induced Senescence Relayed by an Interleukin-Dependent Inflammatory Network. *Cell*, **133**, 1019–1031.
30. Freund,A., Orjalo,A. V., Desprez,P.Y. and Campisi,J. (2010) Inflammatory networks during cellular senescence: causes and consequences. *Trends Mol. Med.*, **16**, 238–246.
31. Gorospe,M. and Abdelmohsen,K. (2011) MicroRegulators come of age in senescence. *Trends Genet.*, **27**, 233–241.
32. Luo,X.-G., Ding,J.-Q. and Chen,S.-D. (2010) Microglia in the aging brain: relevance to neurodegeneration. *Mol. Neurodegener.*, **5**, 12.
33. Ohtani,N., Takahashi,A., Mann,D.J. and Hara,E. (2012) Cellular senescence: a double-edged sword in the fight against cancer. *Exp. Dermatol.*, **21 Suppl 1**, 1–4.
34. Krtolica,A., Parrinello,S., Lockett,S., Desprez,P.-Y. and Campisi,J. (2001) Senescent fibroblasts promote epithelial cell growth and tumorigenesis: A link between cancer and aging. *Proc. Natl. Acad. Sci.*, **98**, 12072–12077.
35. Salama,R., Sadaie,M., Hoare,M. and Narita,M. (2014) Cellular senescence and its effector programs. *Genes Dev.*, **28**, 99–114.

36. Coppé,J.-P., Desprez,P.-Y., Krtolica,A. and Campisi,J. (2010) The Senescence-Associated Secretory Phenotype: The Dark Side of Tumor Suppression. *Annu. Rev. Pathol. Mech. Dis.*, **5**, 99–118.
37. Rodier,F. and Campisi,J. (2011) Four faces of cellular senescence. *J. Cell Biol.*, **192**, 547–556.
38. Collado,M., Blasco,M.A. and Serrano,M. (2007) Cellular Senescence in Cancer and Aging. *Cell*, **130**, 223–233.
39. Campisi,J. (2003) Cancer and ageing: rival demons? *Nat. Rev. Cancer*, **3**, 339–349.
40. Lanigan,F., Geraghty,J.G. and Bracken,A.P. (2011) Transcriptional regulation of cellular senescence. *Oncogene*, **30**, 2901–2911.
41. Wang,W., Yang,X., Cristofalo,V.J., Holbrook,N.J. and Gorospe,M. (2001) Loss of HuR Is Linked to Reduced Expression of Proliferative Genes during Replicative Senescence. *Mol. Cell Biol.*, **21**, 5889–5898.
42. Pont,A.R., Sadri,N., Hsiao,S.J., Smith,S. and Schneider,R.J. (2012) mRNA Decay Factor AUF1 Maintains Normal Aging, Telomere Maintenance, and Suppression of Senescence by Activation of Telomerase Transcription. *Mol. Cell*, **47**, 5–15.
43. Sanduja,S., Kaza,V. and Dixon,D.A. (2009) The mRNA decay factor tristetraprolin (TTP) induces senescence in human papillomavirus-transformed cervical cancer cells by targeting E6-AP ubiquitin ligase. *Aging (Albany. NY)*, **1**, 803–817.
44. Xie,H.-F., Liu,Y.-Z., Du,R., Wang,B., Chen,M.-T., Zhang,Y.-Y., Deng,Z.-L. and Li,J. (2017) miR-377 induces senescence in human skin fibroblasts by targeting DNA methyltransferase 1. *Cell Death Dis.*, **8**, e2663.
45. Xu,D., Takeshita,F., Hino,Y., Fukunaga,S., Kudo,Y., Tamaki,A., Matsunaga,J., Takahashi,R. u., Takata,T., Shimamoto,A., *et al.* (2011) miR-22 represses cancer progression by inducing cellular senescence. *J. Cell Biol.*, **193**, 409–424.
46. Montes,M., Nielsen,M.M., Maglieri,G., Jacobsen,A., Højfeldt,J., Agrawal-Singh,S., Hansen,K., Helin,K., van de Werken,H.J.G., Pedersen,J.S., *et al.* (2015) The lncRNA MIR31HG regulates p16(INK4A) expression to modulate senescence. *Nat. Commun.*, **6**, 6967.
47. Wu,C.L., Wang,Y., Jin,B., Chen,H., Xie,B.S. and Mao,Z. Bin (2015) Senescence-associated long non-coding RNA (SALNR) delays oncogene-induced senescence through NF90 regulation. *J. Biol. Chem.*, **290**, 30175–30192.
48. Drost,J., Mantovani,F., Tocco,F., Elkon,R., Comel,A., Holstege,H., Kerkhoven,R., Jonkers,J., Voorhoeve,P.M., Agami,R., *et al.* (2010) BRD7 is a candidate tumour suppressor gene required for p53 function. *Nat. Cell Biol.*, **12**, 380–389.
49. Kim,D., Pertea,G., Trapnell,C., Pimentel,H., Kelley,R. and Salzberg,S.L. (2013) TopHat2: accurate alignment of transcriptomes in the presence of insertions, deletions and gene fusions. *Genome Biol.*, **14**, R36.
50. Anders,S., Pyl,P.T. and Huber,W. (2015) HTSeq-A Python framework to work with high-throughput sequencing data. *Bioinformatics*, **31**, 166–169.
51. Huang,D.W., Sherman,B.T. and Lempicki,R.A. (2008) Systematic and integrative analysis of large gene lists using DAVID bioinformatics resources. *Nat. Protoc.*, **4**, 44–57.
52. Subramanian,A., Tamayo,P., Mootha,V.K., Mukherjee,S., Ebert,B.L., Gillette,M.A., Paulovich,A., Pomeroy,S.L., Golub,T.R., Lander,E.S., *et al.* (2005) Gene set enrichment analysis: A knowledge-based approach for interpreting genome-wide expression profiles. *PNAS*, **102**, 15545–15550.

53. Soares,R.J., Maglieri,G., Gutschner,T., Diederichs,S., Lund,A.H., Nielsen,B.S. and Holmström,K. (2018) Evaluation of fluorescence in situ hybridization techniques to study long non-coding RNA expression in cultured cells. *Nucleic Acids Res.*, **46**, e4. 10.1093/nar/gkx946.
54. Loayza-Puch,F., Rooijers,K., Buil,L.C.M., Zijlstra,J., F. Oude Vrielink,J., Lopes,R., Ugalde,A.P., van Breugel,P., Hofland,I., Wesseling,J., *et al.* (2016) Tumour-specific proline vulnerability uncovered by differential ribosome codon reading. *Nature*, **530**, 490–494.
55. Korkmaz,G., Lopes,R., Ugalde,A.P., Nevedomskaya,E., Han,R., Myacheva,K., Zwart,W., Elkon,R. and Agami,R. (2016) Functional genetic screens for enhancer elements in the human genome using CRISPR-Cas9. *Nat. Biotechnol.*, **34**, 1–10.
56. Agami,R. and Bernards,R. (2000) Distinct Initiation and Maintenance Mechanisms Cooperate to Induce G1 Cell Cycle Arrest in Response to DNA Damage. *Cell*, **102**, 55–66.
57. Haarhuis,J.H.I., van der Weide,R.H., Blomen,V.A., Yáñez-Cuna,J.O., Amendola,M., van Ruiten,M.S., Krijger,P.H.L., Teunissen,H., Medema,R.H., van Steensel,B., *et al.* (2017) The Cohesin Release Factor WAPL Restricts Chromatin Loop Extension. *Cell*, **169**, 693–707.e14.
58. van de Werken,H.J.G., Landan,G., Holwerda,S.J.B., Hoichman,M., Klous,P., Chachik,R., Splinter,E., Valdes-Quezada,C., Öz,Y., Bouwman,B.A.M., *et al.* (2012) Robust 4C-seq data analysis to screen for regulatory DNA interactions. *Nat. Methods*, **9**, 969–972.
59. Smyth,G.K. (2005) Limma: linear models for microarray data BT - Bioinformatics and Computational Biology Solutions Using R and Bioconductor. *Bioinforma. Comput. Biol. Solut. Using R Bioconductor*, 10.1007/0-387-29362-0_23.
60. Law,C.W., Chen,Y., Shi,W. and Smyth,G.K. (2014) voom: precision weights unlock linear model analysis tools for RNA-seq read counts. *Genome Biol.*, **15**, R29.
61. Vidigal,J.A. and Ventura,A. (2015) Rapid and efficient one-step generation of paired gRNA CRISPR-Cas9 libraries. *Nat. Commun.*, **6**, 8083.
62. Lee,J.T. (2009) Lessons from X-chromosome inactivation: Long ncRNA as guides and tethers to the epigenome. *Genes Dev.*, **23**, 1831–1842.
63. Augui,S., Nora,E.P. and Heard,E. (2011) Regulation of X-chromosome inactivation by the X-inactivation centre. *Nat. Rev. Genet.*, **12**, 429–442.
64. Ørom,U.A., Derrien,T., Beringer,M., Gumireddy,K., Gardini,A., Bussotti,G., Lai,F., Zytnicki,M., Notredame,C., Huang,Q., *et al.* (2010) Long noncoding RNAs with enhancer-like function in human cells. *Cell*, **143**, 46–58.
65. Bertani,S., Sauer,S., Bolotin,E. and Sauer,F. (2011) The Noncoding RNA Mistral Activates Hoxa6 and Hoxa7 Expression and Stem Cell Differentiation by Recruiting MLL1 to Chromatin. *Mol. Cell*, **43**, 1040–1046.
66. Wang,K.C., Yang,Y.W., Liu,B., Sanyal,A., Corces-Zimmerman,R., Chen,Y., Lajoie,B.R., Protacio,A., Flynn,R.A., Gupta,R.A., *et al.* (2011) A long noncoding RNA maintains active chromatin to coordinate homeotic gene expression. *Nature*, **472**, 120–124.
67. Lai,F., Orom,U.A., Cesaroni,M., Beringer,M., Taatjes,D.J., Blobel,G.A. and Shiekhattar,R. (2013) Activating RNAs associate with Mediator to enhance chromatin architecture and transcription. *Nature*, **494**, 497–501.
68. Wesley,U. V, Albino, a P., Tiwari,S. and Houghton, a N. (1999) A role for dipeptidyl peptidase IV in suppressing the malignant phenotype of melanocytic cells. *J. Exp. Med.*, **190**, 311–322.
69. Pethiyagoda,C.L., Welch,D.R. and Fleming,T.P. (2000) Dipeptidyl peptidase IV (DPPIV) inhibits cellular invasion of melanoma cells. *Clin. Exp. Metastasis*, **18**, 391–400.

70. Wesley,U. V, Tiwari,S. and Houghton,A.N. (2004) Role for dipeptidyl peptidase IV in tumor suppression of human non small cell lung carcinoma cells. *Int. J. Cancer*, **109**, 855–66.
71. Kajiyama,H., Kikkawa,F., Suzuki,T., Shibata,K., Ino,K. and Mizutani,S. (2002) Prolonged survival and decreased invasive activity attributable to dipeptidyl peptidase IV overexpression in ovarian carcinoma. *Cancer Res.*, **62**, 2753–2757.
72. Kajiyama,H., Kikkawa,F., Khin,E.E., Shibata,K., Ino,K. and Mizutani,S. (2003) Dipeptidyl peptidase IV overexpression induces up-regulation of E-cadherin and tissue inhibitors of matrix metalloproteinases, resulting in decreased invasive potential in ovarian carcinoma cells. *Cancer Res.*, **63**, 2278–2283.
73. Kikkawa,F., Kajiyama,H., Ino,K., Shibata,K. and Mizutani,S. (2003) Increased adhesion potency of ovarian carcinoma cells to mesothelial cells by overexpression of dipeptidyl peptidase IV. *Int. J. Cancer*, **105**, 779–783.
74. Mizokami,Y., Kajiyama,H., Shibata,K., Ino,K., Kikkawa,F. and Mizutani,S. (2004) Stromal cell-derived factor-1alpha-induced cell proliferation and its possible regulation by CD26/dipeptidyl peptidase IV in endometrial adenocarcinoma. *Int J Cancer*, **110**, 652–659.
75. Wesley,U. V, McGroarty,M. and Homoyouni,A. (2005) Dipeptidyl peptidase inhibits malignant phenotype of prostate cancer cells by blocking basic fibroblast growth factor signaling pathway. *Cancer Res.*, **65**, 1325–1334.
76. Arscott,W.T., LaBauve, a E., May,V. and Wesley,U. V (2009) Suppression of neuroblastoma growth by dipeptidyl peptidase IV: relevance of chemokine regulation and caspase activation. *Oncogene*, **28**, 479–491.
77. Busek,P., Stremenova,J., Sromova,L., Hilser,M., Balaziová,E., Kosek,D., Trylcová,J., Strnad,H., Krepela,E. and Sedo,A. (2012) Dipeptidyl peptidase-IV inhibits glioma cell growth independent of its enzymatic activity. *Int. J. Biochem. Cell Biol.*, **44**, 738–747.
78. Kim,K.M., Noh,J.H., Bodogai,M., Martindale,J.L., Yang,X., Indig,F.E., Basu,S.K., Ohnuma,K., Morimoto,C., Johnson,P.F., *et al.* (2017) Identification of senescent cell surface targetable protein DPP4. *Genes Dev.*, **31**, 1529–1534.

Supplemental data for chapter 2

A

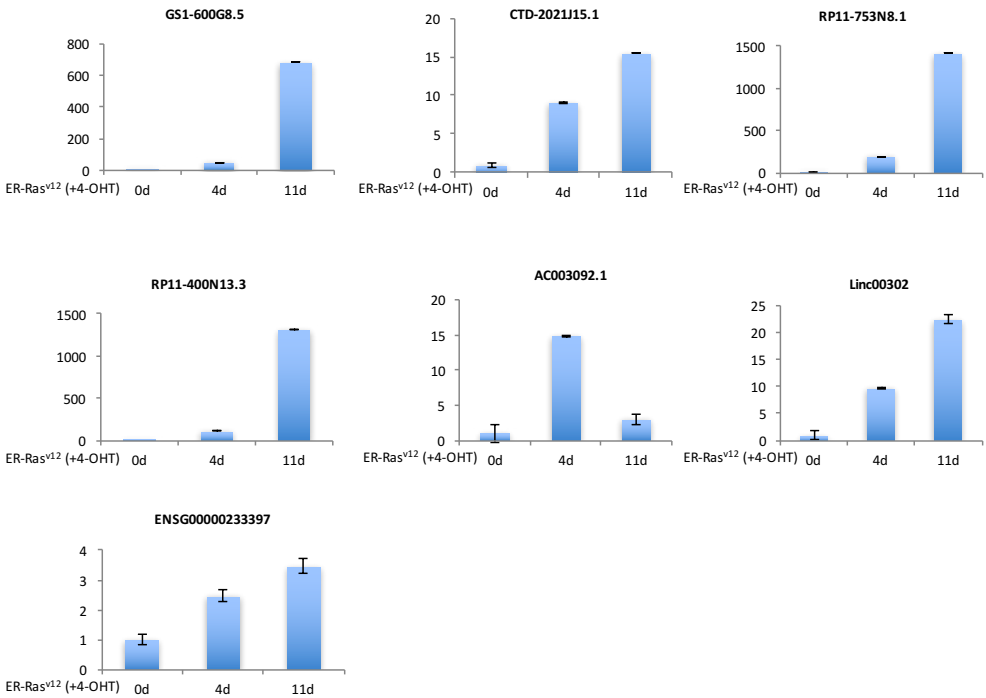
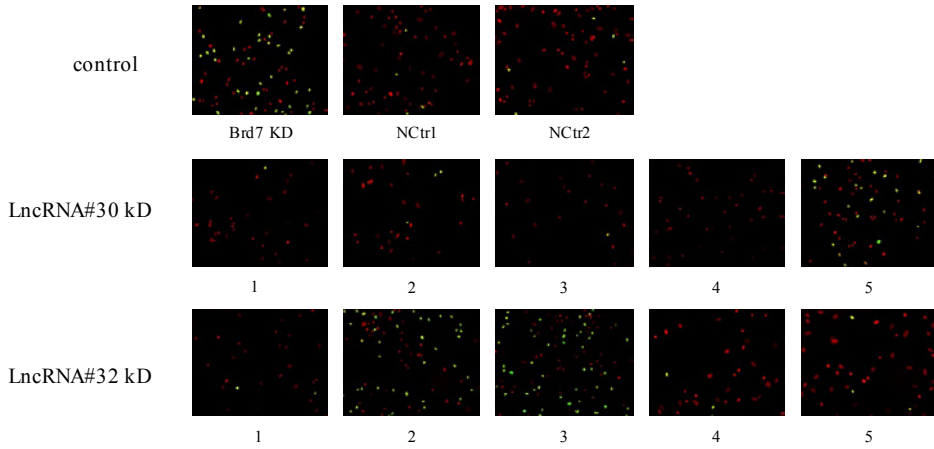


Figure SI. Confirmation of some lncRNAs expression upon RAS induction. (A) qRT-PCR expression analysis of seven different lncRNAs in BJ/ET/RasV¹² cells treated with 4-OHT relative to untreated cells.

A



B

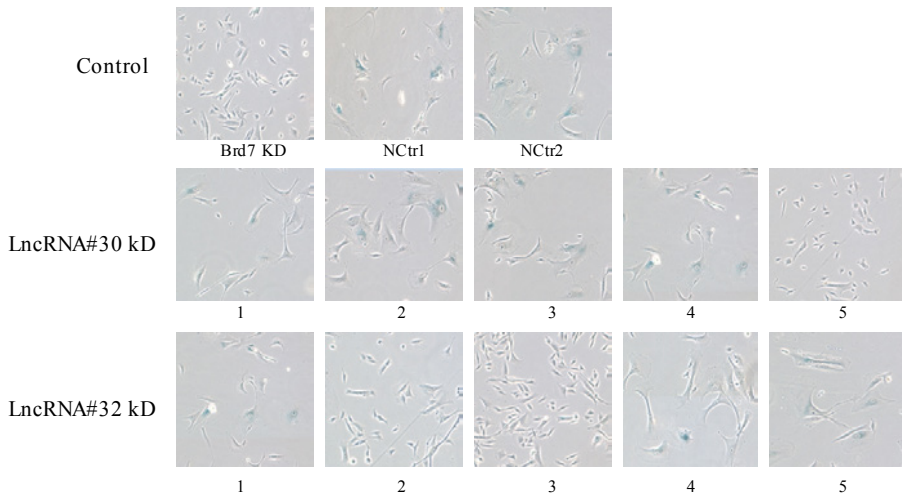


Figure S2. Validation of selected lncRNAs.

(A) Representative images of the BrdU assay of cells under the indicated conditions and after 14 days 4-OHT treatment. (B) Representative images of the SA-β-gal staining of cells under the indicated conditions and after 14 days 4-OHT treatment.

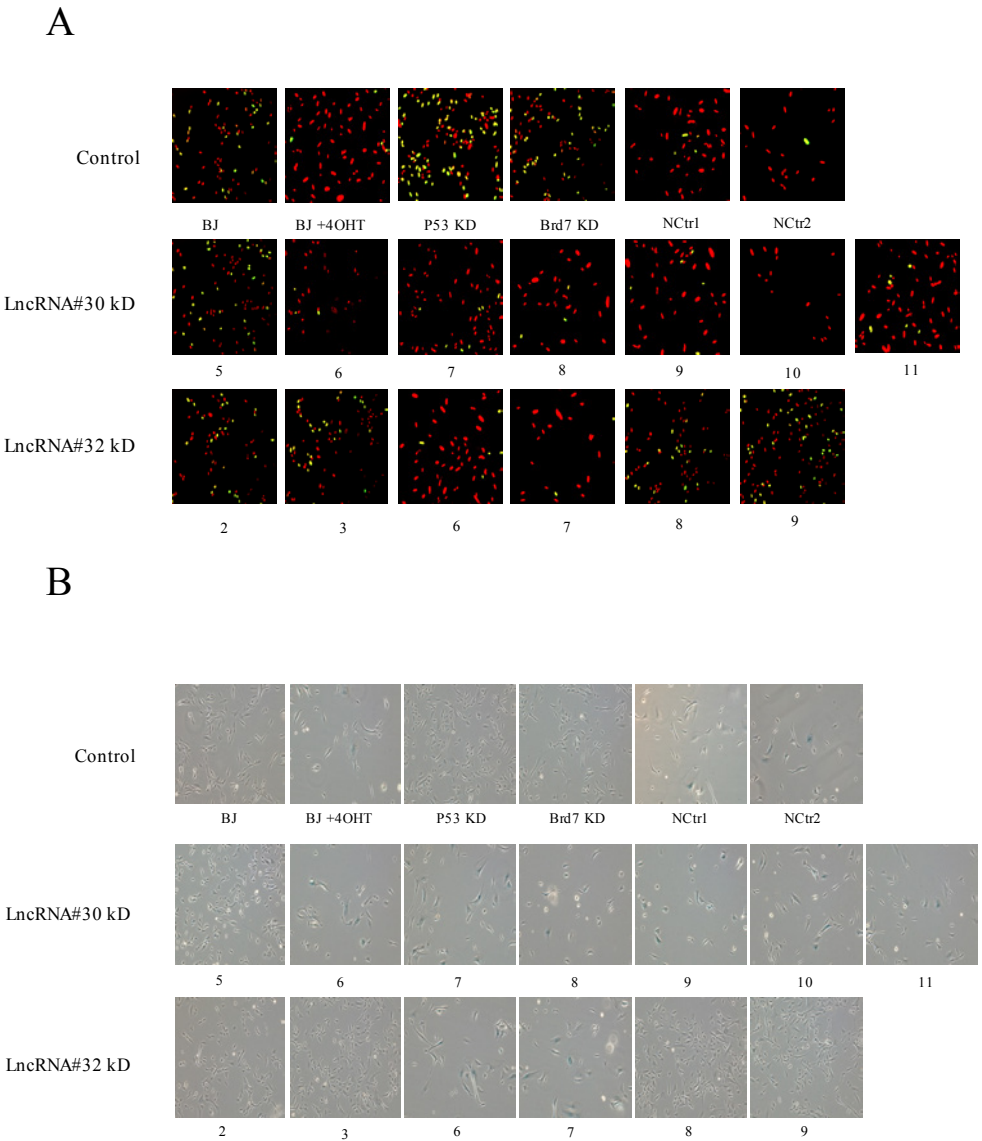


Figure S3. Validation of additional shRNA vectors.
(A) Representative images of the BrdU assay of cells under the indicated conditions and after 14 days 4-OHT treatment. (B) Representative images of the SA-β-gal staining of cells under the indicated conditions and after 14 days 4-OHT treatment.

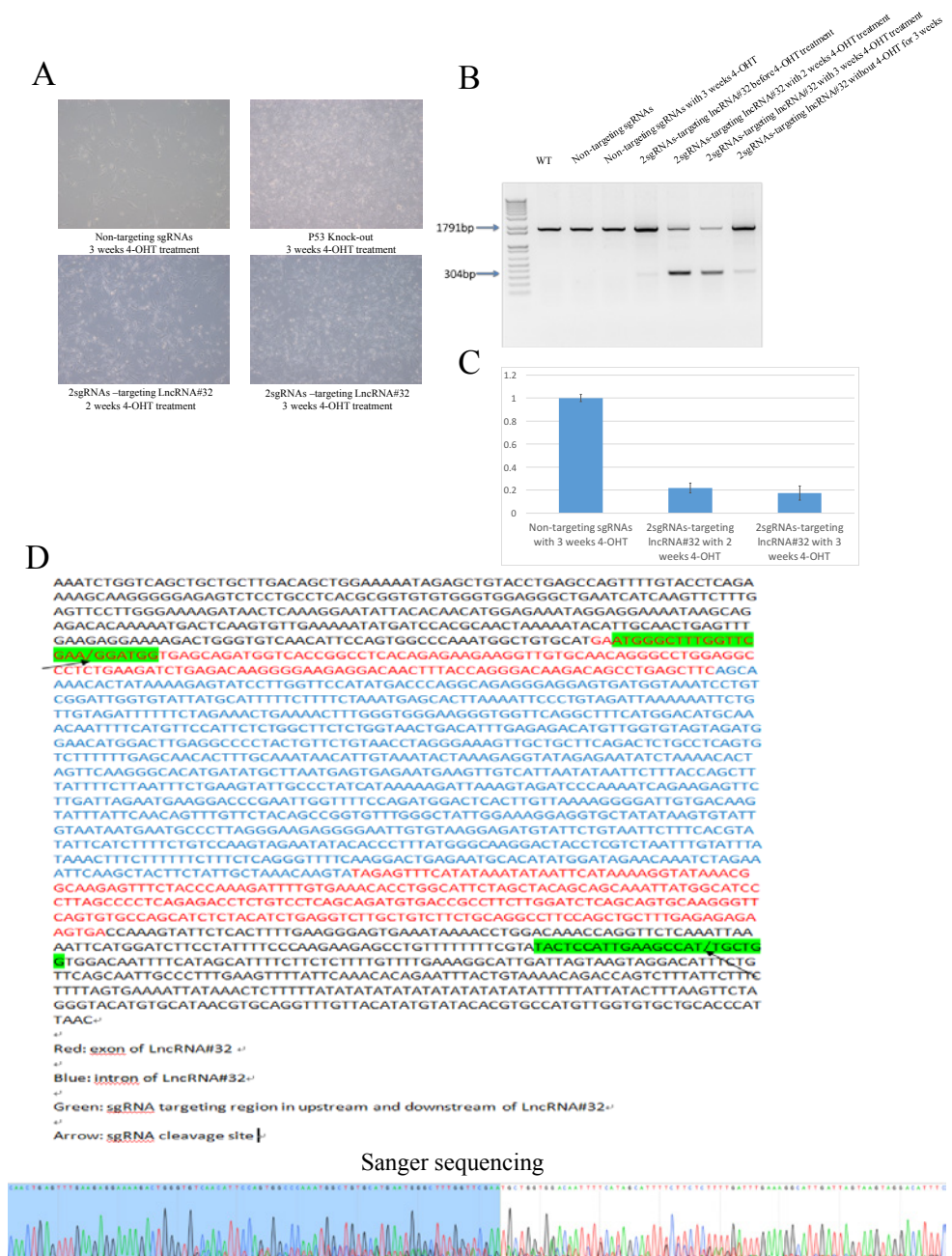


Figure S4. LncRNA#32 deleted BJ cells have growth advantage during OIS.

(A) Representative images of cells under the indicated conditions. (B) PCR analysis of genomic DNA was used to quantify lncRNA#32 deletion. (C) qRT-PCR analysis of lncRNA#32 in the indicated conditions. (D) Sanger sequencing of the PCR fragments obtained in B confirms the deletion of lncRNA#32.

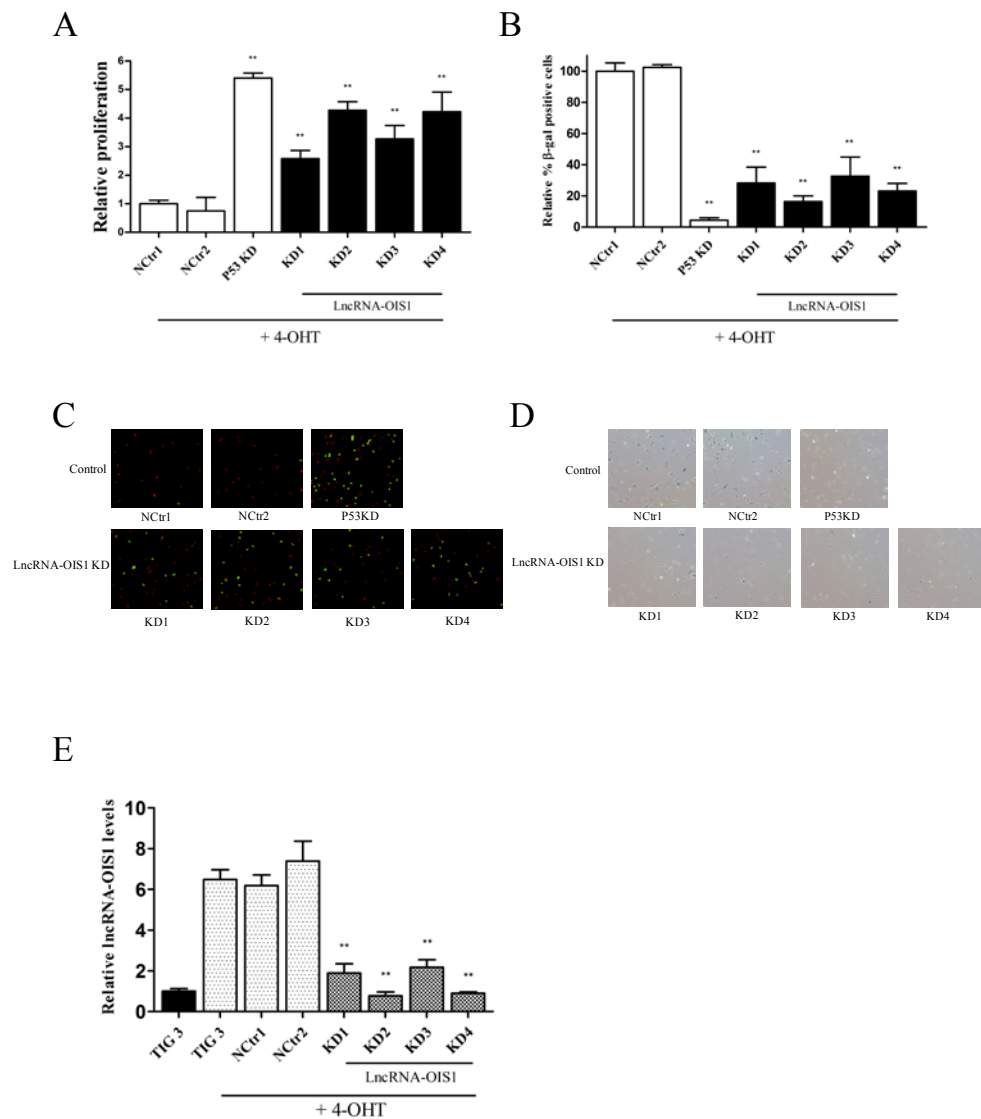


Figure S5. Validation of lncRNA-OIS1 kd in TIG3 cells.

(A) The proliferation of the various shRNA-transduced TIG3/ET/RAS^{v12} cells was quantified using BrdU assay, $**P < 0.002$, two-tailed Student's t-test. For every condition, percentage of BrdU-positive cells was normalized to negative control cells. (B) Senescent cells were quantified using SA-β-gal assay, $**P < 0.0005$, two-tailed Student's t-test. For every condition, percentage of β-gal-positive cells was normalized to negative control cells. (C, D) Representative images of the BrdU assay and the SA-β-gal staining of cells under the indicated conditions and after 13 days 4-OHT treatment. (E) qRT-PCR analysis of lncRNA-OIS1 in the various shRNA-transduced TIG3 cells treated with 4-OHT relative to untreated cells. Data were normalized to a housekeeping gene and the levels in untreated cells set to 1, $**P < 0.0005$, two-tailed Student's t-test.

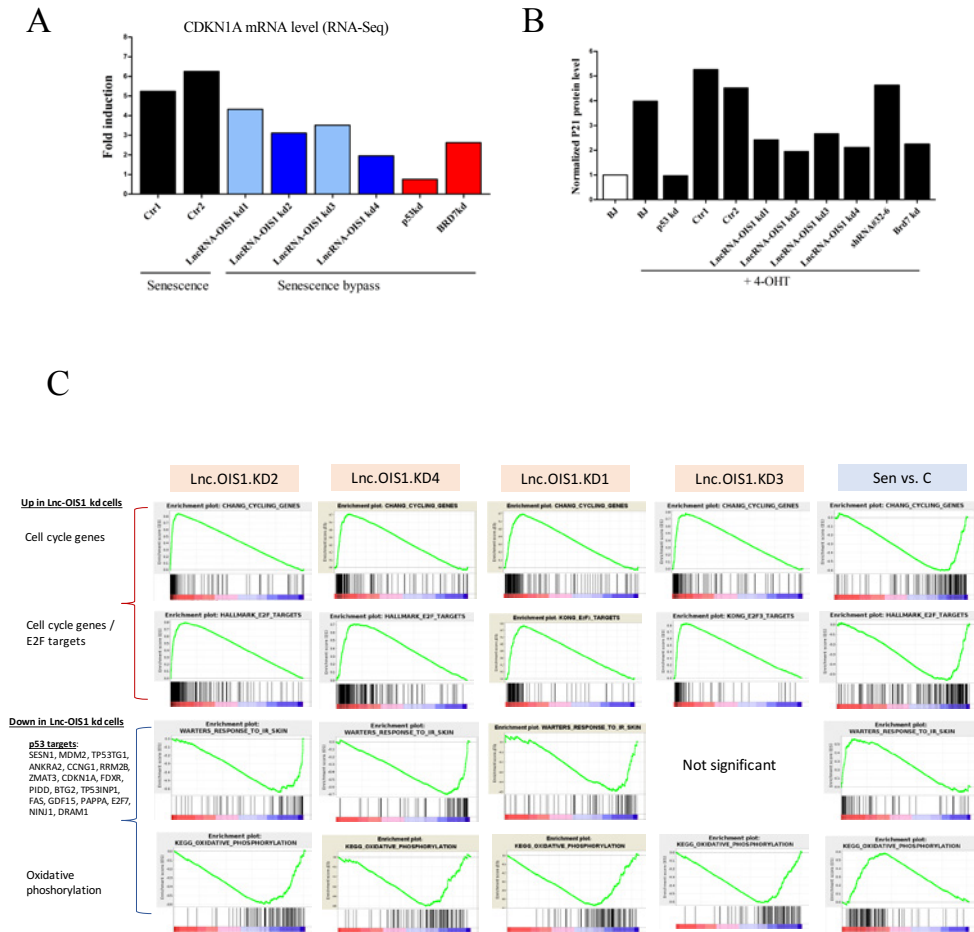


Figure S6. Loss-of lncRNA-OIS1 reverses senescence-induced gene expression pattern.

(A) CDKN1A RNA levels were calculated based on RNA-seq. (B) Quantification of WB results using Image J. (C). Selected gene sets that were significantly affected by knocking-down lncRNA-OIS1 (for all sets shown in this figure, p-value adjusted for multiple testing < 0.05). These sets were identified by GSEA analysis comparing gene expression profiles between BJ cells transfected with shRNAs against lncRNA-OIS1 and control shRNAs, both in the background of induced oncogenic RAS. GSEA comparison between BJ cells with and without induced RAS (senescent vs. control BJ cells) is shown in the right column. Knocking-down lncRNA-OIS1 reverse transcriptional signatures that characterize OIS.

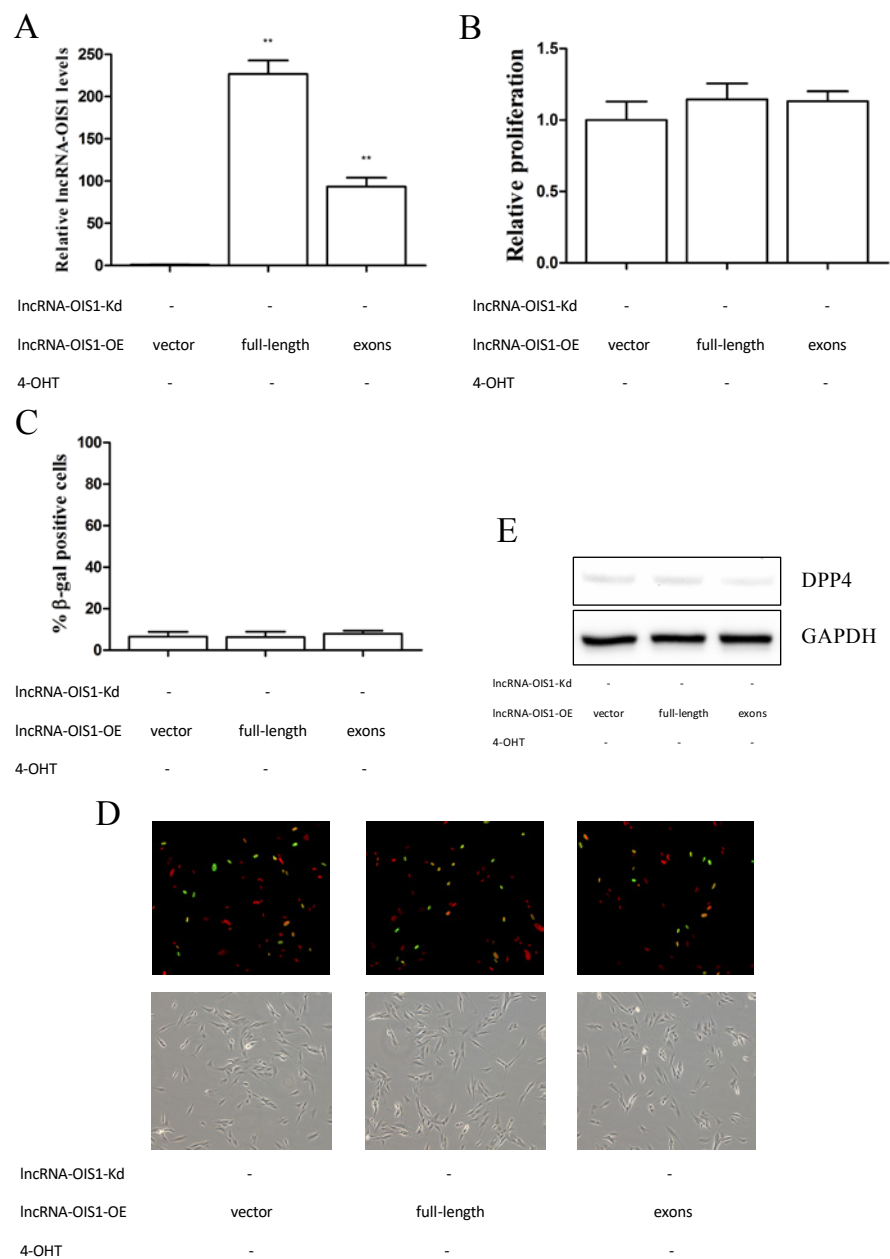


Figure S7. lncRNA-OIS1 overexpression in wild type BJ cells does not affect cell proliferation.

(A) qRT-PCR analysis of lncRNA-OIS1 expression under the indicated conditions. Data were normalized to a housekeeping gene, and the levels in control cells was set to 1, $**P < 0.0001$, two-tailed Student's t-test. (B) Proliferation of the cells under indicated conditions was quantified using BrdU assay. The percentage of BrdU-positive cells was normalized to control cells. (C) Senescent cells were quantified using SA-β-gal assay. (D) Representative images of the BrdU and SA-β-gal assays. (E) WB analysis to determine DPP4 protein levels.

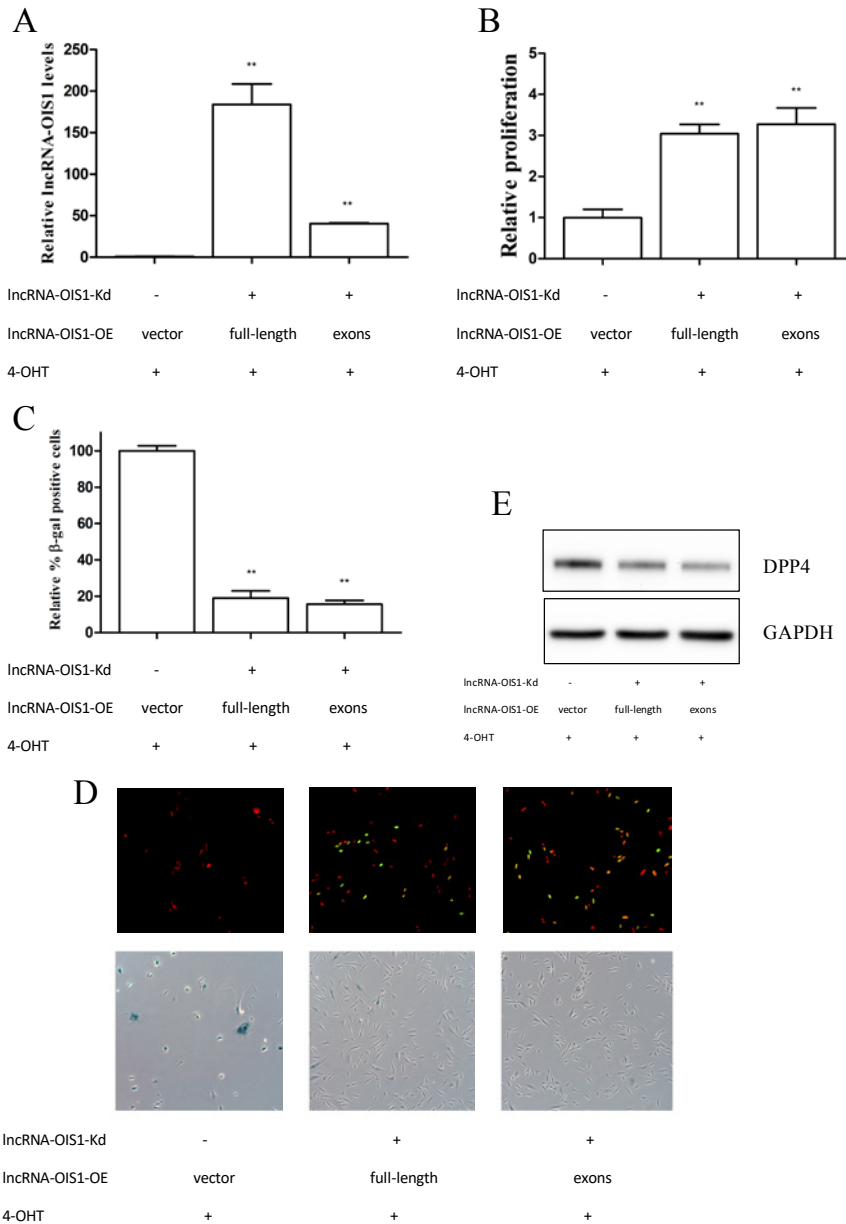


Figure S8. LncRNA-OIS1 overexpression in lncRNA-OIS1kd cells does not affect senescence-bypass under RAS^{V12} induction conditions.

(A) qRT-PCR analysis of lncRNA-OIS1 expression in the indicated conditions. Data were normalized to a housekeeping gene, and the levels in control cells were set to 1. ** $P < 0.0005$, two-tailed Student's t-test. (B) Proliferation of the cells under indicated conditions was quantified using BrdU assay. ** $P < 0.001$, two-tailed Student's t-test. The percentage of BrdU-positive cells was normalized to control cells. (C) Senescent cells were quantified using SA- β -gal assay. ** $P < 0.0001$, two-tailed Student's t-test. The percentage of SA- β -gal-positive cells was normalized to control cells. (D) Representative images of the BrdU and SA- β -gal assays of cells under the indicated conditions. (E) Western blot analysis determines DPP4 protein levels.

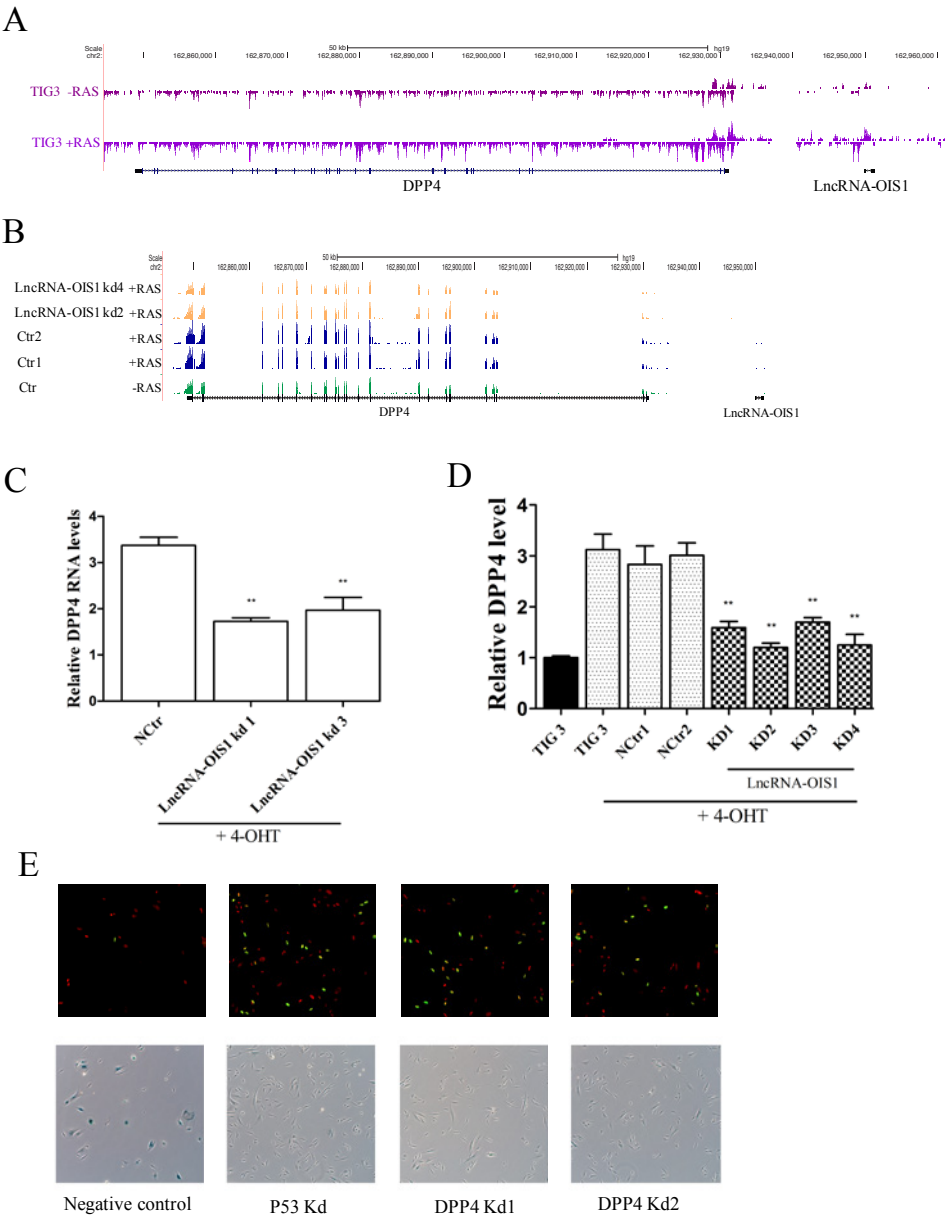
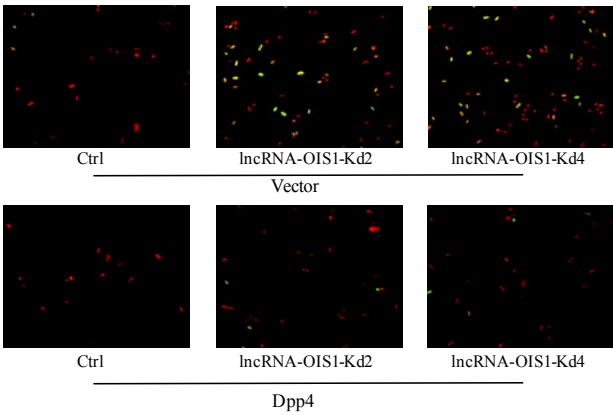


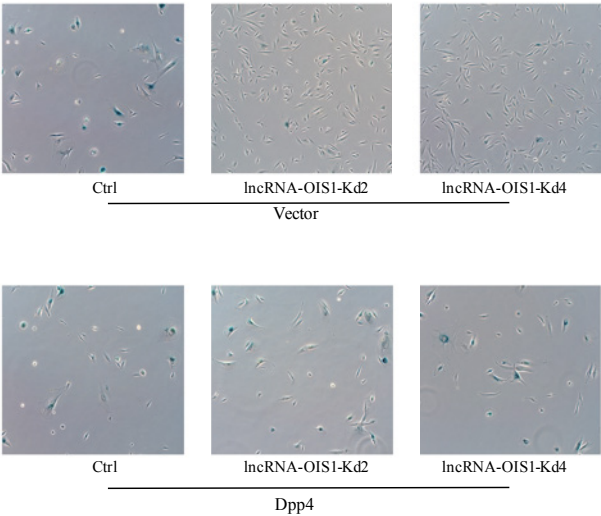
Figure S9. lncRNA-OIS1 knockdown in TIG3 cells affects the activation of DPP4 following oncogene induction, and loss-of DPP4 shows OIS bypass.

(A) Screenshots of GRO-seq data of the lncRNA-OIS1 and DPP4 genomic locus in TIG3 cells. (B) Screenshots of RNA-seq data of DPP4 and lncRNA-OIS1. (C) qRT-PCR analysis of DPP4 expression upon lncRNA-OIS1 kd treated with 4-OHT in BJ cells, $**P < 0.002$, two-tailed Student's t-test. (D) qRT-PCR analysis of DPP4 expression upon lncRNA-OIS1 kd treated with or without 4-OHT in TIG3 cells, $**P < 0.01$, two-tailed Student's t-test. (E) Representative images of the BrdU assay and β -gal staining of cells under indicated conditions.

A



B



C

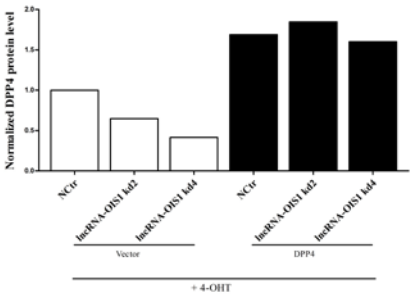


Figure S10. Ectopic expression of DPP4 abolishes OIS-bypass induced by lncRNA-OIS1kd. (A) Representative images of the BrdU assay of cells under the indicated conditions and after 14 days of 4-OHT treatment. (B) Representative images of SA-β-gal staining of cells under the indicated conditions and after 14 days of 4-OHT treatment. (C) Quantification of western blot pictures by Image J.

A

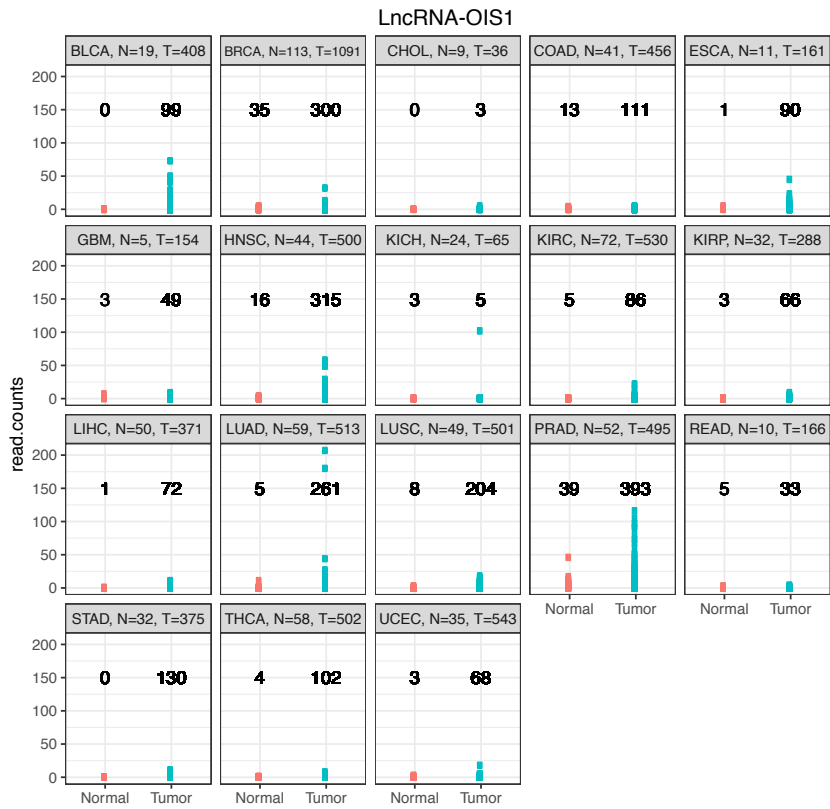


Figure SII. LncRNA-OIS1 expression is extremely low in most tumors.

(A) TCGA data analysis of lncRNA-OIS1. We plotted the read counts of lncRNA-OIS1 in normal and tumor samples. Indicated in each tumor type the number of samples with at least 1 read count for lncRNA-OIS1. Of all 33 TCGA tumor types only those with at least 5 normal and 5 tumor samples are shown.

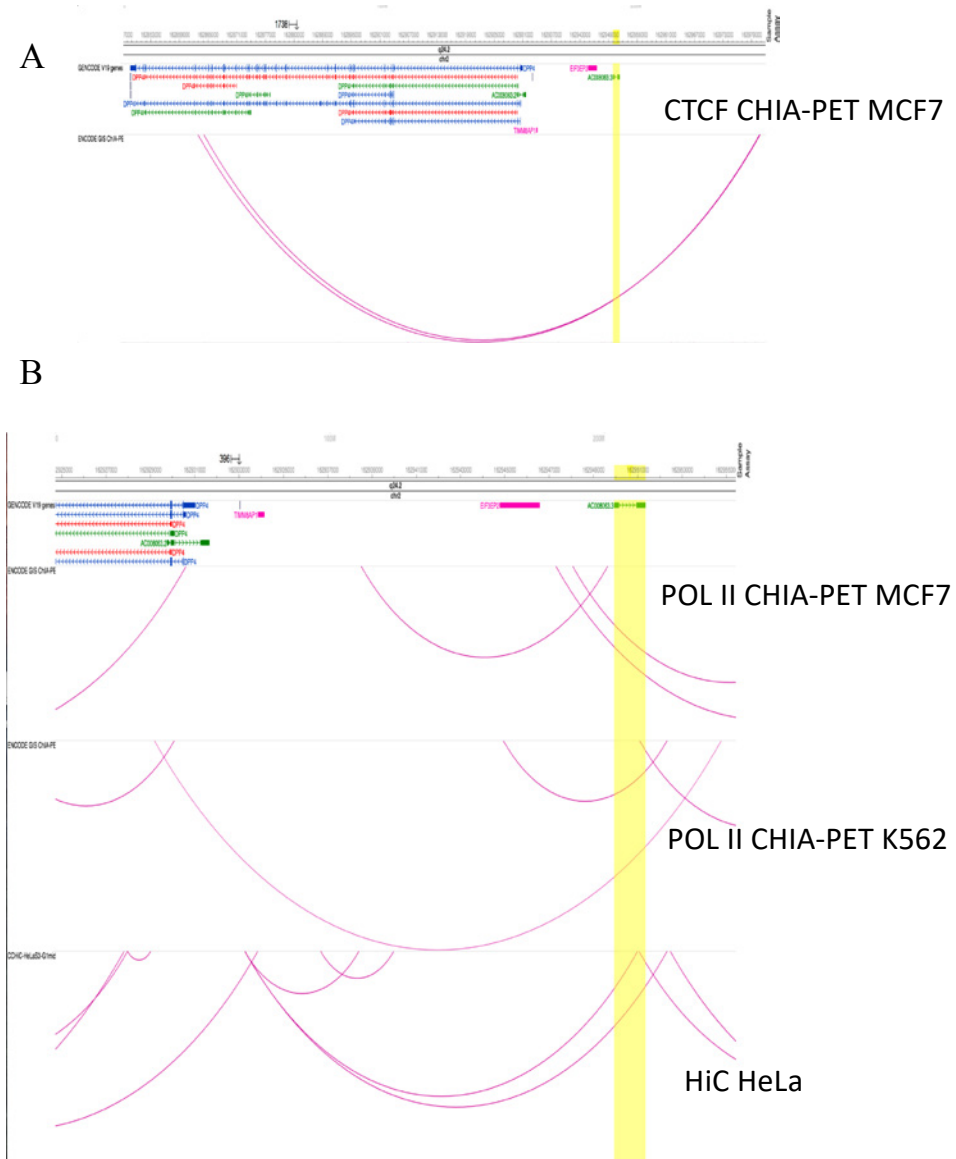
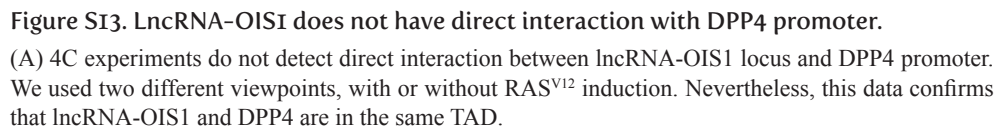


Figure SI2. LncRNA-OISI and DPP4 are in the same topological associated chromatin domain.

(A) Screenshot of CTCF ChIA-PET data in MCF7 cells. (B) Screenshot of RNA Polymerase II (POL-II) ChIA-PET data in MCF7, K562 cells, and Hi-C data of HeLa cells.







Chapter 3

Functional CRISPR screen identifies AP1-associated enhancer regulating FOXF1 to modulate oncogene-induced senescence

Ruiqi Han^{1,3,5}, Li Li^{1,3,5}, Alejandro Piñeiro Ugalde¹, Arie Tal¹, Zohar Manber⁴,
Eric Pinto Barbera^{1,3}, Veronica Della Chiara¹, Ran Elkon^{4,6}, Reuven Agami^{1,2,3,6}

¹Division of Oncogenomics, The Netherlands Cancer Institute, Plesmanlaan 121, 1066 CX Amsterdam, The Netherlands.

²Department of Genetics, Erasmus University Medical Center, Wytemaweg 80, 3015 CN Rotterdam, The Netherlands.

³Oncode Institute, Amsterdam, The Netherlands.

⁴Department of Human Molecular Genetics and Biochemistry, Sackler School of Medicine, Tel Aviv University,
Tel Aviv, Israel

⁵These authors contributed equally

⁶Co-corresponding authors

Abstract

Background

Functional characterization of noncoding elements in the human genome is a major genomic challenge, and the maturation of genome-editing technologies is revolutionizing our ability to achieve this task. Oncogene-induced senescence (OIS), a cellular state of irreversible proliferation arrest that is enforced following excessive oncogenic activity, is a major barrier against cancer transformation, and therefore bypassing OIS is a critical step in tumorigenesis. Here, we aimed at further identification of enhancer elements that are required for the establishment of OIS.

Results

We first applied genome-wide profiling of enhancer-RNAs (eRNAs) to systematically identify enhancers that are activated upon oncogenic stress. DNA motif analysis of these enhancers indicated AP-1 as a major regulator of the transcriptional program induced by OIS. We thus constructed a CRISPR-Cas9 sgRNA library designed to target OIS-induced enhancers that are putatively regulated by AP-1, and used it in a functional screen. We identified a critical enhancer that we dub *Enh^{AP1-OIS1}* and validated that mutating the AP-1 binding site within this element results in OIS bypass. Furthermore, we identified *FOXF1* as the gene regulated by this enhancer, and demonstrated that this target gene mediates *Enh^{AP1-OIS1}* effect on the senescence phenotype.

Conclusion

Our study elucidates a novel cascade mediated by AP-1 and FOXF1 that regulates OIS and further demonstrates the power of CRISPR-based functional genomic screens in deciphering the function of noncoding regulatory elements in the genome.

Keywords

CRISPR – Functional screen – Enhancers – Oncogene-induced senescence - Gene regulation – AP1- FOS – JUN – FOXF1

Background

Over the last decade, large-scale genomic projects identified hundreds of thousands of regulatory elements in the human genome, most of them are putative enhancers(1,2). Identification of candidate enhancer regions was mainly based on profiling of characteristic histone modifications (e.g., H3K27ac and H3K4me1) and binding of transcriptional activators (e.g., p300). Recently, eRNA expression, typically transcribed bi-directionally at promoter-distal cis-regulatory elements, was indicated as a sharp feature of active enhancers, and was utilized for systematic discovery of enhancers across the genome(3). Importantly, changes in eRNA production correlate with changes in the enhancer activity(4,5). Yet, functional characterization of the plethora of candidate enhancer elements is a major genomic challenge(6). High-throughput reporter assays to probe the functions of regulatory regions were developed in recent years(7). However, these methods separate putative regulatory elements from their native chromosome, so that any effect of chromatin context and long range regulatory interactions is lost. Furthermore, definitive demonstration of the function of regulatory element requires their perturbation in situ. The maturation of novel genome-editing technologies is revolutionizing our ability to interrogate the function of the noncoding genome. This potential was demonstrated by pioneering CRISPR-based functional genomic screens that systematically targeted noncoding elements in the human genome(8–11).

In one of these CRISPR-based functional genomic screens we focused on oncogene-induced senescence (OIS), which is a cellular state of irreversible proliferation arrest that is enforced in face of excessive oncogenic activity (oncogenic stress) (8). OIS is a major barrier against cancer transformation (12,13) and therefore overcoming OIS is a critical step in tumorigenesis (14). Activation of this process is largely dependent on p53 (13,15), and consequently its bypass by cancer cells is mainly achieved by emergence of somatic mutations in p53 or other components of its pathway (16,17). As p53 is an enhancer binding transcription factor (TF), whose function in transcriptional regulation is required for its tumor suppressive activity, we previously performed a CRISPR-based functional genomic screen that systematically targeted p53-bound enhancers(18). That screen uncovered several p53-bound regulatory elements that are required for the activation of OIS. However, aberrant expression of oncogenes can lead to activation of additional transcription factors (TFs) whose function is also critical for the establishment and/or maintenance of OIS. In the current study, we aimed at the identification of such TFs and discovery of additional enhancers that are required for the establishment of OIS. We carried out an unbiased profiling of enhancers activated upon oncogenic stress, which indicated AP-1 as a major regulator of the transcriptional program induced by OIS. We thus generated a CRISPR-Cas9 sgRNA library designed to target enhancers putatively regulated by AP-1, and used it in a functional screen to identify those required for OIS. This screen detected *Enh^{API-OIS1}*, an AP-1 bound enhancer that is hyper-activated

in OIS and whose abrogation results in OIS bypass. Furthermore, we identified *FOXF1* as the target gene of this enhancer, and demonstrated that it regulates the senescence phenotype.

Material and methods

Cell culture

BJ/ET/Ras^{V12} and HEK293-T cells were cultured in DMEM medium (Gibco), supplemented with 1% penicillin/streptomycin (Gibco) and 10% FCS (Hyclone). To induce OIS, BJ cells were treated with 100 nM 4-OHT (Sigma) for 14 days.

Analysis of GRO-seq data

GRO-seq was applied to control and RAS^{G12V}-induced hTERT immortalized BJ cells (14 days after RAS induction). These conditions were probed using biological duplicates. Sequenced reads were aligned to the human genome (hg19) using bowtie2 (43). Transcriptional units (TUs) were inferred from the GRO-seq data using HOMER (44). Read counts per TU were calculated using HTseq-count (45). 76,200 TUs covered by at least 20 reads in at least one sample were detected. TU expression levels were then normalized using quantile normalization to allow comparison between samples, and fold-change (FC; presented in log₂ base) were calculated between the RAS-induced and control samples. To avoid inflation of high FC value for lowly expressed TUs, we set a floor value of 10 (that is, all expression levels below 10 were set to 10). Next, we defined bi-directional TUs as TUs whose start site is separated by no more than 800 bp and are transcribed on opposite strands (TU+ and TU-). As bi-directional transcription is a hallmark of transcriptional regulatory elements, we refer to these loci as regulatory elements (REs). Overall, this analysis defined 36,497 regulatory elements. Last, a regulatory element (bi-directional TU) was defined as OIS-induced if the expression level of both its mates was elevated by at least 2-folds upon RAS induction, in both duplicates. In total, 1,821 OIS-induced REs were identified in our dataset (Table S1).

Motif enrichment analysis

The sequences of the OIS-induced regulatory elements were searched for statistically over-represented TF binding motifs. We performed this *de novo* motif analysis using DREME (46). For each bi-directional TUs, we scanned the region between the start site of the opposite mates (TU+ and TU-) plus a margin of 200 bp to each direction. As control sequences, we extracted adjacent sequences of the same length are immediately upstream and downstream the test sequence. The binding motif of JUN/FOS was highly enriched ($p=1.2 \times 10^{-88}$) on the OIS-induced REs. Specific occurrences of the enriched JUN/FOS motif were identified using FIMO with default parameters (47). Overall, 762 JUN/FOS motif occurrences were found on 638 OIS-induced REs.

CRISPR library construction and analysis

We designed a CRISPR library to target the FOS/JUN motifs in the OIS-induced REs. For 398 of the 638 OIS-induced REs with FOS/JUN motif, we found an occurrence of the NGG PAM in a location that is expected to induce a Cas9 DNA cleavage within a margin of 5 bp with respect to the motif (that is, the cut is expected to occur within the motif or up to 5 bp from its edges). Overall, we designed 840 distinct sgRNAs, collectively targeting FOS/JUN motif in 398 OIS-induced REs. We cloned these sgRNAs into pLentiCRISPRv2 vector and generated a plasmid library (which we call *CRISPR-API-EnhLib*). Induced and control BJ-indRAS^{G12V} were transduced with four independent lentiviral pools of *CRISPR-API-EnhLib*. Following four weeks of culturing, we harvested library-transduced cells, isolated genomic DNA, amplified integrated vectors by PCR, and used next-generation sequencing (NGS) to quantify the abundance of integrated sgRNAs present in each population. Read counts were normalized to 1M reads and enrichment ratio (fold-change in log₂) were calculated for each sgRNA between the induced and control samples per replicate. (To avoid inflation of FC for sgRNAs covered by low number of reads, counts below 50 were set to 50). Next, average enrichment factor was calculated per sgRNA over the four replicates and was transformed to a Z score (Fig. 2B, Table S3).

Senescence-associated β -galactosidase assay

BJ cells were transduced with different sgRNA constructs and selected with puromycin. After selection, cells were seeded in triplicate in 6-well plates and treated with 100 nM 4-OHT for 14 days. β -galactosidase measurement was performed by following the protocol of the Senescence β -Galactosidase Staining Kit (Cell Signaling), and at least 1000 cells were analyzed for each condition.

BrdU proliferation assay

BJ cells were seeded in 6-well plates on day 1. Next morning, cells were incubated in fresh medium for 3 h with 30 μ M bromodeoxyuridine (BrdU, Sigma) followed by two times PBS wash and then fixed with 4% formaldehyde. Cells were washed two times with PBS and treated with 5M HCl/0.5% Triton to denature DNA. Cells were neutralized with 0.1M Na₂B₄O₇. The cells were then treated with blocking buffer (3% BSA in 0.5% Tween PBS) for 30min and incubated with anti-BrdU antibody (Dako) with blocking buffer for 2 hours at room temperature. Cells were washed with PBS three times, and finally incubated with FITC-conjugated anti-mouse Alexa Fluor 488 secondary antibody (Dako) in blocking buffer for 1 hour, washed three times, stained with propidium iodide for 30min. BrdU incorporation was measured by immunofluorescence (at least 1000 cells were scored for each condition). The numbers of individual nucleus and BrdU-stained nucleus were counted using imageJ software.

Luciferase reporter assay

The constructs with the enhancers were cloned based on pGL3-promoter (Promega) vector. The enhancer region was PCR amplified from BJ genomic DNA and inserted downstream of the firefly luciferase reporter gene. The transfection was performed by seeding 1×10^5 of cultured cells in 6-well plates. The next day, 500ng of each construct (pGL3-promoter, pGL3-Enh^{API-OIS1}-Fw, and pGL3-Enh^{API-OIS1}-Rv) were co-transfected with 50ng of Renilla luciferase reporter construct using Fugene-6 (Promega) following manufacturer's protocol. Luciferase reporter assay was performed 24h post transfection using Dual-Luciferase Reporter assay kit (Promega). Cells were lysed directly on the plate with passive lysis buffer for 15min at room temperature. Firefly and Renilla luciferase activity was measured with the substrates from the kit using Centro XS3 LB960 machine (Berthold technologies). For BJ-indRAS^{G12V}, cells were pre-treated with 100nM 4-OHT for 48h prior transfection. For HCT116, cells were treated with UV-C (50J/m²) or MG132 (5μM) 18h after transfection. The luciferase assay was performed 5h post treatment.

Mutagenesis of Enh^{API-OIS1}

Mutations of Enh^{API-OIS1} were performed using QuikChange Lightning site-directed mutagenesis kit (Agilent) according to the manufacture's manual. Briefly, primers for mutagenesis were designed using the online tool from Agilent. pGL3-Enh^{API-OIS1}-Fw and pGL3-Enh^{API-OIS1}-Rv were PCR amplified and transformed into DH5α bacteria. Single colonies from each mutant were sequence verified and used for transfection.

RNA isolation, reverse transcription and qRT-PCR

Total RNA was extracted by using TRIsure (Bioline) reagent and following the manufacturer's protocol. Reverse transcription was done with SuperScript III (Invitrogen) using 1 μg of total RNA per reaction. qRT-PCR reaction was performed using SensiFAST SYBR No-ROX Kit (Bioline) in LightCycler 480 (Roche). Primers used are listed in Table S4.

Western blot

1×10^6 Cells were seeded in 10cm dish and treated with DMSO or 4-OHT for 14 days. Cells were trypsinized and cell pellets were lysed with RIPA buffer supplemented with 1x cOmplete protease inhibitor cocktail (Roche) following the manufacturer's protocol. Protein concentrations were determined using Pierce BCA protein assay kit (Thermo Scientific). Lysates were separated on SDS-PAGE gels and transferred Membranes were immunoblotted with the following antibodies: CDKN1A (Sc-397, Santa Cruz; 1: 1,000), HRAS (C-20, Santa Cruz; 1: 1,000), FoxF1 (ab168383, Abcam, 1:1000), HSP90 (610418, BD biosciences, 1:3000). Protein bands were visualized using corresponding secondary antibodies (Dako) and ECL reagent (GE Healthcare).

Lentiviruses production and infection

HEK293T cells were seeded at the density of 5×10^6 cells per 10cm dish one day prior transfection. Transfection was performed using PEI (Polyethylenimine, Polysciences) and medium was refreshed after 16h. Virus-containing supernatant was collected 48h post transfection by filtering through a $0.45 \mu\text{m}$ membrane (Milipore Steriflip HV/PVDF) and snap-frozen, stored at -80°C . BJ cells were infected and selected with the proper antibiotics 48 h after transduction for at least 4 days until no surviving cells remained in the no-transduction control plate.

Chromatin Conformation Capture (3C) analysis

10×10^6 cells were harvested in PBS for each 3C sample. Cells were centrifuged at 300xg for 5min at RT, and resuspended PBS / 10% FBS. Then cells were incubated with equal volume of 4% formaldehyde (2% end concentration) for 10min and quenched with 2M glycine solution (0.2M end concentration), followed by centrifugation at 300xg for 5min at 4°C . Cell pellet was then resuspended in PBS / 10% PBS and centrifuged at 300xg for 5min at 4°C . The supernatant was then discarded and snap-frozen, stored at -80°C . The cell pellet was lysed in 3mL lysis buffer (50mM Tris -HCl pH 7.5, 0.5% NP-40, 1% Triton X-100, 150mM NaCl, 5mM EDTA, protease inhibitor cocktail (Roche)) for 1.5h at 4°C , followed by centrifugation at 1000xg for 3min. The pellet was washed once in 1.2x restriction buffer and resuspended again in 500 μL of 1.2x restriction buffer. 15 μL of 10% SDS was added to the suspension and incubated at 37°C while shaking at 400rpm. 75 μL of 20% Triton X-100 was added to the suspension and incubated at 37°C while shaking at 400rpm. The samples were then centrifuged at 1000 x g for 3min and resuspended in 500 μL of 1x restriction buffer. The digestion was performed with addition of 200U of Csp6I (Thermo Fisher Scientific) at 37°C overnight. The digestion efficiency was assessed the next day on agarose gel. The enzyme was then inactivated at 65°C for 20min and then samples were centrifuged at 1000 x g for 3min to remove the restriction buffer. The pellet was resuspended in 7mL of 1x ligation buffer, and the ligation was performed with addition of 50U of T4 DNA ligase at 16°C overnight. Again, the ligation efficiency was examined on agarose gel. De-crosslinking was performed by addition of 30 μL of protease K (Roche) at 65°C overnight. To remove residual RNA, 15 μL of RNaseA cocktail (Ambion) was added to the samples and incubated at 37°C for 45min. DNA was recovered by adding 7mL of isopropanol and 70 μL of NucleoMag 96 PCR beads (Bioke) and incubated for 30min at room temperature. The samples were centrifuged for 3min at 1000 x g and washed with 80% ethanol twice. Finally, the beads were dried and eluted in 300 μL of 10mM Tris-HCl pH 7.5. To assess the physical interactions between Enh^{API-OIS1} and target regions, we designed a constant primer (C1) that amplify the Enh^{API-OIS1} region overlapping the junction created by Csp6I enzyme. For each assessed region, we designed two primers (reverse and forward) to examine the interactions with Enh^{API-OIS1}. The first PCR was performed with primer C1 and each candidate primer for 25 cycles. Afterwards, a nested PCR was performed using a second

constant primer (C2) and each candidate primer for another 18 cycles. Finally, PCR products were resolved on 2% agarose gel. To assess the primer efficiency, we PCR amplified the genomic regions of *Enh^{API-OIS1}* and *FOXF1*, and mixed equal molar of each fragments as the template. The template DNA was then digested and ligated as mentioned. Finally, the quantifications were normalized with the primer efficiencies. To examine the sequences of the PCR products, DNA bands were cut, isolated, and sanger-sequenced.

Mutation analysis of enhancer regions

Genomic DNA of the cells transduced with sgRNAs were isolated and quantified. 500ng of the genomic DNA was used for PCR to amplify the enhancer region. We performed a two-step PCR by introducing the P5 adapter sequences in the first PCR and P7 adapters with the indexes in the second PCR. After the second PCR, the libraries were purified with CleanPCR beads (CleanNA) and quantified on 2100 Bioanalyzer using a 7500 chip (Agilent). Equimolar of each sample was taken for the final library. Libraries were sequenced using the Mi-Seq platform. Sequenced reads were aligned to the amplified enhancer region using bowtie. Bam files were analysed to count the number of mutations (mismatches, insertions or deletions) identified at each location in that region.

RNA-seq library construction

Total RNA was isolated using Trisure reagent (Bioline) following the manufacturer's protocol. Briefly, cells were lysed in Trisure, precipitated with isopropanol, and dissolved in RNase-free water. To generate strand-specific libraries, we used the TruSeq Stranded mRNA sample preparation kit (Illumina) following the manufacturer's instructions. Briefly, 1000ng of total RNA was polyA-enriched using oligo-dT beads, and the RNA was fragmented, random primed and reverse transcribed using SuperScript II Reverse Transcriptase (Invitrogen). Second strand cDNA was then synthesized, 3'-adenylated and ligated to Illumina sequencing adapters and subsequently amplified by 12 cycles of PCR. The sequencing libraries were analyzed on a 2100 Bioanalyzer using a 7500 chip (Agilent), and pooled equimolar into a 10nM multiplex sequencing pool.

Sequencing

Sequencing of the CRISPR screen and RNA-seq was done using single reads of 65bp on the Hi-Seq2500 platform (Illumina). Mutation analysis of enhancer regions were performed with single reads of 150bp on the Mi-Seq system with Mi-Seq reagent v2 Nano kit.

RNA-seq analysis

Gene expression profiles were recorded in BJ-indRAS^{G12V} (14 days after RAS induction by 4-OHT treatment) transduced with CRISPR vectors that either targeted the *Enh^{API-OIS1}* using sgRNA-API⁶⁹, sgRNA-API⁷¹, targeted *FOXF1* itself or transduced with a

control non-targeting sgRNA (sgRNA-NT). Sequenced reads were aligned to the human genome (hg19) using TopHat2 (48). Number of reads mapped to each annotated gene was counted using HTseq-count (45), and then converted to RPKMs (using GENCODE v25 annotations). RPKM levels were further normalized using quantile normalization and expression levels in each sample relative to the control non-targeting sample were calculated (in log2 base). Biological pathways and processes affected by targeting the *Enh^{AP1-OIS1}* or *FOXF1* were sought using gene-set enrichment analysis (GSEA) (23).

Results

Genome-wide identification of OIS-induced enhancers

We previously carried out a CRISPR-based screen aimed at identification of p53-bound enhancers that are required for OIS(17). That screen was confined to regions that are directly bound by p53 as detected by p53 ChIP-seq analysis, and therefore missed enhancers that are critical for OIS enforcement and are regulated by other TFs, in either p53-dependent or independent manner. To overcome this limitation and to globally screen DNA regulatory elements activated by OIS without being biased by preselection of a candidate TF, we first sought to comprehensively detect all the enhancers that are activated upon oncogenic stress. To this goal we utilized Global Run-On sequencing (GRO-seq), a nascent RNA detection method (19), that allow robust determination of eRNA expression, as a quantitative measure for enhancer activity (7,8,18). We used a cellular system in which the oncogene RAS^{G12V} was induced in hTERT-immortalized BJ cells (BJ-indRAS^{G12V}). As these cells contain wild-type p53, oncogenic stress results in a very potent activation of OIS and proliferation arrest (20). Exploiting bi-directional transcription as a hallmark of transcriptional activity at enhancers and promoters (7,21,22), we detected 1,821 regulatory elements whose activity was induced in BJ-indRAS^{G12V} upon oncogene induction for 14 days (Fig. 1A; Table S1). Next, we bioinformatically searched for TFs that potentially mediate the activation of these regions by performing *de novo* DNA motif enrichment analysis. Remarkably, we found that the regulatory regions activated during the induction of OIS were significantly enriched for the binding motif of the AP1 (FOS:JUN) transcription factor (TF) (Fig. 1B). Overall, these results suggest an important role for AP1 in the regulation of the transcriptional response to oncogenic stress.

Therefore, we constructed a CRISPR library that systematically targets OIS-induced DNA elements that are putatively regulated by AP1, and performed a functional genetic screen to identify those that are required for OIS activation. The *de novo* motif analysis detected 762 AP1 motifs in 638 OIS-induced regulatory elements (over-representation p-value=1.2*10⁻⁸⁸). We examined which of these motif occurrences can be targeted by CRISPR-Cas9, given the requirement for the presence of the NGG PAM motif near the

AP-1 motif. We required that the Cas9-mediated DNA cut will occur either within the motif itself or up to a margin of 5 nt with respect to it (Fig. 1C). 398 (62%) of the 638 OIS-induced regulatory elements (REs) containing AP1 motif met this criterion, with most motifs targeted by 2-3 distinct sgRNAs. Accordingly, we designed 840 sgRNAs that target AP1 motifs in 398 OIS-induced regulatory elements. We cloned these sgRNAs as a pool into pLentiCRISPRv2 vector, and generated a plasmid library referred herein as *CRISPR-AP1-EnhLib* (Fig. 1D and Table S2).

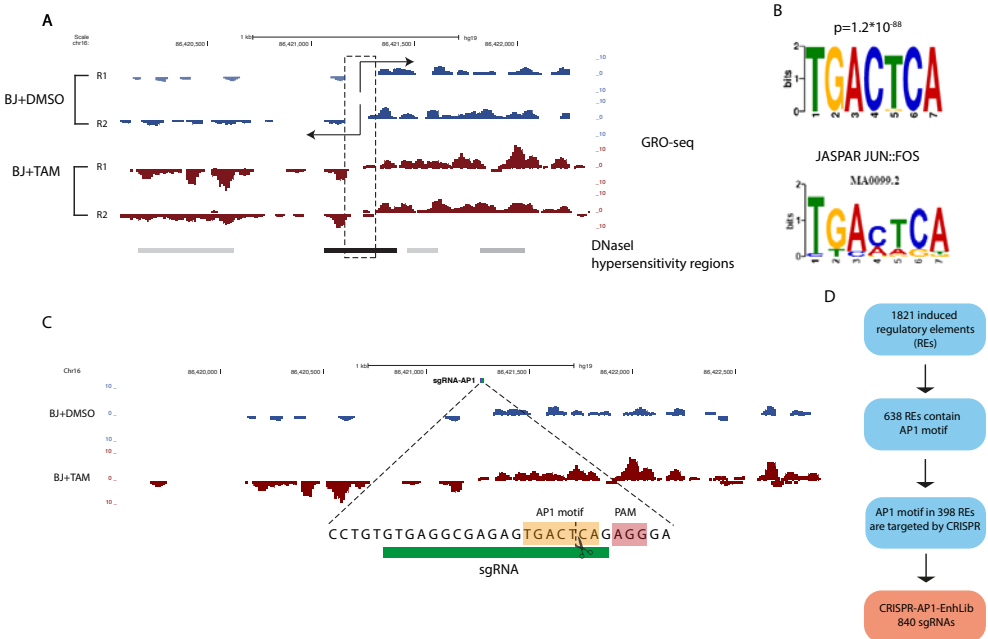


Figure I. Design of a CRISPR screen targeting API enhancers which are activated upon oncogenic stress.

A. An example of an enhancer whose activity is induced in response to oncogenic stress. Enhancer activity is inferred from the typical bi-directional transcription of eRNAs (BJ+DMSO indicates proliferating cells, and BJ+4-OHT indicates senescent cells); Genomic regions that show DNase hypersensitivity (DHS), as determined by ENCODE, are shown by the grey track). Overall, our GRO-seq analysis identified 1,821 regulatory elements (REs; enhancers or promoters) whose activity was induced in BJ cells in face of RAS activation. **B.** *De novo* motif analysis detected highly significant enrichment of the FOS:JUN (AP1) DNA motif in the regulatory elements that were induced upon oncogenic stress. Top – the enriched motif detected in our dataset; bottom – the AP1 motif from the JASPAR DB (49). **C.** An example for occurrence of an AP1 motif within an enhancer that was induced upon oncogenic stress, that is located close enough to an NGG PAM motif, resulting in Cas9-mediated DNA cleavage that occur within the motif (Cas9 cleavage occurs ~3 nt before the PAM). Overall, we identified 398 induced REs with AP1 motif that met this requirement (Cas9 cleavage within a margin of 5 nt with respect to the motif). **D.** Statistical summary of the *CRISPR-AP1-EnhLib* used in our functional screen.

CRISPR screen targeting OIS-induced enhancers with AP-I motif

We used the *CRISPR-API-EnhLib* library to screen for DNA elements that are putatively regulated by API and are required for the activation of OIS. BJ-indRAS^{G12V} were transduced with four independent lentiviral pools of *CRISPR-API-EnhLib* and selected with puromycin. Then we treated the cells with 4-OHT (RAS induction) or DMSO (control) as shown in Figure 2A. Following four weeks of culturing, we harvested the cells, isolated genomic DNA, amplified integrated vectors by PCR, and used next-generation sequencing (NGS) to quantify the abundance of integrated sgRNAs present in each population. We reasoned that sgRNAs targeting regulatory elements that are required for OIS would cause bypass of senescence, sustained cell proliferation, and thus would be enriched in the cell population under oncogenic stress compared to control (Fig. 2A). Indeed, our screen detected several sgRNAs that were highly enriched in the OIS population (Fig. 2B; Table S3), among them, five showed an average enrichment fold above 1.75 over the four replicates of the screen. Notably, two of these five sgRNAs, sgRNAs-API⁶⁹ and sgRNA-API⁷¹, are independent sgRNAs that target the same enhancer region (Fig. 2B), hence increasing the confidence that these are true positive hits. ENCODE ChIP-seq data confirmed a strong binding of both FOS and JUN to this region (Figure S1). Moreover, our GRO-seq data showed ~2-fold induction of eRNA expression from this enhancer in response to oncogenic stress. Thus, we selected this regulatory region for further validation and functional characterization and named it *Enh*^{API-OIS1}.

First, using individual transductions, we validated that the introduction of sgRNAs API⁶⁹ and API⁷¹ to BJ-indRAS^{G12V} cells causes a potent bypass of OIS, as judged by cell number and morphology (Fig. 2C). Second, we confirmed that introduction of these two sgRNAs to BJ-indRAS^{G12V} cells indeed results in an array of small deletions and insertions at the expected position within the API binding motif in the targeted enhancer (Figure S2). Third, following induction of oncogenic stress, sgRNAs API⁶⁹ and API⁷¹ transduced BJ-indRAS^{G12V} cells showed a significant reduction in senescent-associated-β-Gal (SA-β-Gal) staining (Fig. 2D, Figure S3) and an elevated BrdU staining (Fig. 2E, Figure S3), indicative of attenuated activation of cellular senescence and of sustained cellular proliferation compared to the NT control. As expected, while the effect caused by these two sgRNAs was highly significant, it was not as strong as the effect elicited by targeting p53 (Fig. 2D-E). Last, we examined the activity of *Enh*^{API-OIS1} following the transduction of sgRNAs API⁶⁹ and API⁷¹ by measuring eRNA expression at the *Enh*^{API-OIS1} locus. As expected, targeting *Enh*^{API-OIS1} by these two sgRNAs significantly compromised its activity during OIS compared to the control sgRNA (Fig. 2F).

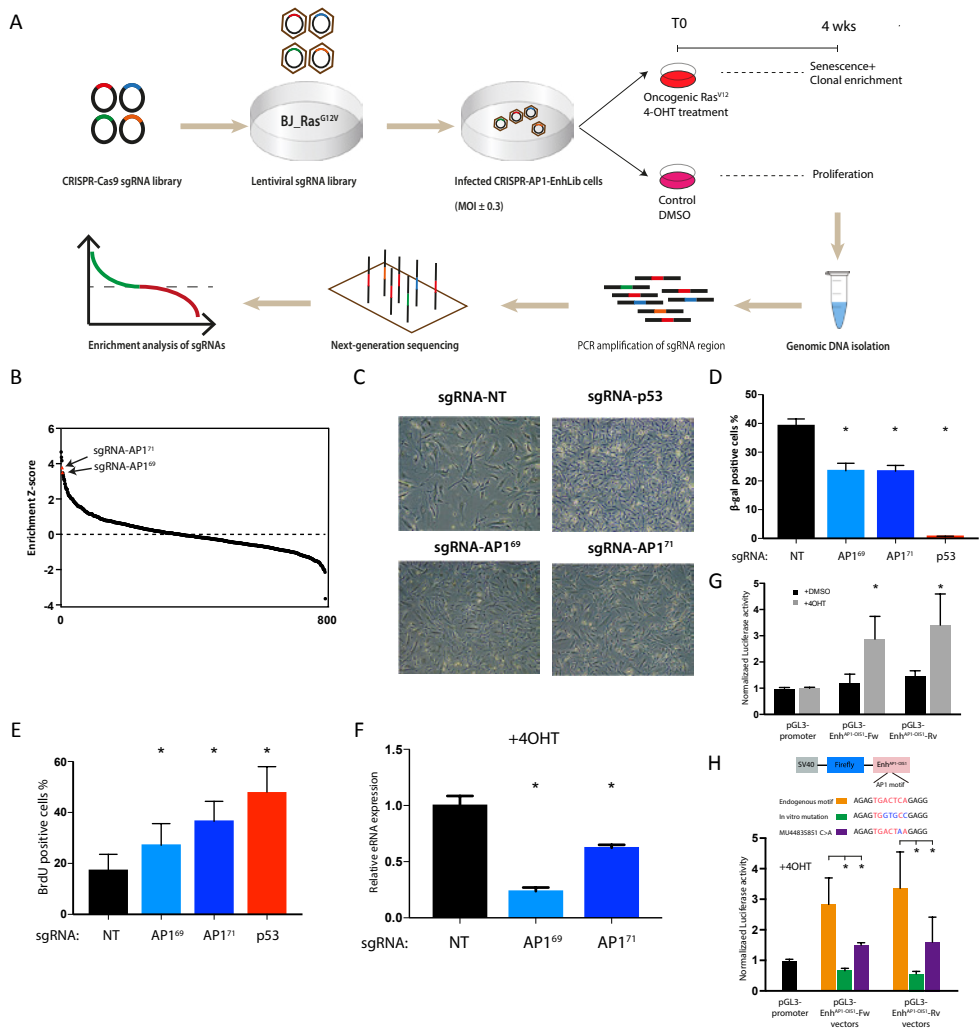


Figure 2. Functional CRISPR screen discover a novel enhancer required for OIS.

A. Schematic representation of the set-up of our functional screen. **B.** Results of the CRISPR screen. sgRNAs are sorted by the enrichment score based on the ratio between their prevalence in the BJ+4-OHT and BJ +DMSO control populations (measured 4 weeks after 4-OHT treatment). Y-axis shows Z scores of the mean sgRNA enrichment scores (calculated over the four replicates of the screen). Coloured in red are two sgRNAs, sgRNA-AP1⁶⁹ and sgRNA-AP1⁷¹, that target the same enhancer, called here *Enh*^{AP1-OIS1}. **C.** Individual transductions of sgRNA- AP1⁶⁹ and sgRNA-AP1⁷¹ validated that they cause OIS bypass. sgRNA targeting p53 was used as a positive control and a non-targeting (NT) sgRNA was used as a negative control. **D.** Targeting *Enh*^{AP1-OIS1} by either sgRNA- AP1⁶⁹ or sgRNA-AP1⁷¹ caused OIS bypass as measured by β-gal staining, a canonical mark for senescence (p53ko used as a positive control). Data shown represents mean (SD), n=4. *p<0.05. **E.** Targeting *Enh*^{AP1-OIS1} by either sgRNA- AP1⁶⁹ or sgRNA-AP1⁷¹ resulted in enhanced proliferation as measured by BrdU staining (p53ko used as a positive control). Data shown represents mean (SD), n=4. *p<0.05. **F.** Measurement of eRNA production at *Enh*^{AP1-OIS1} in cells with the indicated sgRNAs. eRNA levels are significantly decreased upon mutagenesis of the AP1 binding site caused by either sgRNA- AP1⁶⁹ or sgRNA-AP1⁷¹. Data shown represents mean (SD), n=3. *p<0.05. **G.** BJ-indRAS^{G12V} cells were transfected with

the indicated plasmids, and treated with DMSO or 4-OHT for 72h. pGL3 constructs contain firefly luciferase reporter gene with the corresponding enhancer (none for pGL3-promoter, two different orientations for *Enh^{AP1-OIS1}*). Relative luciferase activity is calculated by dividing the firefly luciferase activity to that of Renilla luciferase. Normalized luciferase activity is calculated by dividing the relative luciferase activity to that of pGL3-promoter for each condition. Data shown represents mean (SD), n=6. *p<0.05. **H.** BJ-indRAS^{G12V} cells were transfected with the indicated enhancer constructs. Endogenous motif represents the original sequence of *Enh^{AP1-OIS1}*, in vitro mutation construct represents mutagenesis of the AP1 consensus motif, and MU44835851 represents mutant construct bearing a C>A mutation as indicated. The cells were treated with 4-OHT for 48h prior transfections. Data shown represents mean (SD), n=3. *p<0.05.

Next, we carried out *in vitro* reporter assays to verify that *Enh^{AP1-OIS1}* functions as enhancer and promotes transcription of target genes. We cloned *Enh^{AP1-OIS1}* downstream of the Firefly luciferase gene in two orientations in pGL3-promoter vector followed by transfection into BJ-indRAS^{G12V} cells. While we did not observe a noticeable elevation of luciferase activity in cells treated with DMSO, there was a significant increase of 3-fold in cells treated with 4-OHT (Fig. 2G). To verify that mutations in the AP1 binding site disrupts the enhancer activity as we observed in sgRNA-AP1^{69/71} cells, we mutated the AP1 motif of *Enh^{AP1-OIS1}* and examined the effect on the enhancer activity, in condition of oncogenic stress. Indeed, the mutations completely abolished the ability of *Enh^{AP1-OIS1}* to stimulate luciferase expression (Fig. 2H). In addition, we searched for tumor somatic mutations within the AP1 binding motif (using ICGC data), and found one case in a lung cancer patient (Figure S4). The mutation is a C to A substitution within the consensus motif of AP1, and located at the cut site of sgRNA-AP1⁶⁹. To examine if this somatic mutation disrupts the activity of *Enh^{AP1-OIS1}*, we performed mutagenesis of *Enh^{AP1-OIS1}* on the reporter construct with a single nucleotide substitution. Remarkably, we observed a 50% reduction of the enhanced luciferase activity (Fig. 2H), suggesting an important role of the specified nucleotide in determining binding affinity of AP1 to this enhancer. Taken together, our functional genetic screen and subsequent focused experiments have identified and validated a novel AP1-bound enhancer whose activity is required for proper induction of OIS.

FoxF1 is a target gene of *Enh^{AP1-OIS1}*

Next, we set up experiments to elucidate the mode of action by which *Enh^{AP1-OIS1}* is required for OIS. Enhancers regulate gene expression of cis-located target genes that can reside hundreds of kbp away. Examination of our GRO-seq data indicated that *FOXF1*, the nearest gene to the *Enh^{AP1-OIS1}* locus (located >100 kbp downstream of it), was ~2 fold induced following oncogenic stress (Fig. 3A), suggesting a potential functional connection. No other gene in a 1 Mbp distance from *Enh^{AP1-OIS1}* showed such a strong effect. Furthermore, we performed RNA-seq with cells transduced with sgRNA-AP1⁶⁹ and sgRNA-AP1⁷¹, and observed a significant reduction in the expression of FOXF1 (Figure S5). We validated this result using qRT-PCR analysis, which also indicated that targeting *Enh^{AP1-OIS1}* by either sgRNA-AP1⁶⁹ or sgRNA-AP1⁷¹ results in a significant

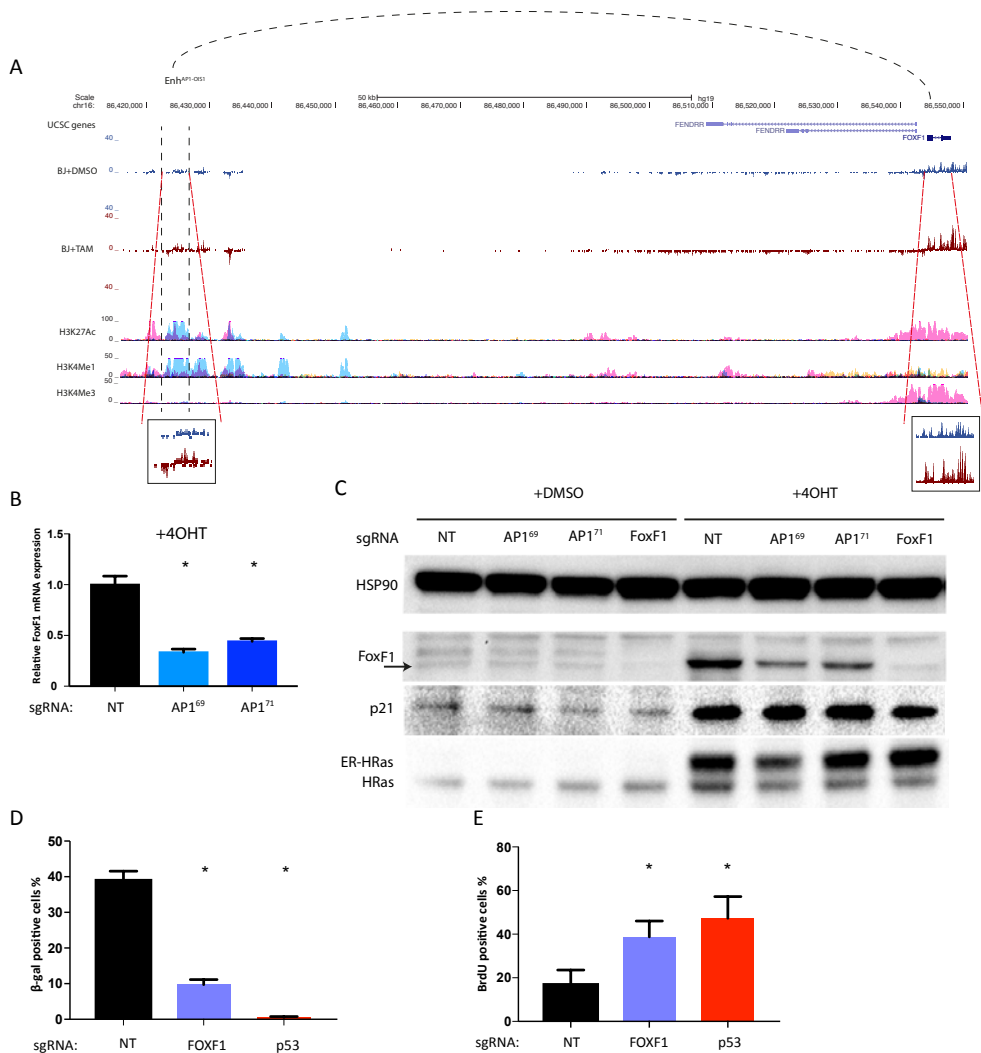


Figure 3. FOXF1 is the target gene regulated by $Enh^{AP1-OIS1}$.

A. UCSC screenshot of GRO-seq analysis of BJ-indRAS^{G12V} cells. BJ cells were treated with DMSO or 4-OHT for 14 days. Bidirectional transcription is represented by using positive and negative values for expression in the Crick and Watson strands, respectively. The genomic regions of $Enh^{AP1-OIS1}$ and $FOXF1$ are enlarged. Note the enhancement in GRO-seq signal for both $Enh^{AP1-OIS1}$ and $FOXF1$ in BJ+4-OHT (brown track) compared to BJ+DMSO (blue track). **B.** mRNA levels of FOXF1 are reduced in sgRNA-AP1⁶⁹ and sgRNA-AP1⁷¹ targeted cells under 4-OHT treatment. Data shown represents mean (SD), n=3. *p<0.05. **C.** BJ-indRAS^{G12V} cells transduced with the specified sgRNAs were treated with DMSO or 4-OHT for 14 days, and FOXF1, p21, and HRas protein levels were measured by western blot. HSP90 was used as the loading control. The band of FOXF1 is marked with an arrow. ER-HRas indicates the induced version of HRas. **D.** Targeting the $FOXF1$ and $p53$ genes caused OIS bypass as measured by β -gal staining. Note the stronger effect of FOXF1ko compared to the effect elicited by targeting $Enh^{AP1-OIS1}$ (Fig. 2D). Data shown represents mean (SD), n=4. *p<0.05. **E.** Targeting $FOXF1$ and $p53$ gene resulted in enhanced proliferation as measured by BrdU staining. Data shown represents mean (SD), n=4. *p<0.05.

reduction in the expression level of FOXF1 under OIS conditions (Fig. 3B). Western blotting analysis confirmed this result at the protein level, in addition to confirming that FOXF1 expression is increased following oncogenic stress (Fig. 3C). Publicly available RNA Pol II ChIA-PET data (from HeLa cells) indicate physical interaction between *Enh^{API-OIS1}* and the 3' region of *FOXF1* (Figure S6), which was confirmed in the chromatin conformation capture (3C) experiments of senescent BJ cells (Figure S7). More importantly, the physical interactions between *Enh^{API-OIS1}* and the promoter region of *FOXF1* were significantly stronger (Figure S7), suggesting a robust transcriptional regulation of *Enh^{API-OIS1}*. Collectively, these results strongly point to *FOXF1* as the target gene of *Enh^{API-OIS1}*.

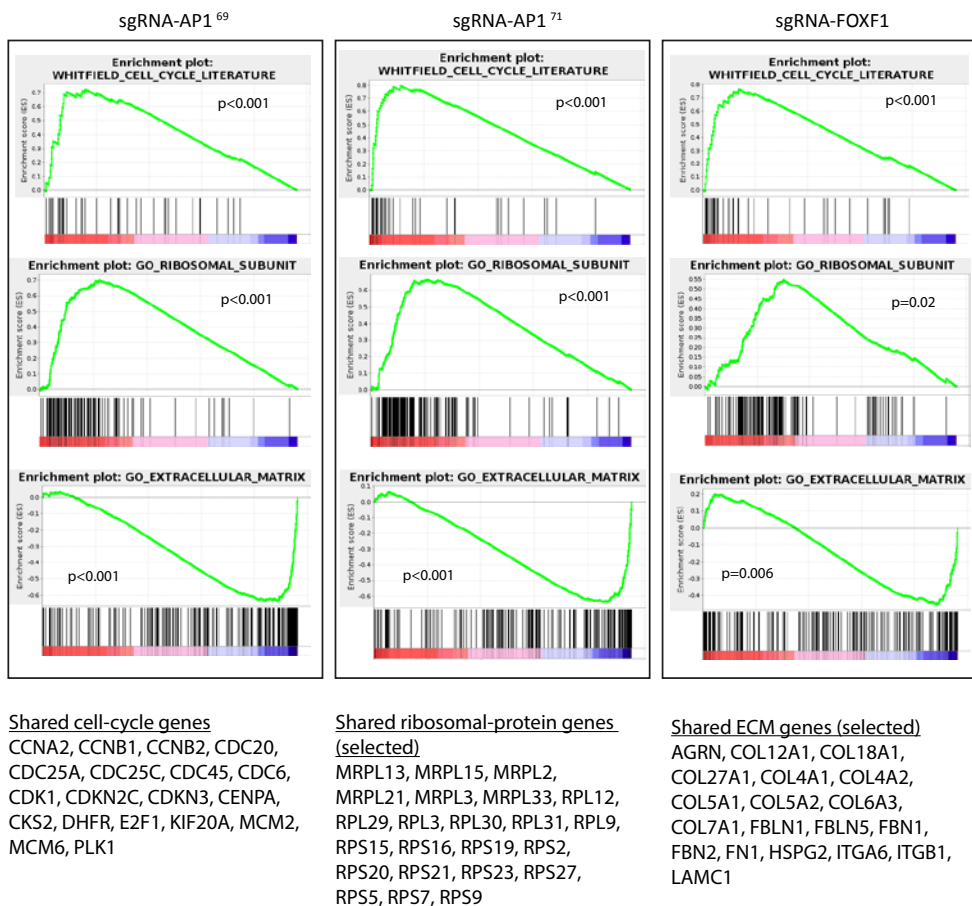


Figure 4. *Enh^{API-OIS1}* and FOXF1 knockouts display expression profiles of senescence bypass.

GSEA analysis of expression profiles measured in 4OHT-treated BJ-indRAS^{G12V} cells targeted by sgRNA-AP1⁶⁹, sgRNA-AP1⁷¹, or sgRNA-FOXF1 compared to the profile of control 4OH-treated cells transduced with non-targeting sgRNA. A list of shared genes within each group is shown.

Loss of FOXF1 causes senescence bypass and abolishes senescence expression signatures

To further establish *FOXF1* as the target gene that links *Enh^{AP1-OIS1}* to senescence, we examined the phenotypic effect of knocking out *FOXF1*. Indeed, targeting *FOXF1* results in a strong senescence bypass phenotype, as evident by significant reduction in SA- β -Gal staining (Fig. 3D) and elevated BrdU staining (Fig. 3E), similar to the effect elicited by targeting *Enh^{AP1-OIS1}* (Fig. 2E-F). Effective *FOXF1* knockout was confirmed by western blotting analysis (Fig. 3C). Last, we used RNA-seq to globally compare expression profiles in BJ-indRAS^{G12V} cells transduced with either sgRNAs targeting *Enh^{AP1-OIS1}* (sgRNA-AP1⁶⁹ or sgRNA-AP1⁷¹), sgRNA targeting *FOXF1*, or a control non-targeting sgRNA. Gene-set enrichment analysis (GSEA) (23) for functional characterization of the biological processes affected by these genetic manipulations showed that cell-cycle genes and genes encoding ribosomal proteins are significantly up-regulated when targeting either *Enh^{AP1-OIS1}* or *FOXF1*, reflecting the bypass of OIS and the subsequent enhanced proliferation experienced by these cells following oncogene hyperactivity (Fig. 4). Conversely, the induction of various extra cellular matrix (ECM) components that is exhibited in OIS was largely attenuated in cells with *Enh^{AP1-OIS1}* or *FOXF1* knockouts (Fig. 4). Taken together, our results strongly indicate that *Enh^{AP1-OIS1}* controls OIS through the regulation of *FOXF1* expression (Fig. 5).

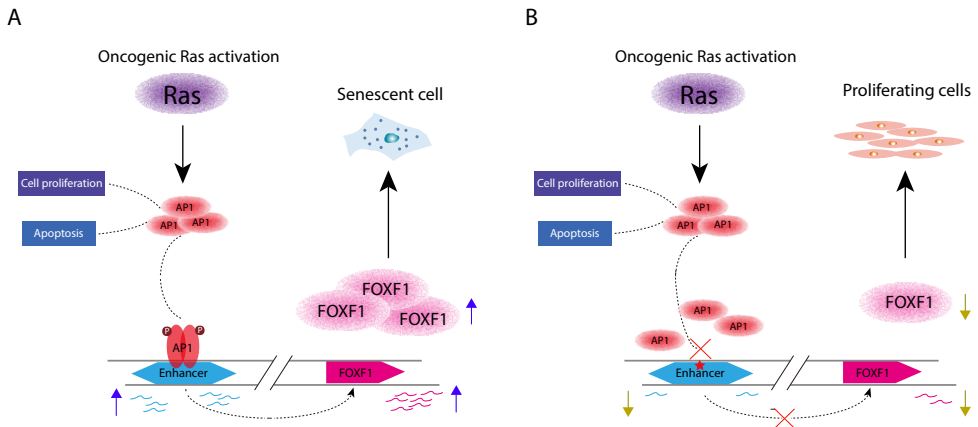


Figure 5. Model of *Enh^{AP1-OIS1}* regulation of OIS.

A. In normal BJ fibroblast cells, hyper-activation of RAS induces MAPK signaling cascade, including AP-1 TFs. Activated AP-1 TFs control different cellular functions, including cell proliferation and apoptosis. AP1 is recruited, among other enhancers, to *Enh^{AP1-OIS1}* and stimulates its activity. This in turn promotes the expression of the target gene FOXF1, diverting oncogenic signals into pre-senescent pathway. **B.** Mutagenesis of the AP-1 binding site in *Enh^{AP1-OIS1}* abrogates its enhancer activity and thus leading to decreased expression of FOXF1. This results in compromised induction of OIS and thus cells continue uncontrolled cell proliferation.

Discussion

In this study, we first found that OIS-induced enhancers are enriched for the binding motif of AP1. Based on this finding, we perform a CRISPR screen focused on AP1 motifs within enhancers that are activated upon oncogenic stress. We discovered a novel AP-1 bound enhancer, *Enh^{AP1-OIS1}*, that is required for establishment of OIS and identified FOXF1 as the target that mediates this role. We propose a new role of AP1 in senescence via activation of FOXF1, providing an additional regulation of cell proliferation during senescence.

AP1 TFs are recruited to enhancer regions to drive oncogenic growth (24) and are broadly required for enhancer selection (25), suggesting a possible role of AP1 at enhancers. As a downstream target of RAS signalling pathway, AP1 is activated to target mitogen-responsive genes (26,27). Earlier studies have shown that mRNA level and activity of AP1 genes are attenuated upon entering replicative senescence (28,29). Altered AP1 activity is mainly due to loss of c-FOS expression and maintained JUN proteins, thus promoting JUN-JUN homodimers instead of FOS-JUN heterodimers (29,30). This suggests that loss of AP1 activity is possibly responsible for the irreversible growth arrest in senescent cells. Conversely, overexpression of c-FOS with increased AP1 activity is not sufficient to initiate DNA synthesis in senescent human fibroblasts (31). Therefore, AP1 is likely not the key factor that regulates senescence, but rather a downstream factor that fine-tune the senescence program under replicative stress (e.g. H-RAS activation). In addition, previous functional genetic screens did not indicate any of the AP1 family members as critical factors in OIS (20,32). Supporting this conclusion, CRISPR-mediated KO of c-FOS and c-JUN did not result in any obvious bypass of OIS (Figure S8). However, it is possible that one or few targets of AP1 mediate OIS while others antagonize it, or are required for cell survival.

FOXF1 belongs to the Forkhead family of transcription factors. FOXA1 has been reported to promote senescence via activation of p16^{INK4a} (33), and FOXO4 inhibition induces p53 nuclear exclusion, which results in apoptosis of senescent cells (34). The functions of FOXF1 remain to be determined, yet recent studies have implicated its role in lung regeneration by targeting genes of extracellular matrix and cell cycle progression (35), as well as promoting prostate cancer growth via MAPK pathway (36). To date, there has been no evidences of any connections between AP1, FOXF1 and OIS, possibly due to regulation via enhancers, rather than proximal promoters, as proposed in this study. It has been proposed that FOXF1 is a target gene of p53, which regulates cell migration and invasion (37); and that FOXF1 is a potential oncogene, which promotes rhabdomyosarcoma by repressing p21^{Cip1} (38). Here we provide the first evidence suggesting that FOXF1 is a potential tumour suppressor, regulating senescence in human cells. In addition, we generated double knockout cell lines (NT+p53 ko, sgRNA-AP1⁶⁹⁺

p53 ko, sgRNA-AP1⁷¹+ p53 ko, and FOXF1 ko + p53 ko), and we observed a strong senescence bypass phenotype (Figure S9A-B). Interestingly, we found an additive effect of proliferation in the EnhAP1-OIS1 ko and FOXF1 ko cell lines (sgRNA-AP1⁶⁹+ p53 ko, sgRNA-AP1⁷¹+ p53 ko, and FOXF1 ko + p53 ko) compared with NT + p53 ko cells (Figure S9B). This suggests that FOXF1 regulates OIS in a p53 independent manner. In parallel with the canonical p53 pathway, FOXF1 regulates the expression of a subset of cell cycle and ribosomal genes (Fig. 4). Further studies should explore the exact function of FOXF1 in regulating senescence.

We propose a model in which following oncogenic induction, AP1 TFs are activated to promote cellular proliferation in response to stimuli. However, under excessive exposure to RAS, AP1 is recruited to *Enh^{AP1-OIS1}* to promote the expression of FOXF1 to drive cells into senescence. Disruption of the AP1 binding site within *Enh^{AP1-OIS1}* results in attenuated activation of FOXF1, hampering full execution of the OIS program. We attempted to generate a FOXF1 overexpression cell line while targeting *Enh^{AP1-OIS1}*, to rescue the senescence phenotype. However, this was not successful, possibly due to the intolerance of the cells under ectopic FOXF1 expression. This result show that although AP1 is activated by MAPK pathway, and stimulates the expression of many cell cycle genes, upon oncogenic stress it also mediates tumor suppressive effects.

Our current knowledge on cancer driver non-coding somatic mutations (SMs) is still very rudimentary, yet several studies suggested that the role of such SMs is underappreciated(39,40). Genome-wide analysis has revealed AP1 as a key factor at regulatory elements in cancers(41), and AP1 binding sites are frequently mutated in various cancer types (42). Analysing ICGC data, we found a somatic mutation within the AP1 motif of *Enh^{AP1-OIS1}* in a lung cancer patient, and validated its functional effect by using in vitro reporter assays (Fig. 2H). This suggests a possible cancer driver effect for somatic mutations in AP1 binding motifs. Our study further demonstrates the power of CRISPR-based screens in exploring the function of the noncoding genome.

Conclusions

Our study provides evidence that AP1 TFs are broadly stimulated during OIS and are localized to enhancer regions to activate specific gene programs. We show that AP1 controls senescence program via *Enh^{AP1-OIS1}* and its target gene *FOXF1*. We propose that AP1 is a double-edged sword in regulating cell proliferation and senescence, providing a restrictive feedback on unlimited cell proliferation.

Acknowledgement

We thank Hans Teunissen and Elzo de Wit for the help on the 3C experiment and all members of the Agami laboratory for technical help and discussions. We are grateful to the NKI Genomics Core Facility for deep-sequencing our samples.

Funding

This work was supported by the ERC-AdG enhReg (322493 to R.A.), ERC-ITN RNA TRAIN (607720 to R.A.), China Scholarship Council (CSC) (to L.L.). The Human Frontier Science Program LT000640/2013 (to APU), The Dutch organization for research NWO-TOP 91216002 (to R.A). R.E. is supported by the Israeli Cancer Association (ICA), with the generous assistance of the ICA Netherlands friends, and by the Marguerite Stolz Research Fellowship Fund. Z.M. was supported in part by the Gad, Nava and Shye Shtacher fellowship. R.E. is a Faculty Fellow of the Edmond J. Safra Center for Bioinformatics at Tel Aviv University.

Data availability

RNA-seq data is available from the GEO DB accession number GSE112458.
GRO-seq data is available from the GEO DB accession number GSE109290.

References

1. ENCODE Project Consortium (2012) An integrated encyclopedia of DNA elements in the human genome. *Nature*, **489**, 57–74.
2. Djebali,S., Davis,C.A., Merkel,A., Dobin,A., Lassmann,T., Mortazavi,A., Tanzer,A., Lagarde,J., Lin,W., Schlesinger,F., *et al.* (2012) Landscape of transcription in human cells. *Nature*, **489**, 101–108.
3. Andersson,R., Gebhard,C., Miguel-Escalada,I., Hoof,I., Bornholdt,J., Boyd,M., Chen,Y., Zhao,X., Schmidl,C., Suzuki,T., *et al.* (2014) An atlas of active enhancers across human cell types and tissues. *Nature*, 10.1038/nature12787.
4. Banerji,J., Rusconi,S. and Schaffner,W. (1981) Expression of a β -globin gene is enhanced by remote SV40 DNA sequences. *Cell*, 10.1016/0092-8674(81)90413-X.
5. Heintzman,N.D., Stuart,R.K., Hon,G., Fu,Y., Ching,C.W., Hawkins,R.D., Barrera,L.O., Van Calcar,S., Qu,C., Ching,K.A., *et al.* (2007) Distinct and predictive chromatin signatures of transcriptional promoters and enhancers in the human genome. *Nat. Genet.*, 10.1038/ng1966.
6. Rada-Iglesias,A., Bajpai,R., Swigut,T., Brugmann,S.A., Flynn,R.A. and Wysocka,J. (2011) A unique chromatin signature uncovers early developmental enhancers in humans. *Nature*, 10.1038/nature09692.
7. Kim,T.K., Hemberg,M., Gray,J.M., Costa,A.M., Bear,D.M., Wu,J., Harmin,D.A., Laptevich,M., Barbara-Haley,K., Kuersten,S., *et al.* (2010) Widespread transcription at neuronal activity-regulated enhancers. *Nature*, **465**, 182–187.
8. de Santa,F., Barozzi,I., Mietton,F., Ghisletti,S., Polletti,S., Tusi,B.K., Muller,H., Ragoussis,J., Wei,C.L. and Natoli,G. (2010) A large fraction of extragenic RNA Pol II transcription sites overlap enhancers. *PLoS Biol.*, 10.1371/journal.pbio.1000384.
9. Amano,T., Sagai,T., Tanabe,H., Mizushima,Y., Nakazawa,H. and Shiroishi,T. (2009) Chromosomal Dynamics at the Shh Locus: Limb Bud-Specific Differential Regulation of Competence and Active Transcription. *Dev. Cell*, **16**, 47–57.
10. Bulger,M. and Groudine,M. (2011) Functional and mechanistic diversity of distal transcription enhancers. *Cell*, **144**, 327–339.
11. Levine,M. (2010) Transcriptional Enhancers in Animal Development and Evolution. *Curr. Biol.*, **20**, R754–R763.
12. Braig,M., Lee,S., Loddenkemper,C., Rudolph,C., Peters,A.H.F.M., Schlegelberger,B., Stein,H., Dörken,B., Jenuwein,T. and Schmitt,C.A. (2005) Oncogene-induced senescence as an initial barrier in lymphoma development. *Nature*, 10.1038/nature03841.
13. Lin,A.W., Barradas,M., Stone,J.C., Van Aelst,L., Serrano,M. and Lowe,S.W. (1998) Premature senescence involving p53 and p16 is activated in response to constitutive MEK/MAPK mitogenic signaling. *Genes Dev.*, **12**, 3008–3019.
14. Sage,J., Miller,A.L., Pérez-Mancera,P.A., Wysocki,J.M. and Jacks,T. (2003) Acute mutation of retinoblastoma gene function is sufficient for cell cycle re-entry. *Nature*, **424**, 223–228.
15. Serrano,M., Lin,A.W., McCurrach,M.E., Beach,D. and Lowe,S.W. (1997) Oncogenic ras provokes premature cell senescence associated with accumulation of p53 and p16(INK4a). *Cell*, **88**, 593–602.
16. Smogorzewska,A. and de Lange,T. (2002) Different telomere damage signaling pathways in human and mouse cells. *EMBO J.*, **21**, 4338–48.

17. Korkmaz,G., Lopes,R., Ugalde,A.P., Nevedomskaya,E., Han,R., Myacheva,K., Zwart,W., Elkon,R. and Agami,R. (2016) Functional genetic screens for enhancer elements in the human genome using CRISPR-Cas9. *Nat. Biotechnol.*, **34**, 1–10.
18. Melo,C.A., Drost,J., Wijchers,P.J., van de Werken,H., de Wit,E., Vrieling,J.A.F.O., Elkon,R., Melo,S.A., Léveillé,N., Kalluri,R., *et al.* (2013) ERNAs Are Required for p53-Dependent Enhancer Activity and Gene Transcription. *Mol. Cell*, **49**, 524–535.
19. Core,L.J., Waterfall,J.J. and Lis,J.T. (2008) Nascent RNA sequencing reveals widespread pausing and divergent initiation at human promoters. *Science (80-)*, **322**, 1845–1848.
20. Drost,J., Mantovani,F., Tocco,F., Elkon,R., Comel,A., Holstege,H., Kerkhoven,R., Jonkers,J., Voorhoeve,P.M., Agami,R., *et al.* (2010) BRD7 is a candidate tumour suppressor gene required for p53 function. *Nat. Cell Biol.*, **12**, 380–389.
21. Melgar,M.F., Collins,F.S., Sethupathy,P., Maniatis,T., Reed,R., Komili,S., Silver,P., Wyrick,J., Young,R., Kim,H., *et al.* (2011) Discovery of active enhancers through bidirectional expression of short transcripts. *Genome Biol.*, **12**, R113.
22. Wang,D., Garcia-Bassets,I., Benner,C., Li,W., Su,X., Zhou,Y., Qiu,J., Liu,W., Kaikkonen,M.U., Ohgi,K.A., *et al.* (2011) Reprogramming transcription by distinct classes of enhancers functionally defined by eRNA. *Nature*, **474**, 390–397.
23. Subramanian,A., Tamayo,P., Mootha,V.K., Mukherjee,S., Ebert,B.L., Gillette,M.A., Paulovich,A., Pomeroy,S.L., Golub,T.R., Lander,E.S., *et al.* (2005) Gene set enrichment analysis: A knowledge-based approach for interpreting genome-wide expression profiles. *Proc. Natl. Acad. Sci.*, **102**, 15545–15550.
24. Zancanato,F., Forcato,M., Battilana,G., Azzolin,L., Quaranta,E., Bodega,B., Rosato,A., Bicciato,S., Cordenonsi,M. and Piccolo,S. (2015) Genome-wide association between YAP/TAZ/TEAD and AP-1 at enhancers drives oncogenic growth. *Nat. Cell Biol.*, 10.1038/ncb3216.
25. Vierbuchen,T., Ling,E., Cowley,C.J., Couch,C.H., Wang,X., Harmin,D.A., Roberts,C.W.M.M. and Greenberg,M.E. (2017) AP-1 Transcription Factors and the BAF Complex Mediate Signal-Dependent Enhancer Selection. *Mol. Cell*, **68**, 1067–1082.e12.
26. Deng,T. and Karin,M. (1994) c-Fos transcriptional activity stimulated by H-Ras-activated protein kinase distinct from JNK and ERK. *Nature*, **371**, 171–175.
27. Kampfer,S., Hellbert,K., Villunger,A., Doppler,W., Baier,G., Grunicke,H.H. and Überall,F. (1998) Transcriptional activation of c-fos by oncogenic Ha-Ras in mouse mammary epithelial cells requires the combined activities of PKC- λ , ϵ and ζ . *EMBO J.*, 10.1093/emboj/17.14.4046.
28. Seshadri,T. and Campisi,J. (1990) Repression of c-fos transcription and an altered genetic program in senescent human fibroblasts. *Science*, **247**, 205–209.
29. Irving,J., Feng,J., Wistrom,C., Pikaart,M. and Villeponteau,B. (1992) An altered repertoire of fos jun (AP-1) at the onset of replicative senescence. *Exp. Cell Res.*, 10.1016/0014-4827(92)90415-5.
30. Riabowol,K., Schiff,J. and Gilman,M.Z. (1992) Transcription Factor Ap-1 Activity Is Required for Initiation of DNA-Synthesis and Is Lost during Cellular Aging. *Proc Natl Acad Sci U S A*, DOI 10.1073/pnas.89.1.157.
31. Rose,D.W., McCabe,G., Feramisco,J.R. and Adler,M. (1992) Expression of c-fos and AP-1 activity in senescent human fibroblasts is not sufficient for DNA synthesis. *J. Cell Biol.*, 10.1083/jcb.119.6.1405.

32. Burrows,A.E., Smogorzewska,A. and Elledge,S.J. (2010) Polybromo-associated BRG1-associated factor components BRD7 and BAF180 are critical regulators of p53 required for induction of replicative senescence. *Proc. Natl. Acad. Sci.*, 10.1073/pnas.1009559107.
33. Li,Q., Zhang,Y., Fu,J., Han,L., Xue,L., Lv,C., Wang,P., Li,G. and Tong,T. (2013) FOXA1 mediates p16INK4a activation during cellular senescence. *EMBO J.*, **32**, 858–873.
34. Baar,M.P., Brandt,R.M.C., Putavet,D.A., Klein,J.D.D., Derks,K.W.J., Bourgeois,B.R.M., Stryeck,S., Rijkse,Y., van Willigenburg,H., Feijtel,D.A., *et al.* (2017) Targeted Apoptosis of Senescent Cells Restores Tissue Homeostasis in Response to Chemotoxicity and Aging. *Cell*, **169**, 132–147.e16.
35. Bolte,C., Flood,H.M., Ren,X., Jagannathan,S., Barski,A., Kalin,T. V. and Kalinichenko,V. V. (2017) FOXF1 transcription factor promotes lung regeneration after partial pneumonectomy. *Sci. Rep.*, 10.1038/s41598-017-11175-3.
36. Fulford,L., Milewski,D., Ustiyani,V., Ravishankar,N., Cai,Y., Le,T., Masineni,S., Kasper,S., Aronow,B., Kalinichenko,V. V., *et al.* (2016) The transcription factor FOXF1 promotes prostate cancer by stimulating the mitogen-activated protein kinase ERK5. *Sci. Signal.*, 10.1126/scisignal.aad5582.
37. Tamura,M., Sasaki,Y., Koyama,R., Takeda,K., Idogawa,M. and Tokino,T. (2014) Forkhead transcription factor FOXF1 is a novel target gene of the p53 family and regulates cancer cell migration and invasiveness. *Oncogene*, 10.1038/onc.2013.427.
38. Milewski,D., Pradhan,A., Wang,X., Cai,Y., Le,T., Turpin,B., Kalinichenko,V. V. and Kalin,T. V. (2017) FoxF1 and FoxF2 transcription factors synergistically promote rhabdomyosarcoma carcinogenesis by repressing transcription of p21 Cip1 CDK inhibitor. *Oncogene*, 10.1038/onc.2016.254.
39. Weinhold,N., Jacobsen,A., Schultz,N., Sander,C. and Lee,W. (2014) Genome-wide analysis of noncoding regulatory mutations in cancer. *Nat. Genet.*, 10.1038/ng.3101.
40. Melton,C., Reuter,J.A., Spacek,D. V. and Snyder,M. (2015) Recurrent somatic mutations in regulatory regions of human cancer genomes. *Nat. Genet.*, **47**, 710–716.
41. Davie,K., Jacobs,J., Atkins,M., Potier,D., Christiaens,V., Halder,G. and Aerts,S. (2015) Discovery of transcription factors and regulatory regions driving in vivo tumor development by ATAC-seq and FAIRE-seq open chromatin profiling. *PLoS Genet.*, **11**, e1004994.
42. Kaiser,V.B., Taylor,M.S. and Semple,C.A. (2016) Mutational Biases Drive Elevated Rates of Substitution at Regulatory Sites across Cancer Types. *PLoS Genet.*, **12**.
43. Langmead,B. and Salzberg,S.L. (2012) Fast gapped-read alignment with Bowtie 2. *Nat. Methods*, **9**, 357–359.
44. Heinz,S., Benner,C., Spann,N., Bertolino,E., Lin,Y.C., Laslo,P., Cheng,J.X., Murre,C., Singh,H. and Glass,C.K. (2010) Simple Combinations of Lineage-Determining Transcription Factors Prime cis-Regulatory Elements Required for Macrophage and B Cell Identities. *Mol. Cell*, **38**, 576–589.
45. Anders,S., Pyl,P.T. and Huber,W. (2015) HTSeq-A Python framework to work with high-throughput sequencing data. *Bioinformatics*, **31**, 166–169.
46. Bailey,T.L. (2011) DREME: Motif discovery in transcription factor ChIP-seq data. *Bioinformatics*, **27**, 1653–1659.
47. Grant,C.E., Bailey,T.L. and Noble,W.S. (2011) FIMO: Scanning for occurrences of a given motif. *Bioinformatics*, **27**, 1017–1018.

48. Kim,D., Pertea,G., Trapnell,C., Pimentel,H., Kelley,R. and Salzberg,S.L. (2013) TopHat2: accurate alignment of transcriptomes in the presence of insertions, deletions and gene fusions. *Genome Biol.*, **14**, R36.
49. Khan,A., Fornes,O., Stigliani,A., Gheorghe,M., Castro-Mondragon,J.A., van der Lee,R., Bessy,A., Chèneby,J., Kulkarni,S.R., Tan,G., *et al.* (2017) JASPAR 2018: update of the open-access database of transcription factor binding profiles and its web framework. *Nucleic Acids Res.*, 10.1093/nar/gkx1126.
50. Zhou,X., Maricque,B., Xie,M., Li,D., Sundaram,V., Martin,E.A., Koebbe,B.C., Nielsen,C., Hirst,M., Farnham,P., *et al.* (2011) The human epigenome browser at Washington University. *Nat. Methods*, **8**, 989–990.

Supplemental data for chapter 3

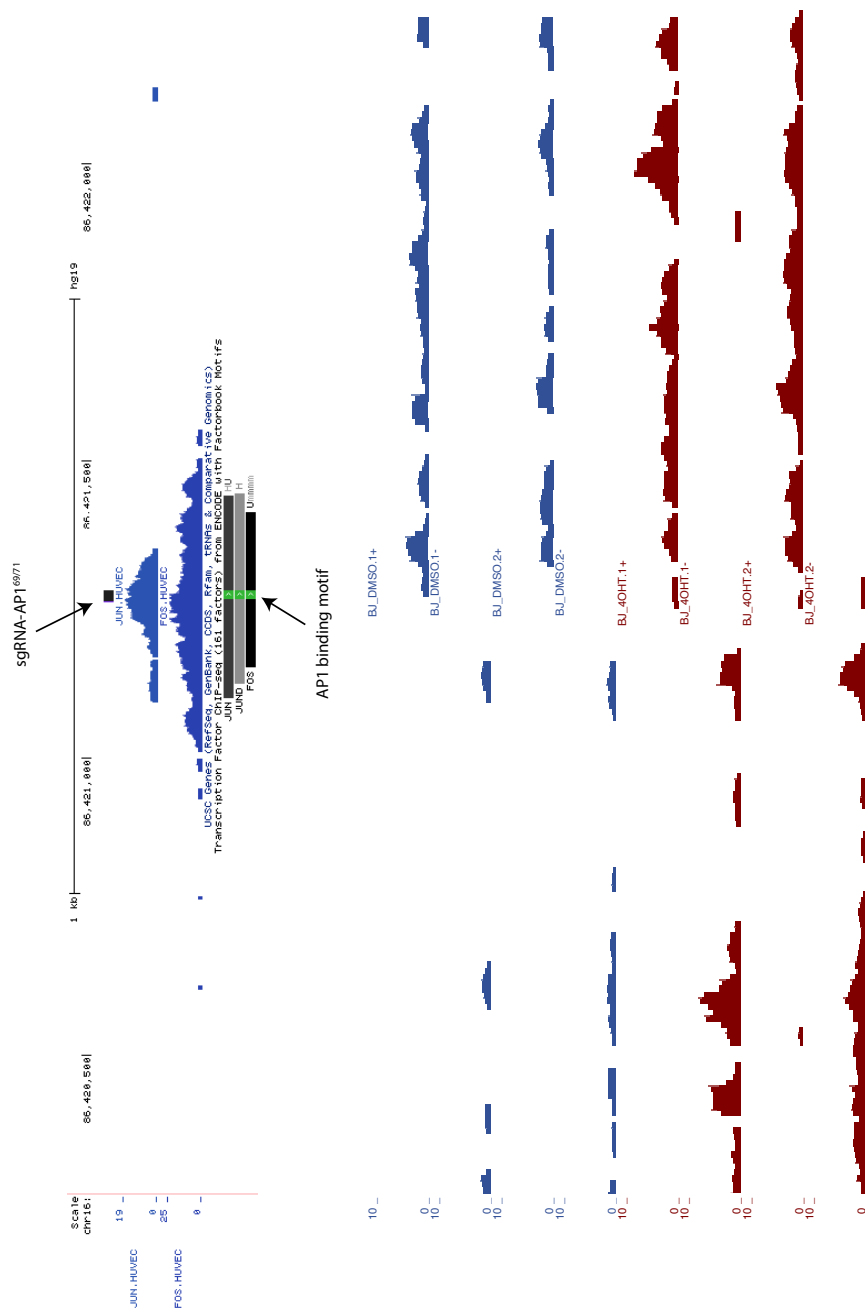


Figure S1. UCSC screenshot of Enh^{APT-OIS1} with ENCODE CHIP-seq data.

ENCODE CHIP-seq data shows a significant binding of c-Fos and c-Jun to *Enh^{AP1-OSI}*. The binding of these factors coincides with the API family consensus motif (Jun, JunD, and Fos in this case).

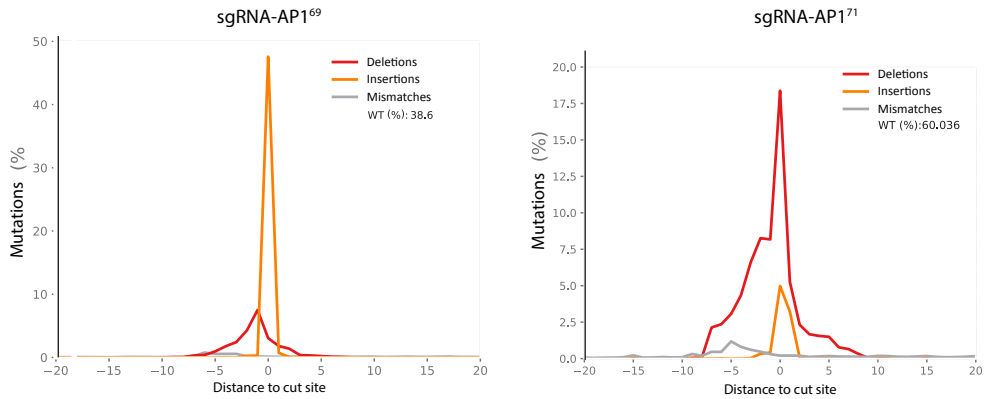


Figure S2. Mutation profiles of BJ-indRAS^{G12V} cells transduced with sgRNA-API⁶⁹ and -API⁷¹. Genomic DNA of BJ-indRAS^{G12V} cells with the indicated sgRNAs was isolated, and *Enh*^{API-OIS1} region was PCR amplified, subjected to deep sequencing and analysed for mutations. Proportion of wild-type or mutated (by mismatch, deletion or insertion) base calls is indicated as a function of its distance from the Cas9 cleavage site. For sgRNA-API⁶⁹, the majority of the mutations are single nucleotide insertions, while for sgRNA-API⁷¹ deletions around the cleavage site were more prevalent.

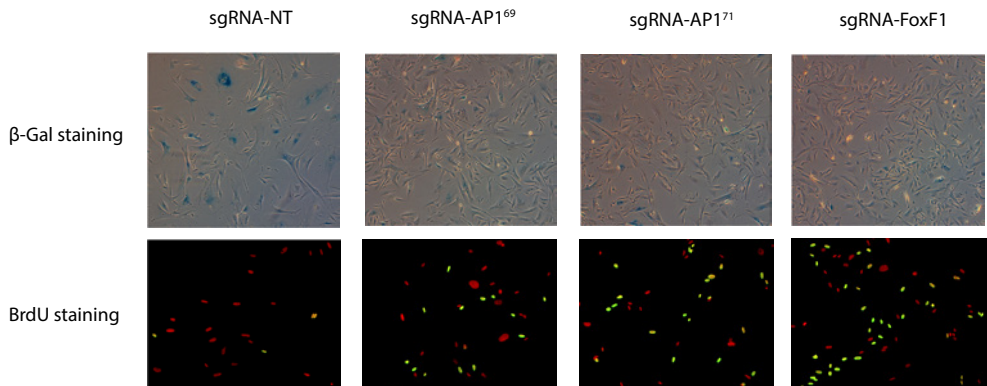


Figure S3. Representative pictures of β -Gal assay and BrdU staining.

A. Representative pictures of β -Gal assay and BrdU staining experiments used for the analysis of the results shown in Fig. 2-3. Each column represents the cells infected with the indicated sgRNA. The cells were treated with 4-OHT for 14 days prior analysis. Upper panel shows the β -Gal staining experiments with senescent cells stained as blue. Lower panel shows the BrdU staining experiments with cells incorporated with BrdU stained as green and nucleus stained as red.

Summary



Figure S4. Somatic mutation in the AP1 motif within *Enh^{AP1-OIS1}*. Screenshots from ICGC portal show a single nucleotide substitution within the AP1 motif in *Enh^{AP1-OIS1}* detected in a patient with lung cancer.

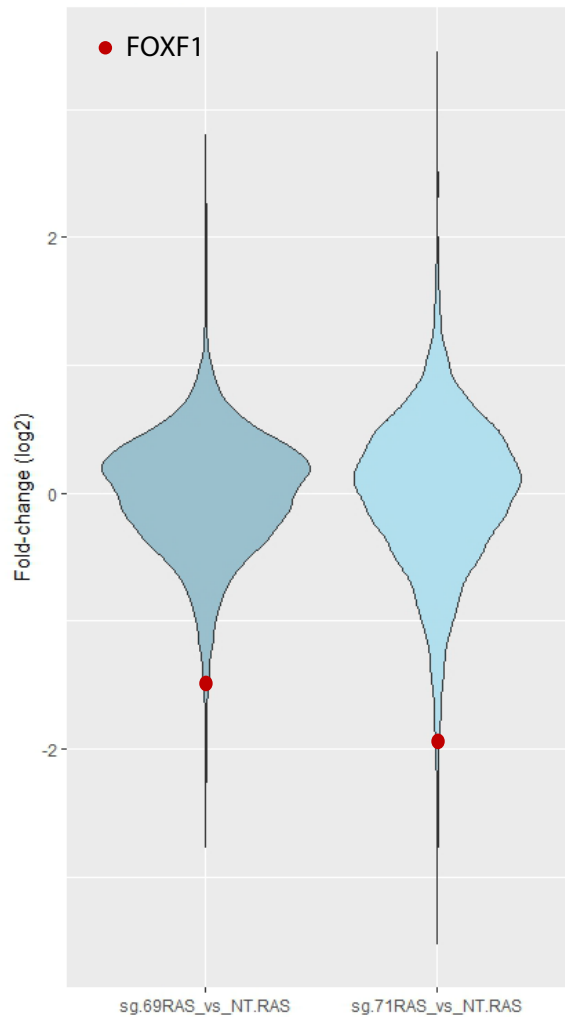


Figure S5. RNA-seq analysis indicates *FOXF1* as a target gene of *Enh^{API-OIS1}*.

Gene expression levels were measured in BJ cells targeted by either sgRNA-API⁶⁹, sgRNA-API⁷¹ or sgRNA-NT negative control. Violin plots show the distribution of fold change of gene expression (in log2 base) calculated for the comparison between the sgRNA-API⁶⁹ and sgRNA-API⁷¹ samples and the sgRNA-NT control. *FOXF1* is marked by a rod dot. Its expression was markedly decreased by targeting *Enh^{API-OIS1}* by either sgRNA-API⁶⁹ or sgRNA-API⁷¹.

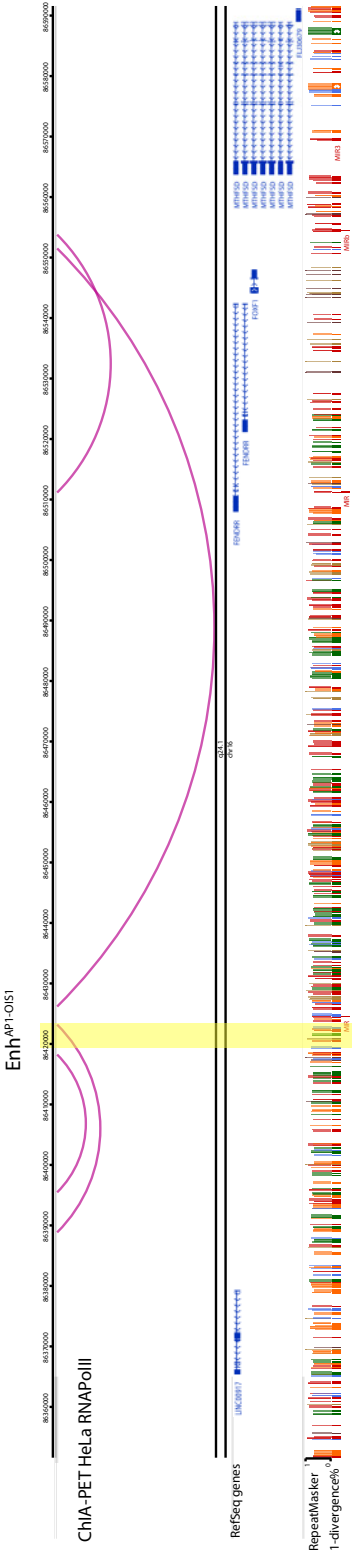
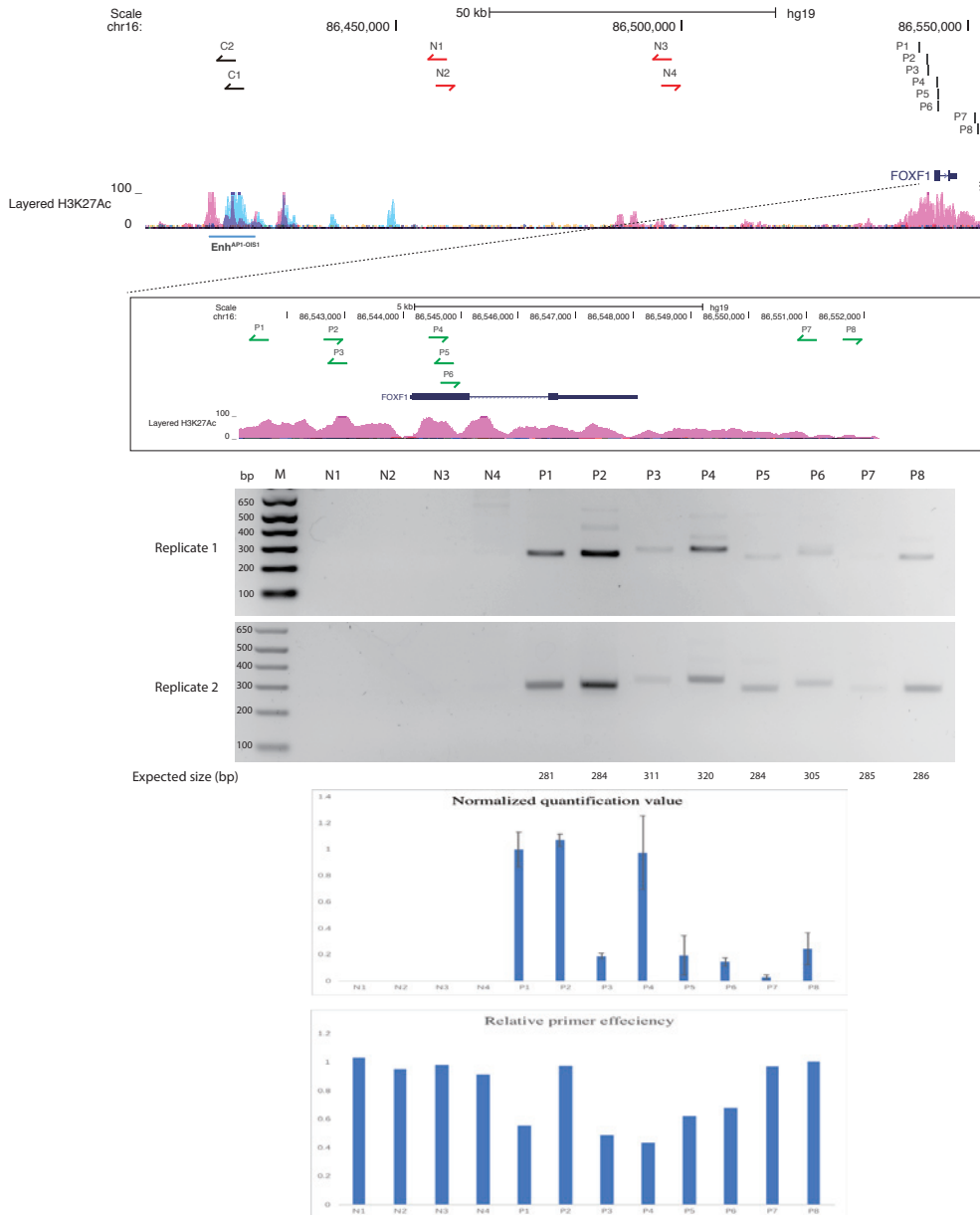


Figure S6. RNA PolII ChIA-PET data support direct interaction between *Enh^{AP1-OIS1}* and *FOXFI*. Each ChIA-PET experiment is indicated with the name of cell lines and the antibody used for the pull down on the left. *Enh^{AP1-OIS1}* is highlighted in yellow and inferred physical interactions between two regions are presented by loops. Data is taken from the WashU epigenome browser (50).

Functional CRISPR screen identifies API-associated enhancer regulating FOXF1

A



3

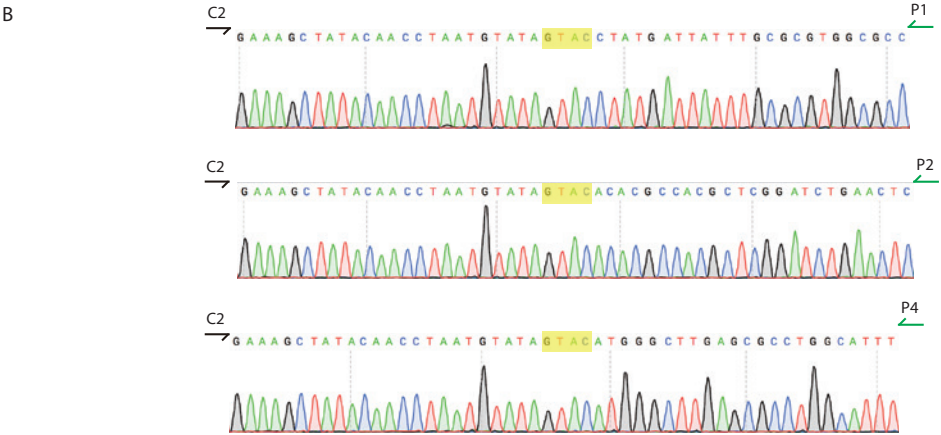


Figure S7. 3C experiment reveal direct interaction between *Enh^{AP1-OIS1}* and *FOXF1*.

A. Genome browser presentation of the location of each primer used in 3C analysis. Constant primers (C1, C2) used to amplify *Enh^{AP1-OIS1}* are indicated in black arrows. Negative control regions with no interaction with *Enh^{AP1-OIS1}* are amplified with primers indicated in red arrows (N1-N4). *FOXF1* regions with potential interactions with *Enh^{AP1-OIS1}* are amplified with primers indicated in green arrows (P1-P8). Agarose gel images from two independent biological replicates are shown with the expected sizes of the PCR products. The quantification of the gels was performed by normalizing to the primer efficiencies. Values shown are further normalized to the quantification value of P1. **B.** Sanger sequencing results from the indicated PCR products. Csp6I restriction sites are highlighted in yellow. The PCR were performed using the indicated primer pairs.

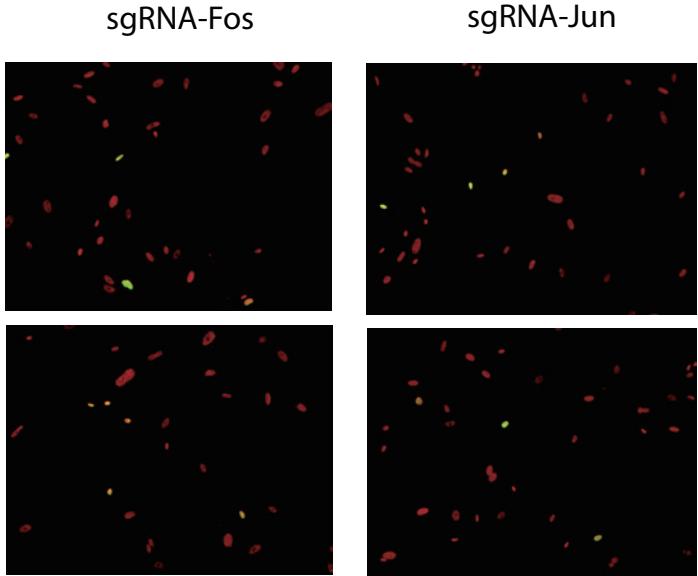
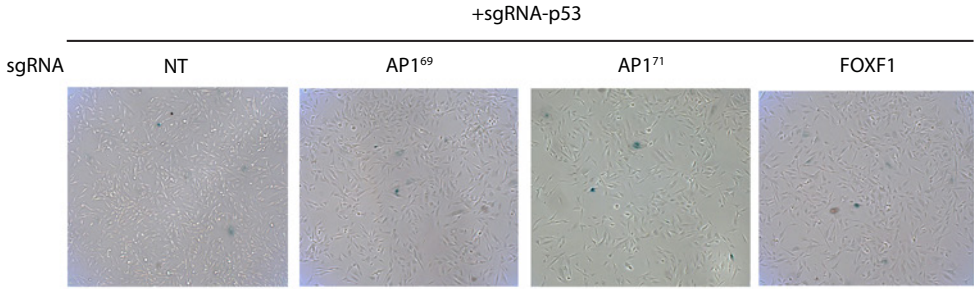


Figure S8. Disruption of Fos and Jun could not bypass senescence.

Representative pictures of BrdU staining experiments with sgRNAs against c-Fos and c-Jun genes. BJ cells were treated with 4-OHT for 14 days. Each column shows two pictures from the same experiment.

A



B

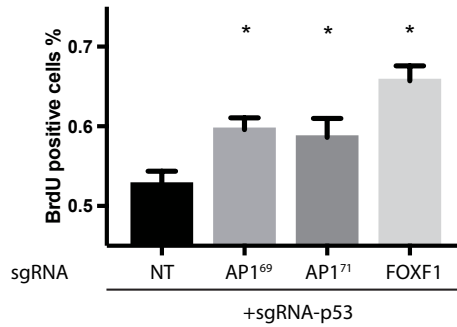


Figure S9. FOXF1 function is independent of p53 during OIS.

A. Representative images of the SA-β-gal staining of cells under the indicated conditions and after 14 days 4-OHT treatment. **B.** The proliferation levels of the various sgRNA-transduced BJ-indRAS^{G12V} cells (indicated in the figures) was quantified using BrdU assay, (* $p < 0.05$, two-tailed Student's t-test). For every condition, the percentage of BrdU-positive cells was normalized to control cells (NT+p53 ko).

A large, stylized number 4 is centered on a white background. The number is white and has a thick, slightly irregular outline. Behind the number is a large, textured, charcoal-like smudge in shades of gray and black, which has a rough, hand-drawn appearance. The smudge is roughly circular but has many irregular edges and internal textures, giving it a sense of depth and movement.

4



Chapter 4

A functional genetic screen identifies TRAM2 as a key target of YAP-mediated proliferation and oncogenesis

Li Li^{1,5}, Alejandro P Ugalde^{1,5}, Zohar², Gozde Korkmaz¹, Remco Nagel¹,
Ilyomchev¹, Rui Lopes¹, Ran Elkon^{2,*} & Reuven Agami^{1,3,4,*}

¹Division of Oncogenomics, Oncode Institute, Netherlands Cancer Institute, Plesmanlaan 121,
1066CX, Amsterdam, the Netherlands

²Department of Human Molecular Genetics and Biochemistry, Sackler School of Medicine, Tel Aviv University,
Tel Aviv, Israel

³Erasmus MC, Rotterdam University, Rotterdam, the Netherlands

⁴Oncode institute, Netherlands Cancer Institute, Plesmanlaan 121, 1066CX, Amsterdam, the Netherlands

⁵These authors contributed equally

* To whom correspondence should be addressed. Tel: +20512199; Email: r.agami@nki.nl
Correspondence may also be addressed to Ran ElkonTel; Email: ranel@tauex.tau.ac.il

Manuscript in preparation

Abstract

YAP and TAZ are potent regulators of cell proliferation and key drivers of tumorigenesis. They can shuttle to the nucleus when they are activated and will be recruited to specific enhancers through the interaction with the DNA binding protein TEAD. Although a genome-wide mapping of YAP/TAZ/TEAD binding at enhancers has already been described, a comprehensive identification of critical YAP/TAZ/TEAD targets in cancer has never been attempted before. Here, we first identified several YAP-associated enhancers in YAP mediated proliferation. Using the CRISPR-Cas9 system, we performed a proliferation drop-out screen by targeting the TEAD binding motif in MCF10A cells and MCF10A-YAP/AP1 cells (ectopically expressing YAP^{5SA} and AP1) and identified enhancer^{Tram2} as a critical enhancer required for YAP-mediated cell growth. Disruption of enhancer^{Tram2} decreased the expression of Tram2 and affected proliferation of MCF10A-YAP/AP1 cells. Similar to enhancer^{Tram2} knockout, knockout of Tram2 caused a reduction in growth rate. Importantly, ectopic expression of Tram2 restored proliferation of enhancer^{Tram2} knockout cells. Thus, our findings indicated that TRAM2 is a key target of YAP-mediated proliferation.

Introduction

YAP and TAZ have attracted increasing attention in the last decade for their ability to stimulate cell proliferation and their frequent activation in a large number of solid tumors (1). These two highly related transcription factors are historically known for being the downstream effectors of the Hippo pathway, an evolutionarily conserved signaling network that senses cell polarity, and regulates adhesion, cell death and differentiation. Importantly, accumulating evidence indicates that YAP and TAZ constitute a signaling hub that integrates signals from numerous inputs and pathways and therefore are able to control multiple aspects of cancer biology (2). For example, YAP and TAZ are mediators of the Wnt/ β -catenin signaling pathway. In addition, their activities are regulated by growth factors and hormones via G-protein-coupled receptors (GPCRs). Recently YAP and TAZ also emerged as important tumor energy regulators that sense and regulate glucose and lipid metabolism (3).

Mechanistically, dephosphorylated YAP and TAZ are able to translocate to the nucleus, where they activate gene expression by association to DNA-binding transcription factors, more specifically the TEAD family. It has been reported that YAP regulates the expression of some target genes through binding to the promoters. However, recent studies have shown that YAP and TAZ modulate gene transcription through binding to more distal enhancer regions, which are far from the putative target genes (4).

Enhancers are functional regulatory elements that activate the expression of their target genes through chromatin interactions (5). These elements are highly abundant in mammalian genomes (in the range of hundreds of thousands) and they are currently viewed as the main determinants of the spatiotemporal regulation of gene expression. Enhancers can be predicted indirectly by specific chromatin marks, most notably high H3K4me1 and H3K27ac, and low H3K4me3 (6). Mechanistically, enhancers serve as binding platforms for transcription factors to regulate target gene transcription through chromatin loops. Enhancers are typically bound by multiple transcription factors. Conversely, transcription factors can bind to thousands of enhancers. It is important to note that binding of transcription factors at enhancers is not always the direct evidence for enhancer activity (7).

The functions of the vast majority of the enhancers are poorly understood and little is known about the rules that determine the interaction between enhancers and their regulated target genes. In this regard, we have previously shown that genome-wide screens using CRISPR-Cas9 offer an unprecedented opportunity to define enhancer elements required for transcription factor binding to exert their transcriptional reprogramming (8).

Although, many potential enhancers were found to be bound by YAP/TAZ/TEAD, a focused functional genetic screen was not described before. We therefore sought to identify YAP-associated enhancers using our established cellular system-MCF10A-YAP/AP1 cells (MCF10A expressing constitutively activated YAP^(SSA) and AP1). We identified a number of potential YAP regulated enhancers using the public ChIP-seq data. Next, we performed the functional screen and discovered several of these enhancers that are required for YAP-mediated proliferation. We demonstrated that enhancer B (enhancer^{Tram2}) is required for proliferation by controlling the Tram2 gene. Collectively, our results provide a new enhancer-mediated regulatory pathway for YAP induced growth and oncogenesis. Our findings support the role of enhancers as DNA regulators in critical processes such as cell proliferation and a potential role in cancer.

Material and methods

Cell culture

MCF10A and MCF10A-YAP/AP1 cells were cultured in DMEM/F12 medium (Gibco), supplemented with 1% penicillin/streptomycin (Gibco) and 5% horse serum. HEK293-T cells were cultured in DMEM medium (Gibco), supplemented with 1% penicillin/streptomycin (Gibco) and 10% FCS (Hyclone).

Analysis of GRO-seq data

GRO-seq was performed on MDA-MB-231 and MCF-7 cells. Sequencing reads were aligned to the human genome (hg19) using bowtie2 (9), and transcriptional units (TUs) were inferred using HOMER software (10). Read counts per TU were calculated using HTseq-count (11). A total of 76,200 TUs covered by at least 20 reads in at least one sample were detected. TU expression levels were then normalized using quantile normalization to allow comparison between samples. Next, we defined bi-directional TUs as pairs of TUs whose start site is separated by no more than 800 bp and are transcribed on opposite strands (TU+ and TU-). As bi-directional transcription is a hallmark of transcriptional regulatory elements, we refer to these loci as regulatory elements (REs).

CRISPR library construction and analysis

We designed a CRISPR library to target the TEAD and JUN motifs in the potential enhancer regions. For 2508 of the 2902 TEAD motifs and 1141 of the 2071 JUN motifs we found an NGG PAM in a location that is expected to induce a Cas9 DNA cleavage within a distance of 3 bp with respect to the motif (that is, the cut is expected to occur within the motif or up to 3 bp from its edges). Overall, we designed 6489 distinct sgRNAs, including positive and negative controls. To generate a CRISPR-Cas9 lentiviral library (hereafter referred as CRISPR-YAP-enh-lib), the sgRNAs were cloned into pLentiCRISPRv2 using Gibson Assembly from an oligonucleotide pool synthesized by CustomArray

Inc. MCF10A and MCF10A-YAP/AP1 cells were transduced with three independent lentiviral pools of CRISPR-YAP-enh-lib. After selection with puromycin (1 mg/L), half of the transduced cells were harvested at day 0, while the remaining cells were cultured with continuous passaging for 20 days. After 20 days, cells were harvested, genomic DNA was isolated and the integrated sgRNAs were PCR-amplified and submitted for next-generation sequencing (NGS) to quantify their relative abundance. Sequencing reads were first trimmed to remove adaptor sequences and then aligned to the sgRNA library sequences. Read counts per sgRNA were then calculated using a custom R script. To assess the relative change between the starting and final cell population, MAGeCK software was employed using the negative control sgRNAs for normalization. For a comparison between the two cellular models, the average log₂ fold-change obtained in the previous step from the three replicates was transformed to a Z-score.

Luciferase reporter assay

For functional testing of the putative enhancer elements, these sequences were cloned in a pGL3-promoter (Promega) vector. The enhancer region was PCR amplified from DNA of MCF10A cells and inserted downstream of the firefly luciferase reporter gene in the plasmid. For transfection of these plasmids, 1×10^5 of cells were seeded in 6-well plates. The next day, 100 ng of each construct (pGL3-promoter, pGL3-YAP-Enhancer-Fw, and pGL3-YAP-Enhancer-Rv) were co-transfected with 10 ng of Renilla luciferase reporter construct using Fugene-6 (Promega) following the manufacturer's protocol. Luciferase activity was measured 24 h post-transfection using the Dual-Luciferase Reporter assay kit (Promega). Cells were lysed directly on the plate with passive lysis buffer for 15 min at room temperature. Firefly and Renilla luciferase activity was measured using a Centro XS3 LB960 machine (Berthold technologies).

Lentiviruses production and infection

HEK293T cells were seeded at the density of 6×10^6 cells per 10 cm dish one day prior to transfection. Transfection was performed using PEI (Polyethylenimine, Polysciences) and the medium was refreshed 16 h later. Virus-containing supernatant was collected 48 h post-transfection. Next, this was filtered through a 0.45 μ m membrane (Millipore Steriflip HV/PVDF), snap-frozen and stored at -80°C . MCF10A and MCF10A-YAP/AP1 cells were infected and selected with the proper antibiotics 48 h after transduction for at least 4 days until no surviving cells remained in an uninfected control plate.

Mutation analysis of enhancer regions

Genomic DNA of cells transduced with sgRNAs was isolated and the concentration was measured. 500 ng of the genomic DNA was used for PCR-amplification of the enhancer region. We performed a two-step PCR by introducing the P5 adapter sequence in the first PCR and P7 adapters with the indexes in the second PCR. After the second PCR, the libraries were purified with CleanNA beads (GC Biotech) and quantified on the 2100

Bioanalyzer using a 7500 chip (Agilent). Equimolar amounts of each sample were taken for samples ran on the same lane. Libraries were sequenced using the Mi-Seq platform. Sequenced reads were aligned to the amplified enhancer region using Bowtie. Bam files were analyzed to count the number of mutations (mismatches, insertions or deletions) identified at each location in that region.

Sequencing

Sequencing of the CRISPR screen was done using single reads of 65bp on the Hi-Seq2500 platform (Illumina). Mutation analysis of enhancer regions was performed with single reads of 150bp on the Mi-Seq system with Mi-Seq reagent v2 Nano kit.

Results

Generation of the cellular system and library construction

To set up a functional genetic screen for YAP oncogenic activity, we first generated a cellular system. We transduced MCF10A cells with constitutively activate YAP^(SSA), AP1, and YAP^(SSA)+AP1. Next, the effect of introduction of these genes on cell proliferation, morphology and their capacity to form colonies in mammospheres assay was determined. As reported before, ectopic expression of YAP^(SSA) and YAP^(SSA)+AP1, but not the inactive variant YAP^(SSA-S94A), induced accelerated cell proliferation, changes in cellular morphology resembling mesenchymal cells, as well as a transformed phenotype manifested in clonogenic outgrowth (Supplementary Fig.1)(4). Co-expression of AP1 with active YAP enhanced these phenotypes as observed before (4).

As reported by Zanconato et al. (4), most of the binding sites of TEAD, TAZ, YAP, and JUN are potential enhancers. However, the number of functional enhancers is still unclear. Thus, we decided to perform a functional screen to identify the enhancers that are required for the YAP-mediated proliferation and oncogenesis by using the above-generated cellular system (MCF10A-YAP/AP1 cells). To identify all these enhancers, we analyzed publicly-available ChIP-seq data of TEAD, TAZ, YAP, and JUN in MDA231 cells and found 2902 and 2071 sequence motifs for TEAD and JUN binding, respectively (Figure. 1A). Out of these motifs, 2508 and 1141 peaks for TEAD and JUN, respectively, could potentially be targeted by CRISPR-Cas9. Altogether, we constructed CRISPR-YAP-enh-lib, a CRISPR library consisting of 6489 vectors including positive (CRISPR vectors targeting only YAP^(SSA)) and negative controls (CRISPR vectors without target) (Figure. 1A and Table 1).

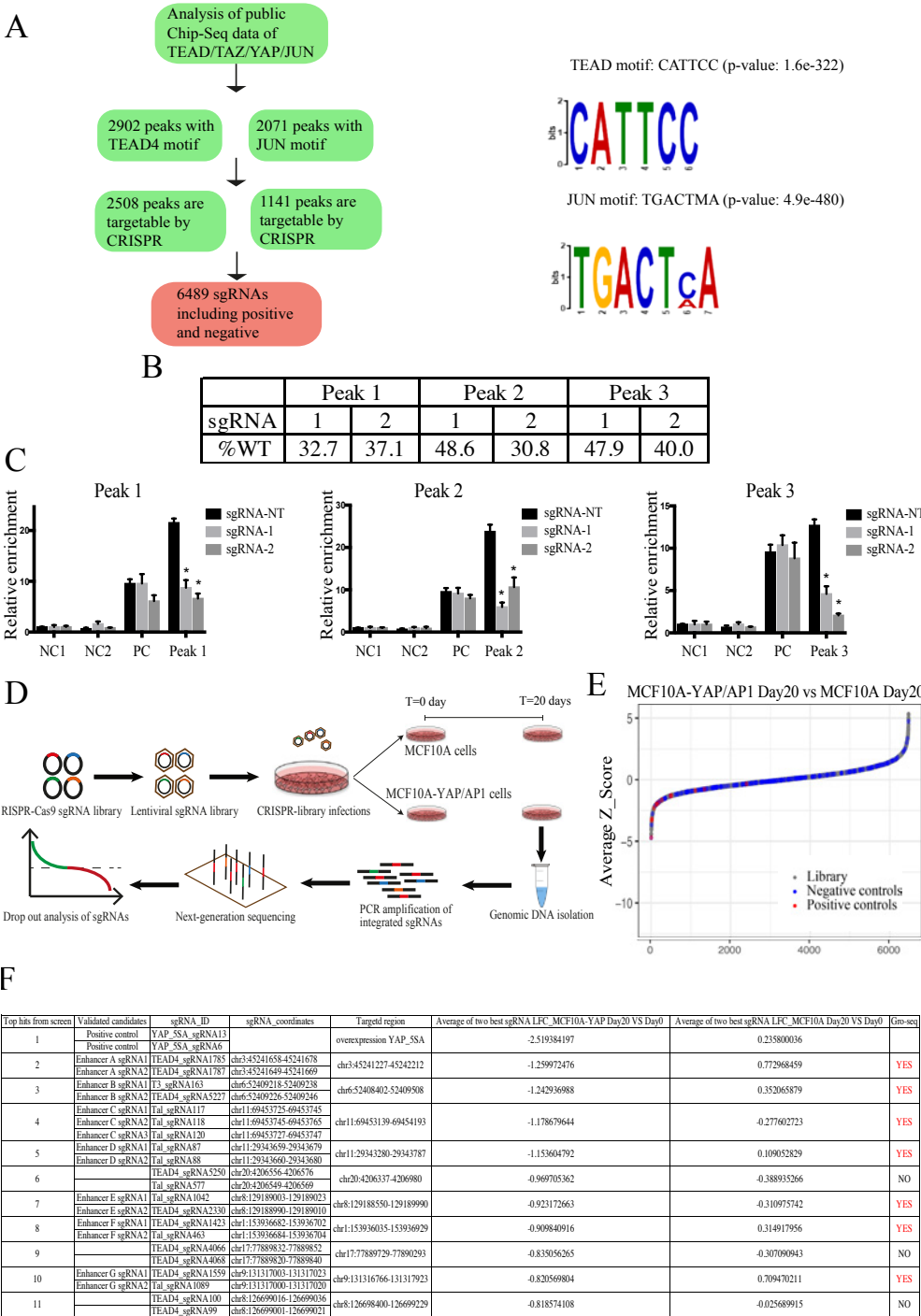


Figure I. Design of a CRISPR screen targeting YAP-associated enhancers to functionally screen for their involvement in proliferation.

A. Schematic representation of the set-up of our library design. B. Mutational profiles of MCF10A-YAP/AP1 cells transduced with sgRNAs. C. Chip-qPCR to measure the YAP binding in each region

after transduction with sgRNAs targeting the TEAD motif. D. Schematic representation of the set-up of our functional screen. E. Results of the CRISPR screen. sgRNAs are sorted by the enrichment score based on the ratio between their prevalence in the MCF10A-YAP/AP1 and MCF10A control populations (measured at 20 days). The y-axis shows the mean Z-score of the sgRNAs (calculated over the 3 replicates of the screen). Colored in red are the sgRNAs targeting the YAP^{SSA} (positive controls), blue dots are the sgRNAs as negative controls. Gray dots are the sgRNAs targeting the TEAD motifs in the genome. F. List of the top 11 candidates with 2 or 3 sgRNAs that showed the same phenotype.

Evaluation of CRISPR efficiency

Next, we evaluated the effectiveness of the CRISPR approach by determining the mutational load in the top 3 YAP-bound regions, which were targeted by at least 2 CRISPR vectors against the TEAD motif (Supplementary Fig.2). In all six cases, we showed that the introduction of the CRISPR vectors into MCF10A-YAP/AP1 cells generated mutations in all target sites with a frequency of >50% (Figure. 1B and Supplementary Fig.3). Importantly, we assessed YAP binding at the target regions using ChIP-qRT-PCR. We demonstrated that YAP can bind all the selected regions very effectively compared with the controls, a feature that was reduced to less than half after CRISPR targeting (Figure. 1C). Altogether, these results indicate that CRISPR targeting of TEAD motifs is robust with less than 20% false-negative rates, considering the fact that 2 or more TEAD motif-targeting CRISPR vectors per region were used.

A functional genetic screen for YAP targets

Ensured by an effective approach, we performed the screen as shown in Figure. 1D. We transduced the CRISPR-YAP-enh-lib into MCF10A and MCF10A-YAP/AP1 cells at a multiplicity of infection of 0.3, drug-selected and cultured the cells for 20 more days. Genomic DNA was isolated from the transduced cells at the start of the experiment (T=0) and at day 20 (T=20). Samples were subjected to PCR-sequencing analysis to determine the abundance of each CRISPR vector. We computed the changes in abundance between T=20 and T=0 for every CRISPR vector in each cell line (Supplementary Fig.4) and executed a differential analysis to identify hits that affect MCF10A-YAP, but not parental MCF10A cells. We found that the abundance of majority negative control vectors (blue dots) showed no significant change in both cell types. The majority of the positive control vectors - targeting the YAP^{SSA} - were significantly depleted in MCF10A-YAP/AP1 cells, indicating a robust assay (Figure. 1E). We selected the top candidates, which were selectively depleted in MCF10A-YAP/AP1 cells with 2 or 3 vectors targeting the same enhancer regions (Figure 1F). For further biological experiments, we selected the 7 enhancer regions with marked production of enhancer RNA transcription as determined by Gro-Seq analysis (Figure. 1F and Supplementary Fig.5).

To confirm the activity of the identified YAP-enhancers, we transduced MCF10A-YAP/AP1 and parental MCF10A cells with individual CRISPR vectors that target the 7 selected enhancers. We observed that each of the targeting vectors was effective in generating

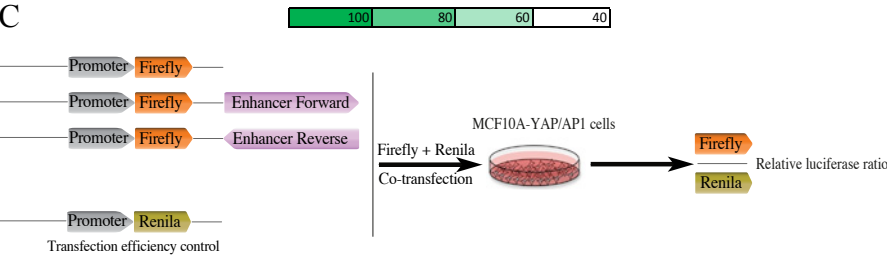
A

	Enhancer A		Enhancer B		Enhancer C			Enhancer D		Enhancer E		Enhancer F		Enhancer G	
sgRNA	1	2	1	2	1	2	3	1	2	1	2	1	2	1	2
%WT	10.2	12.7	1.8	4.4	34.9	26.1	50.4	5	20.1	4.5	9.6	3.8	39.8	4.2	2.3

B

MCF10A-YAP						MCF10A					
		T0	T6	T12				T0	T6	T12	
Enhancer A	sgRNA-1	100	88.32	73.72	***			100	100.30	99.12	
	sgRNA-2	100	91.19	77.72	***			100	100.82	99.92	
Enhancer B	sgRNA-1	100	89.01	73.63	***			100	106.89	99.49	
	sgRNA-2	100	90.08	75.37	***			100	100.00	98.26	
Enhancer C	sgRNA-1	100	87.30	72.49	***			100	100.43	98.43	
	sgRNA-2	100	85.45	68.17	***			100	99.26	96.63	
	sgRNA-3	100	86.02	71.03	***			100	100.47	98.55	
Enhancer D	sgRNA-1	100	89.42	74.20	***			100	101.01	98.95	
	sgRNA-2	100	91.59	77.54	***			100	100.62	98.61	
Enhancer E	sgRNA-1	100	85.37	69.72	***			100	99.77	98.30	
	sgRNA-2	100	85.40	69.59	***			100	100.27	98.42	
Enhancer F	sgRNA-1	100	90.87	76.59	***			100	100.19	98.97	
	sgRNA-2	100	89.06	76.49	***			100	99.41	97.09	
Enhancer G	sgRNA-1	100	89.45	76.97	***			100	99.81	98.21	
	sgRNA-2	100	88.15	75.34	***			100	100.42	99.27	
Positive control		100	63.64	38.22	***			100	100.77	100.08	
Negative control		100	99.15	96.21				100	101.16	100.12	

C



D

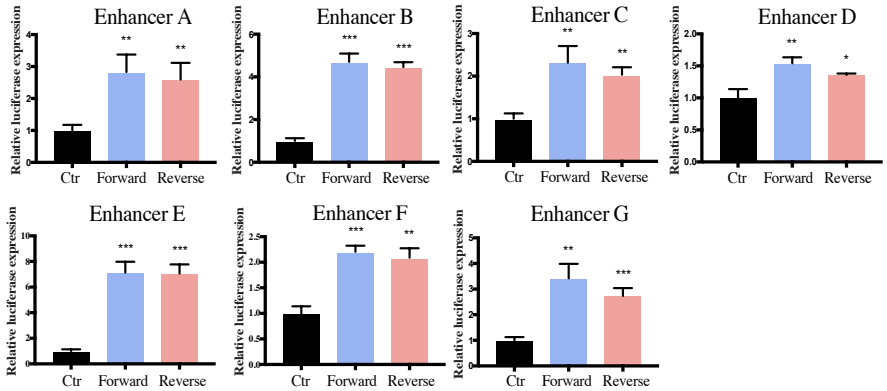


Figure 2. Validation of the selected hits.

A. Mutation profiles of MCF10A-YAP/AP1 cells transduced with indicated sgRNAs. B. Validation of candidate hits by a competitive proliferation assay in MCF10A-YAP/AP1 and MCF10A cells. Negative control indicates a nontargeting sgRNA. Positive control indicates a sgRNA targeting the YAP^{SA}. Values on day 6 (T = 6) and day 12 (T = 12) are normalized to day 0 (T = 0). n = 3; ***P < 0.001, two-tailed Student's t-test. C. Schematic representation of the set-up of luciferase reporter assay. D. MCF10A-YAP/AP1 cells were transfected with the indicated reporter vectors and harvested 25–30 h after transfection. The relative luciferase activities (firefly/Renilla) were normalized to the control (Ctr). P-values for luciferase assay were calculated by two-tailed Student's t-test. ***P < 0.001, **P < 0.01, *P < 0.05.

mutations at target sites ranging from 50 to more than 90% of mutated sequence (Figure. 2A and Supplementary Fig.6). Then, we performed a growth competition assay with these cells. As expected, we showed that while negative vectors did not affect proliferation of either MCF10A-YAP/AP1 or MCF10A cells, the CRISPR vector targeting YAP^{SSA} markedly compromised proliferation of only MCF10A-YAP/AP1 cells. Similarly, targeting all 7 enhancers selected from the screen significantly reduced the proliferation capacity of MCF10A-YAP/AP1 cells but not MCF10A cells (Figure. 2B). However, the extent of the effect of targeting the identified enhancers on the cellular growth rate was small in comparison to that found when targeting YAP^{SSA}. This suggested that YAP might be able to activate cell proliferation via a network of targets, each of which exhibit a relatively small contribution.

Next, we examined enhancer activity by placing the identified YAP-bound regions downstream of a luciferase reporter gene, either in a forward or reverse orientation as shown in Figure 2C. We demonstrated that all regions could activate firefly luciferase transcription regardless of their orientation, indicating a genuine enhancer activity (Figure 2D).

Discussion

Over the past decades, numerous YAP target genes have been discovered and characterized as critical players in YAP-mediated proliferation and oncogenesis. However, a comprehensive view of the transcriptional function of YAP remains largely unknown. Especially, the role of YAP-bound enhancers in proliferation and metastasis are still unexplored. We observed that ectopic expression of YAP^{SSA} and YAP^{SSA}+AP1 in MCF10A cells induced accelerated cell proliferation and cellular morphological changes which were in line with previous research, indicating that YAP is a very upstream factor regulating these phenotypes. Here, we contributed to the understanding of the function of YAP-associated enhancers by describing an enhancer screen in MCF10A cells transduced or not with YAP. This screen identified several novel enhancers required for YAP-mediated proliferation. However, the extent of the effect of each enhancer was relatively small compared to knockout of YAP^{SSA}, suggesting that YAP regulates cell proliferation via a network of targets. We predicted the target gene of each enhancer based on RNAseq (data is being processed and is not shown here). Some well-known genes, such as *Myc* and *CCND1*, were uncovered as the target genes of two of the identified enhancers. More interestingly, we identified another enhancer (enhancer^{Tram2}) whose target gene is predicted to be *Tram2* (translocation associated membrane protein 2). *Tram2*'s function was previously unexplored in the context of cancer and YAP regulation. Exactly how *Tram2* affects proliferation and how enhancer^{Tram2} controls *Tram2* expression remains to be uncovered and needs to be investigated in more details. Nevertheless, we described

here an important function of YAP-mediated enhancers with potentially influential implications in cancer biology.

YAP is a crucial co-transcription factor of the Hippo pathway, regulating organ growth and tumorigenesis. When Hippo signaling is inactive, YAP and its paralogue TAZ translocate to the nucleus and bind DNA indirectly through interaction with the TEAD family to regulate target genes(12, 13). Hippo signaling ablation or expression of constitutively active YAP leads to increased organ size, oncogenic growth or even occurrence of cancers(4, 14–17). The Hippo pathway is extremely important in cancer, which makes this pathway an attractive target for cancer therapeutics. The identification of YAP enhancers uncovers a network of genes that control various aspects of YAP activity, such as proliferation perhaps EMT. Exactly how these enhancers contribute to YAP activity within the Hippo signaling and which enhancer shows dependency remain to be explored.

Although CRISPR is a powerful approach to edit DNA sequence, it has the off-target effect. We need to test the entire library in order to know the exact false-negative rate. However, it is very challenging. We evaluated the efficiency of the CRISPR by testing the 3 top YAP-bound regions targeted by 2 sgRNA (guide RNA) against the TEAD motif before the screen. We concluded that the CRISPR is very effective with low false-negative rate indicating our functional screen is reliable, which in line with our validation results. Altogether, our preliminary findings here elucidate the importance of enhancers for YAP signaling pathways and in cancer.

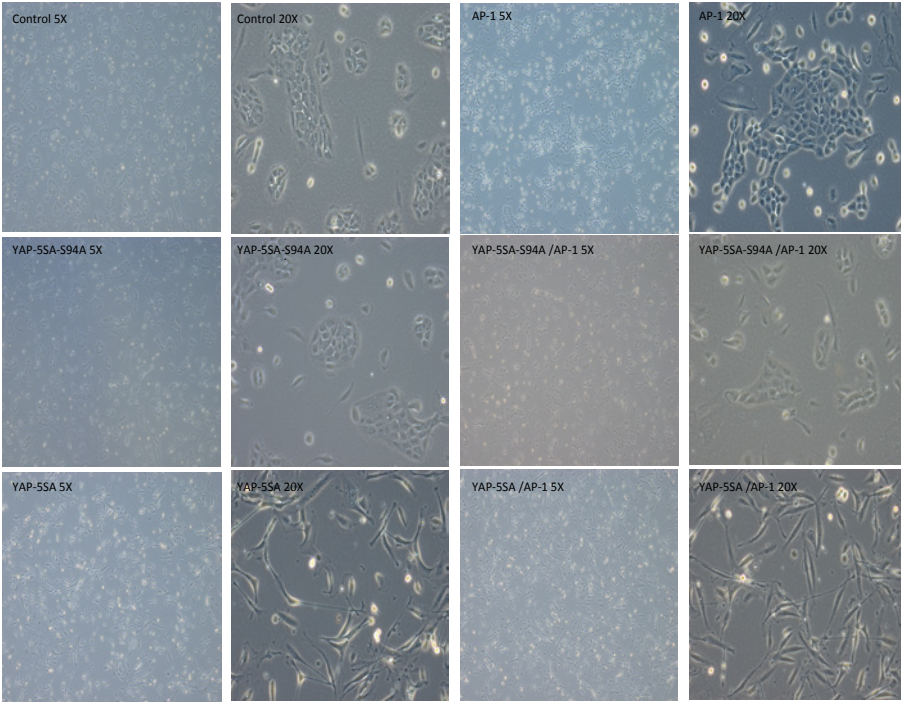
References

1. Harvey,K.F., Zhang,X. and Thomas,D.M. (2013) The Hippo pathway and human cancer. *Nat Rev Cancer*, nrc3458 [pii]n10.1038/nrc3458.
2. Piccolo,S., Dupont,S. and Cordenonsi,M. (2014) The biology of YAP/TAZ: hippo signaling and beyond. *Physiol. Rev.*, **94**, 1287–1312.
3. Zhang,X., Zhao,H., Li,Y., Xia,D., Yang,L., Ma,Y. and Li,H. (2018) The role of YAP/TAZ activity in cancer metabolic reprogramming. *Mol. Cancer*, **17**, 134.
4. Zanconato,F., Forcato,M., Battilana,G., Azzolin,L., Quaranta,E., Bodega,B., Rosato,A., Bicciato,S., Cordenonsi,M. and Piccolo,S. (2015) Genome-wide association between YAP/TAZ/TEAD and AP-1 at enhancers drives oncogenic growth. *Nat. Cell Biol.*, 10.1038/ncb3216.
5. Bulger,M. and Groudine,M. (2010) Enhancers: the abundance and function of regulatory sequences beyond promoters. *Dev. Biol.*, **339**, 250–257.
6. Heintzman,N.D., Stuart,R.K., Hon,G., Fu,Y., Ching,C.W., Hawkins,R.D., Barrera,L.O., Van Calcar,S., Qu,C., Ching,K.A., *et al.* (2007) Distinct and predictive chromatin signatures of transcriptional promoters and enhancers in the human genome. *Nat. Genet.*, 10.1038/ng1966.
7. Wang,J., Zhao,Y., Zhou,X., Hiebert,S.W., Liu,Q. and Shyr,Y. (2018) Nascent RNA sequencing analysis provides insights into enhancer-mediated gene regulation. *BMC Genomics*, **19**.
8. Korkmaz,G., Lopes,R., Ugalde,A.P., Nevedomskaya,E., Han,R., Myacheva,K., Zwart,W., Elkon,R. and Agami,R. (2016) Functional genetic screens for enhancer elements in the human genome using CRISPR-Cas9. *Nat. Biotechnol.*, **34**, 1–10.
9. Langmead,B. and Salzberg,S.L. (2012) Fast gapped-read alignment with Bowtie 2. *Nat. Methods*, **9**, 357–359.
10. Heinz,S., Benner,C., Spann,N., Bertolino,E., Lin,Y.C., Laslo,P., Cheng,J.X., Murre,C., Singh,H. and Glass,C.K. (2010) Simple Combinations of Lineage-Determining Transcription Factors Prime cis-Regulatory Elements Required for Macrophage and B Cell Identities. *Mol. Cell*, 10.1016/j.molcel.2010.05.004.
11. Anders,S., Pyl,P.T. and Huber,W. (2015) HTSeq-A Python framework to work with high-throughput sequencing data. *Bioinformatics*, 10.1093/bioinformatics/btu638.
12. Ramos,A. and Camargo,F.D. (2012) The Hippo signaling pathway and stem cell biology. *Trends Cell Biol.*, 10.1016/j.tcb.2012.04.006.
13. Zhao,B., Ye,X., Yu,J., Li,L., Li,W., Li,S., Yu,J., Lin,J.D., Wang,C.Y., Chinnaiyan,A.M., *et al.* (2008) TEAD mediates YAP-dependent gene induction and growth control. *Genes Dev.*, 10.1101/gad.1664408.
14. Camargo,F.D., Gokhale,S., Johnnidis,J.B., Fu,D., Bell,G.W., Jaenisch,R. and Brummelkamp,T.R. (2007) YAP1 Increases Organ Size and Expands Undifferentiated Progenitor Cells. *Curr. Biol.*, 10.1016/j.cub.2007.10.039.
15. Zhou,D., Conrad,C., Xia,F., Park,J.S., Payer,B., Yin,Y., Lauwers,G.Y., Thasler,W., Lee,J.T., Avruch,J., *et al.* (2009) Mst1 and Mst2 Maintain Hepatocyte Quiescence and Suppress Hepatocellular Carcinoma Development through Inactivation of the Yap1 Oncogene. *Cancer Cell*, 10.1016/j.ccr.2009.09.026.
16. Benhamouche,S., Curto,M., Saotome,I., Gladden,A.B., Liu,C.H., Giovannini,M. and McClatchey,A.I. (2010) Nf2/Merlin controls progenitor homeostasis and tumorigenesis in the liver. *Genes Dev.*, 10.1101/gad.1938710.

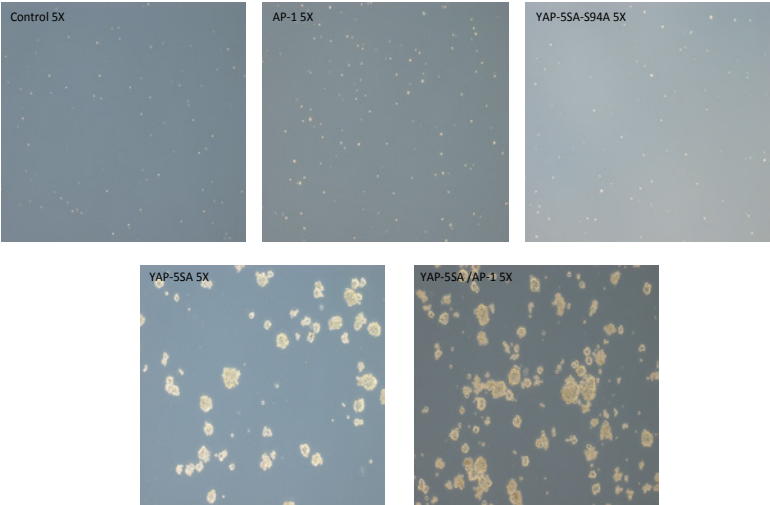
17. Dong,J., Feldmann,G., Huang,J., Wu,S., Zhang,N., Comerford,S.A., Gayyed,M.F., Anders,R.A., Maitra,A. and Pan,D. (2007) Elucidation of a Universal Size-Control Mechanism in Drosophila and Mammals. *Cell*, 10.1016/j.cell.2007.07.019.

Supplemental data for chapter 4

A

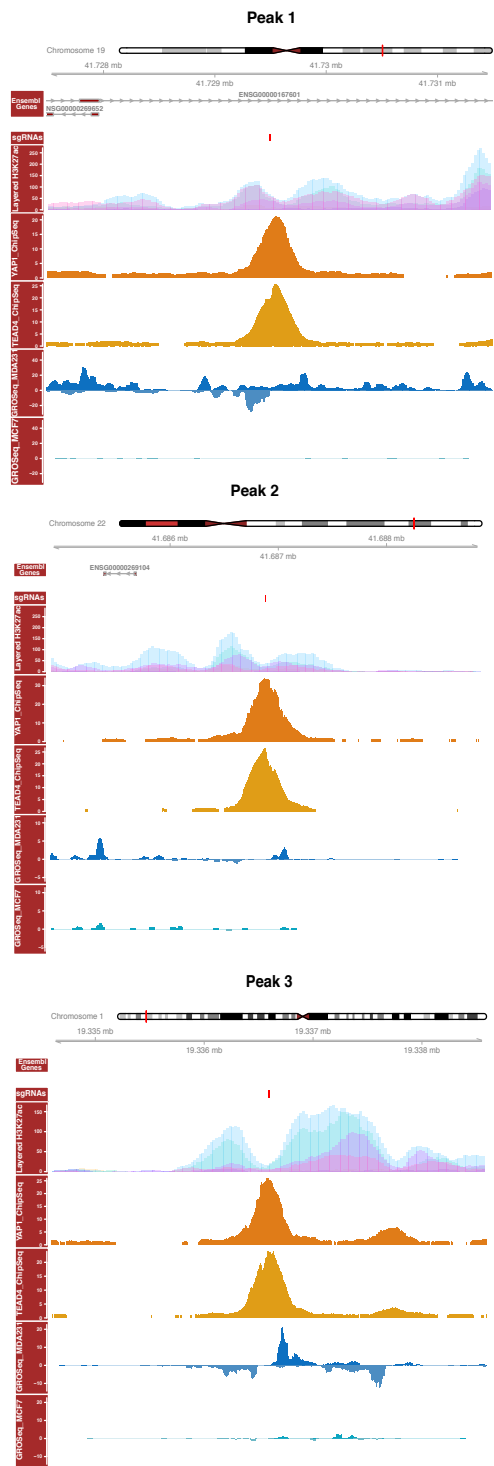


B

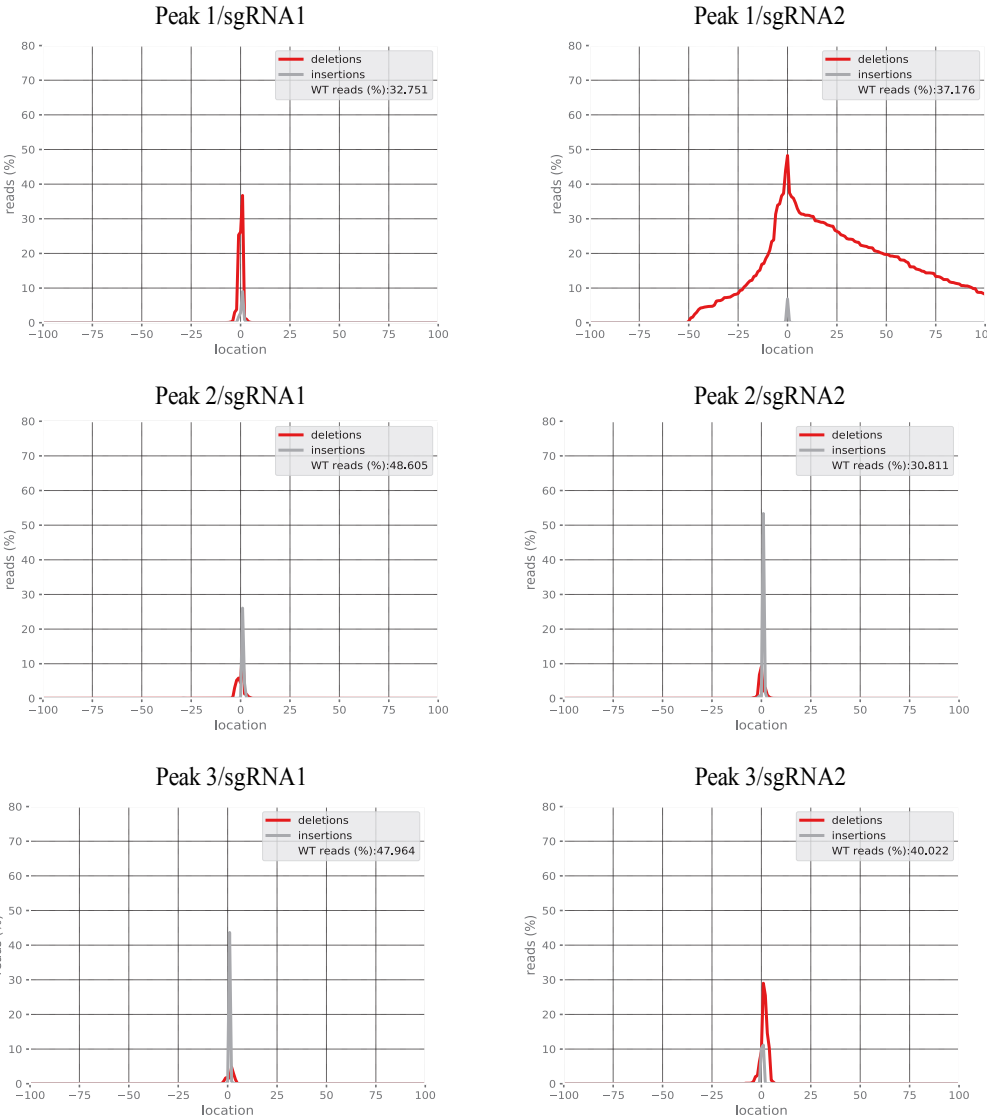


Supplementary Fig. I Generation of MCF10A-YAP/AP1cell system.

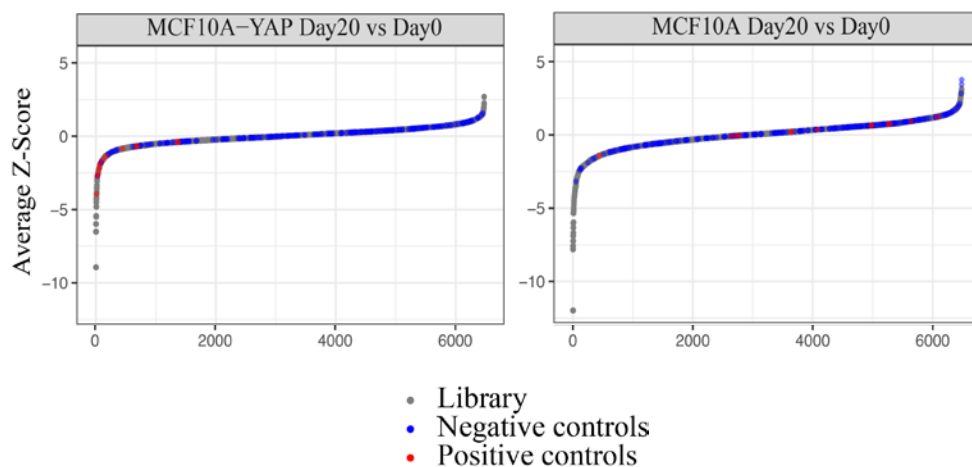
A. Representative images of MCF10A cells transduced with indicated vectors under indicated conditions in 2D culture. B. Representative mammosphere assay images of MCF10A cells transduced with indicated vectors under indicated conditions in 3D culture.



Supplementary Fig. 2 Information of genome location combined with public YAP/TEAD ChIP-seq data and Gro-seq data for the CRISPR sgRNAs efficiency test.

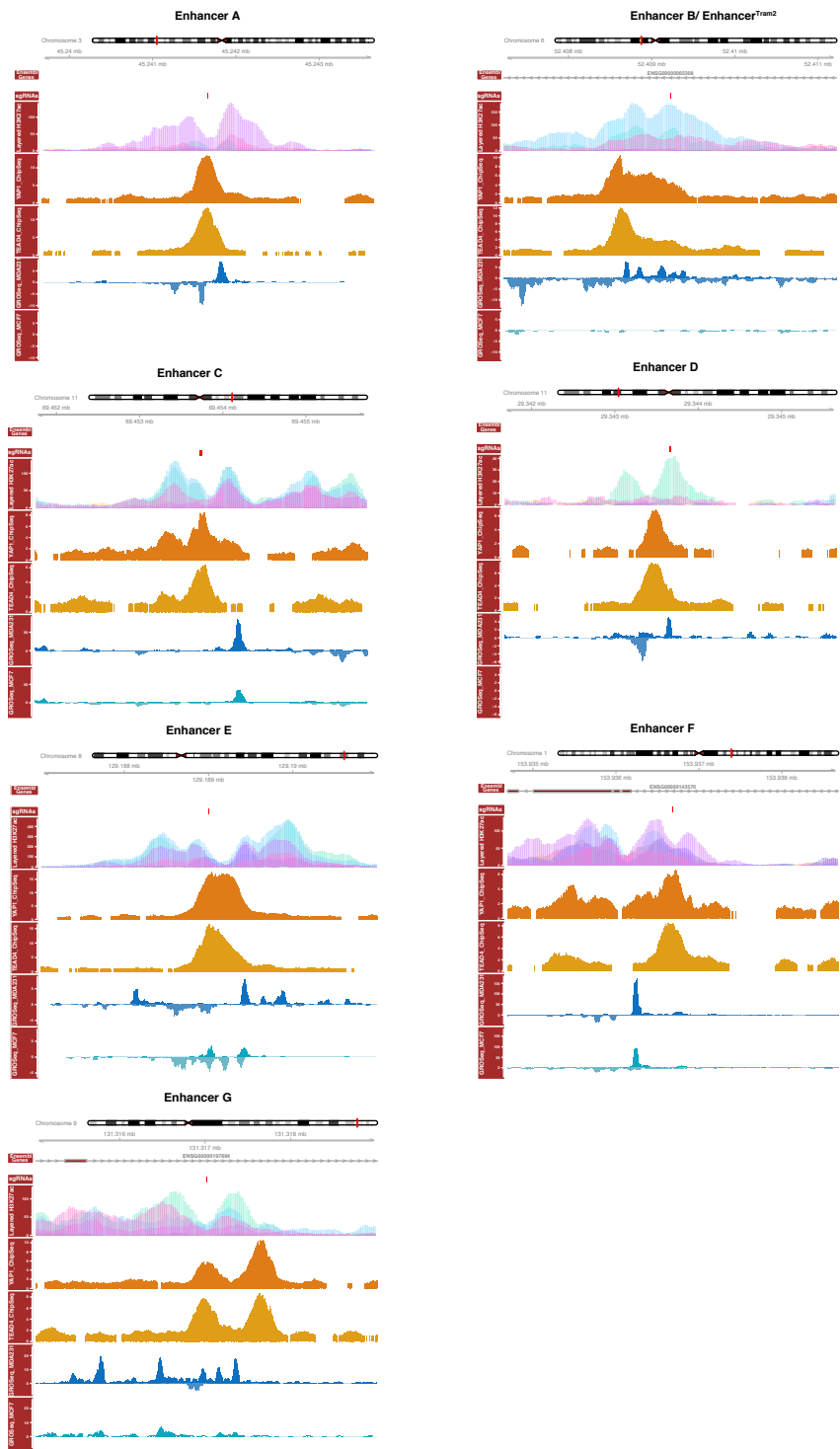


Supplementary Fig. 3 Mutation profiles of MCF10A-YAP/AP1 cells transduced with indicated sgRNAs.

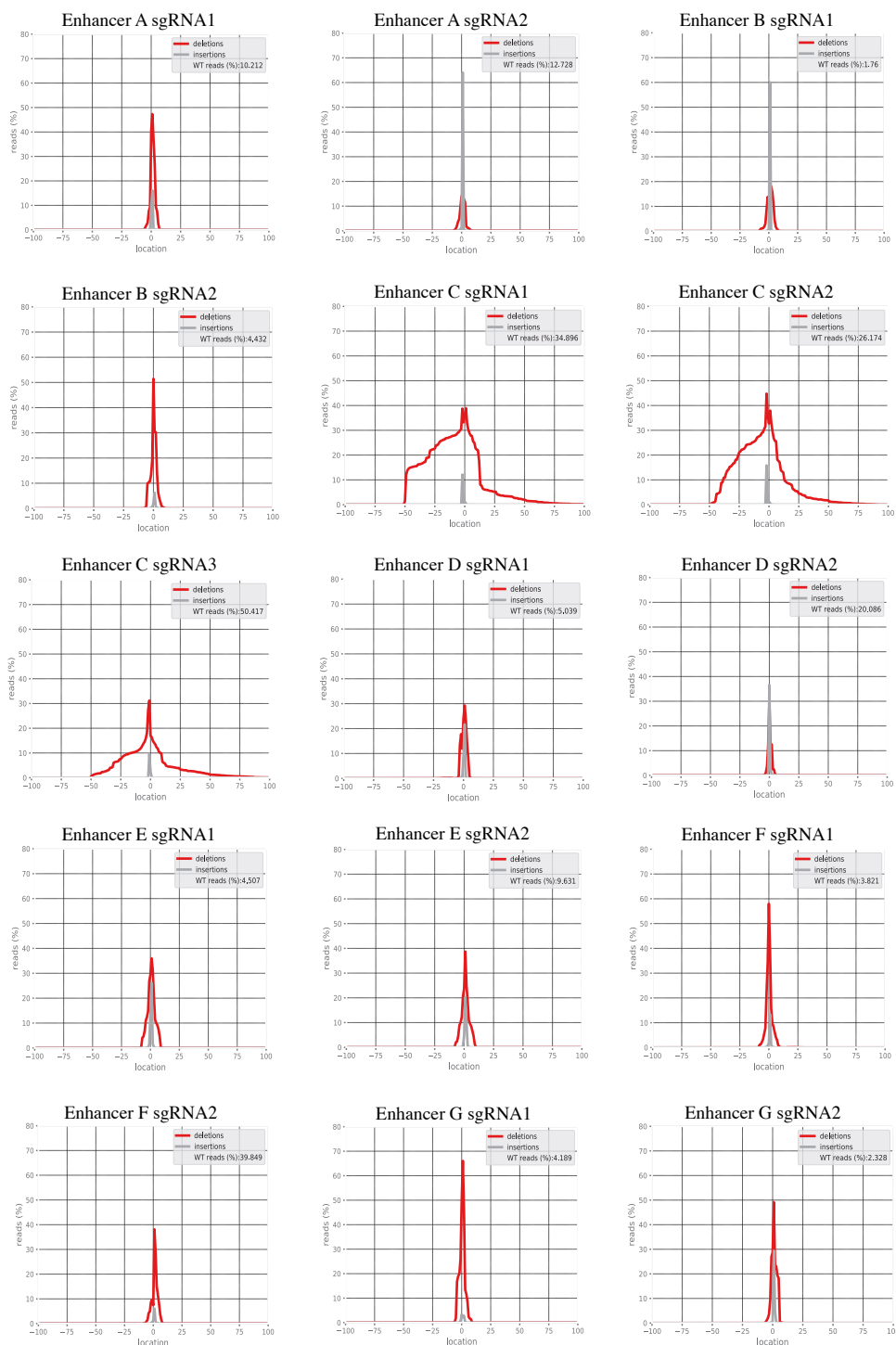


Supplementary Fig. 4 Results of the CRISPR screen.

sgRNAs are sorted by the enrichment score based on the ratio between their prevalence at day 20 and day 0 in MCF10A-YAP/AP1 and MCF10A cells respectively. Y-axis shows Z scores of the mean sgRNA enrichment scores (calculated over the 3 replicates of the screen). Colored in red are the sgRNAs targeting the YAP^{SSA} (positive controls), blue dots are the sgRNAs as negative controls. Gray dots are the sgRNAs targeting the TEAD motifs in the genome.



Supplementary Fig. 5 Information of genome location combined with public YAP/TEAD Chip-seq data and Gro-seq data for the validated hits sgRNAs.



Supplementary Fig. 6 Mutation profiles of MCF10A-YAP/AP1 cells transduced with indicated sgRNAs.



Chapter 5

Discussion



Cancer is a common disease worldwide, but unfortunately its treatment is limited and inefficient. Understanding the tumorigenesis and cancer development can provide additional fundamental knowledge to help develop novel cancer diagnosis and treatment tools. Cellular senescence is a mechanism that suppresses tumorigenesis following the emergence of genetic alterations. Investigation and identification of regulators in cellular senescence will help us to better understand tumorigenesis, allowing the identification of new biomarkers or therapeutic targets for cancer treatment.

Over the past few decades, many lncRNAs have been characterised as important players in a myriad of biological processes, such as differentiation, proliferation, development, as well as in a variety of human diseases including cancer (1–5). However, the roles and functions of lncRNAs in OIS have not been fully elucidated. OIS is a major cellular senescence type which poses a critical barrier to cancer, but so far, few studies have described lncRNAs in OIS. It has been shown that lncRNA-MIR31HG is a senescence modulator in BRAFV600 induced senescence in TIG3 cells (6). Loss of MIR31HG reduced cell growth and promoted a strong senescence phenotype by regulating the tumour suppressor p16^{INK4a}. In the first study described in this thesis (chapter 2), we contributed to the understanding of the function of lncRNAs by presenting the lncRNA-OIS1 as a new regulator of cellular senescence (OIS). LncRNA-OIS1 is a long non-coding RNA whose expression is upregulated during OIS and knockdown of lncRNA-OIS1 bypassed the OIS. The shRNAs were validated from the screen, confirming that knockdown of the corresponding lncRNAs by shRNAs induced this senescence bypass phenotype. However, the off-target effect existed when more shRNAs were included for validation. Recent studies have shown that the CRISPR-Cas13 system can be used to edit the RNA. Remarkably, Cas13 has less off-target effect and was more effective than siRNA (7, 8). It is, therefore, possible that the use of CRISPR-Cas13 to manipulate lncRNA expression may identify in the future additional key lncRNAs that regulate OIS.

Furthermore, the knockdown of lncRNA-OIS1 affects the activation of the nearby gene DPP4 upon oncogene induction. Further investigation indicated that DPP4 is the target gene of lncRNA-OIS1 in the context of senescence. We demonstrated that loss of DPP4, similar to lncRNA-OIS1 knockdown, resulted in bypass of senescence. We reverted the bypass of senescence induced by the lncRNA-OIS1 knockdown through ectopic expression of DPP4. However, exactly how lncRNA-OIS1 controls DPP4 expression and how DPP4 modulates senescence remain to be investigated. Nevertheless, it is hypothesised that lncRNA-OIS1 expression is required for either the recruitment of essential transcription factors to activate DPP4 or alternatively by inhibiting the binding of a transcriptional repressor protein. The results presented in chapter 2 were partly confirmed by Kyoung Mi Kim et al. (9), who described the identification of DPP4 as a regulator and marker for senescence, a promising target of therapeutic intervention to eliminate senescent cells.

As mentioned in the introduction, the bi-directional transcription of eRNAs is the hallmark for active enhancers. Global Run-On sequencing (GRO-seq) was used to detect eRNAs, identifying 1821 regulatory elements activated upon RAS induction in BJ cells. In chapter 3, it was established that those OIS-induced regions (enhancers) are significantly enriched for the AP1 binding motif. Genome-wide functional screen focusing on the AP1 motif within these enhancers uncovered the role of a novel AP1 associated enhancer, EnhA^{P1-OIS1}, in regulating OIS through its target gene FOXF1. AP1 is an important transcription factor consisting of FOS-JUN (heterodimer) or JUN-JUN (homodimers). The FOS-JUN heterodimer is relatively more stable and has higher DNA-binding affinity than JUN-JUN homodimers. It has been reported that AP1 binds with enhancers to drive oncogenic growth and is required for enhancer selection (10, 11), indicating a critical role in regulating enhancers. AP1 is a well-known downstream target of the RAS signalling pathway, which is responsible for mitogen-related genes (12, 13). Previous studies have shown that AP1 mRNA level and activity are attenuated when cells enter replicative senescence (14, 15). It has been demonstrated that AP1 activity is required for initiation of DNA synthesis. Interestingly, AP1 activity is lost during cellular ageing (16), suggesting the loss of AP1 activity is responsible for the irreversible cell cycle arrest in senescent cells. However, c-FOS overexpression with rescued AP1 activity is not sufficient for DNA synthesis in the senescent human fibroblasts (17). Therefore, AP1 is more likely a downstream factor regulating senescence under replicative stress (e.g. H-RAS activation). It is worth noting that none of the AP1 family members were demonstrated as critical players in OIS based on previous functional genetic screens (18, 19). Also, the OIS bypass phenotype was not observed on c-FOS knockout and c-JUN knockout, strongly supporting the previous conclusion. Why AP1 regulates OIS, but the knockout of AP1 did not show OIS bypass still requires further investigation. One possibility is that some AP1 target genes mediate OIS, however, others antagonise it or are required for cell survival.

This thesis contributed to the understanding of AP1 associated enhancer modulating OIS through FOXF1, providing evidence indicating that FOXF1 is a potential tumour suppressor that regulates senescence. Other studies have already shown the role of FOXF1 in lung regeneration by targeting ECM genes and cell cycle progression (20). FOXF1 also promotes prostate cancer growth through the MAPK pathway (21). Moreover, FOXF1 has been proposed to be a target of p53 to regulate cell migration, invasion (22) and promote rhabdomyosarcoma by repressing p21^{Cip1} as a potential oncogene (23). How exactly FOXF1 modulates OIS is not clear. Our results indicate that FOXF1 regulates OIS in a p53 independent manner, but more studies are required to explore the function of FOXF1 in OIS.

YAP is another crucial transcription factor of the Hippo pathway regulating organ growth and tumorigenesis. When Hippo signalling is inactive, YAP and its paralogue TAZ

translocate to the nucleus and bind DNA indirectly through interaction with the TEAD family of transcription factors to regulate target genes (24, 25). Hippo signalling ablation or expression of constitutively active YAP leads to increased organ size, oncogenic growth or even occurrence of cancers (10, 26–29). The Hippo pathway is extremely important in cancer, which makes this pathway a potential target for cancer therapeutics.

Over the past decades, numerous YAP-mediated genes have been discovered and characterised as critical players in YAP-mediated proliferation and oncogenesis. However, the transcriptional function of YAP remains largely unknown, especially the role of YAP-mediated enhancers. In chapter 4, a stable cell line was generated by overexpressing the constitutively active YAP^(SSA) and AP1. As expected, the same oncogenic growth phenotype was observed as previously reported (10). It is known that YAP/TAZ/TEAD together with AP1 can bind with enhancers to drive oncogenic growth (10). However, how many enhancers are functionally important for the oncogenic growth and epithelial-mesenchymal transition phenotypes that are induced by deregulated YAP and AP1 remain unknown. We successfully performed a functional screen and identified seven enhancer targets of YAP. Some well-known genes, such as *Myc* and *CCND1*, were predicted as targets of two identified enhancers based on our RNA-seq. Notably, we found one novel enhancer whose target gene is supposed to be *Tram2*. All target enhancers are required for YAP-oncogenic function, but more detailed investigations and analyses of the function of the identified enhancers and target genes are required. Taken together, chapter 4 described an important function of YAP-mediated enhancers with potentially influential implications in cancer biology.

References

- Guttman,M., Donaghey,J., Carey,B.W., Garber,M., Grenier,J.K., Munson,G., Young,G., Lucas,A.B., Ach,R., Bruhn,L., *et al.* (2011) LincRNAs act in the circuitry controlling pluripotency and differentiation. *Nature*, **477**, 295–300.
- Tsai,M.C., Spitale,R.C. and Chang,H.Y. (2011) Long intergenic noncoding RNAs: New links in cancer progression. *Cancer Res.*, **71**, 3–7.
- Batista,P.J. and Chang,H.Y. (2013) Long noncoding RNAs: Cellular address codes in development and disease. *Cell*, **152**, 1298–1307.
- Qureshi,I.A. and Mehler,M.F. (2012) Emerging roles of non-coding RNAs in brain evolution, development, plasticity and disease. *Nat Rev Neurosci*, **13**, 528–541.
- Ghosal,S., Das,S. and Chakrabarti,J. (2013) Long Noncoding RNAs: New Players in the Molecular Mechanism for Maintenance and Differentiation of Pluripotent Stem Cells. *Stem Cells Dev.*, **22**, 2240–2253.
- Montes,M., Nielsen,M.M., Maglieri,G., Jacobsen,A., Højfeldt,J., Agrawal-Singh,S., Hansen,K., Helin,K., Van De Werken,H.J.G., Pedersen,J.S., *et al.* (2015) The lncRNA MIR31HG regulates p16 INK4A expression to modulate senescence. *Nat. Commun.*, 10.1038/ncomms7967.
- Abudayyeh,O.O., Gootenberg,J.S., Essletzbichler,P., Han,S., Joung,J., Belanto,J.J., Verdine,V., Cox,D.B.T., Kellner,M.J., Regev,A., *et al.* (2017) RNA targeting with CRISPR-Cas13. *Nature*, 10.1038/nature24049.
- Cox,D.B.T., Gootenberg,J.S., Abudayyeh,O.O., Franklin,B., Kellner,M.J., Joung,J. and Zhang,F. (2017) RNA editing with CRISPR-Cas13. *Science (80-.)*, 10.1126/science.aaq0180.
- Kim,K.M., Noh,J.H., Bodogai,M., Martindale,J.L., Yang,X., Indig,F.E., Basu,S.K., Ohnuma,K., Morimoto,C., Johnson,P.F., *et al.* (2017) Identification of senescent cell surface targetable protein DPP4. *Genes Dev.*, **31**, 1529–1534.
- Zanconato,F., Forcato,M., Battilana,G., Azzolin,L., Quaranta,E., Bodega,B., Rosato,A., Bicciato,S., Cordenonsi,M. and Piccolo,S. (2015) Genome-wide association between YAP/TAZ/TEAD and AP-1 at enhancers drives oncogenic growth. *Nat. Cell Biol.*, 10.1038/ncb3216.
- Vierbuchen,T., Ling,E., Cowley,C.J., Couch,C.H., Wang,X., Harmin,D.A., Roberts,C.W.M. and Greenberg,M.E. (2017) AP-1 Transcription Factors and the BAF Complex Mediate Signal-Dependent Enhancer Selection. *Mol. Cell*, 10.1016/j.molcel.2017.11.026.
- Deng,T. and Karin,M. (1994) C-Fos transcriptional activity stimulated by H-Ras-activated protein kinase distinct from JNK and ERK. *Nature*, 10.1038/371171a0.
- Kampfer,S., Hellbert,K., Villunger,A., Doppler,W., Baier,G., Grunicke,H.H. and Überall,F. (1998) Transcriptional activation of c-fos by oncogenic Ha-Ras in mouse mammary epithelial cells requires the combined activities of PKC- λ , ϵ and ζ . *EMBO J.*, 10.1093/emboj/17.14.4046.
- Seshadri,T. and Campisi,J. (1990) Repression of c-fos transcription and an altered genetic program in senescent human fibroblasts. *Science (80-.)*, 10.1126/science.2104680.
- Irving,J., Feng,J., Wistrom,C., Pikaart,M. and Villeponteau,B. (1992) An altered repertoire of fos jun (AP-1) at the onset of replicative senescence. *Exp. Cell Res.*, 10.1016/0014-4827(92)90415-5.
- Riabowol,K., Schiff,J. and Gilman,M.Z. (1992) Transcription Factor Ap-1 Activity Is Required for Initiation of DNA-Synthesis and Is Lost during Cellular Aging. *Proc Natl Acad Sci U S A*, DOI 10.1073/pnas.89.1.157.

17. Rose,D.W., McCabe,G., Feramisco,J.R. and Adler,M. (1992) Expression of c-fos and AP-1 activity in senescent human fibroblasts is not sufficient for DNA synthesis. *J. Cell Biol.*, 10.1083/jcb.119.6.1405.
18. Drost,J., Mantovani,F., Tocco,F., Elkon,R., Comel,A., Holstege,H., Kerkhoven,R., Jonkers,J., Voorhoeve,P.M., Agami,R., *et al.* (2010) BRD7 is a candidate tumour suppressor gene required for p53 function. *Nat. Cell Biol.*, **12**, 380–389.
19. Burrows,A.E., Smogorzewska,A. and Elledge,S.J. (2010) Polybromo-associated BRG1-associated factor components BRD7 and BAF180 are critical regulators of p53 required for induction of replicative senescence. *Proc. Natl. Acad. Sci.*, 10.1073/pnas.1009559107.
20. Bolte,C., Flood,H.M., Ren,X., Jagannathan,S., Barski,A., Kalin,T. V. and Kalinichenko,V. V. (2017) FOXF1 transcription factor promotes lung regeneration after partial pneumonectomy. *Sci. Rep.*, 10.1038/s41598-017-11175-3.
21. Fulford,L., Milewski,D., Ustiyani,V., Ravishankar,N., Cai,Y., Le,T., Masineni,S., Kasper,S., Aronow,B., Kalinichenko,V. V., *et al.* (2016) The transcription factor FOXF1 promotes prostate cancer by stimulating the mitogen-activated protein kinase ERK5. *Sci. Signal.*, 10.1126/scisignal.aad5582.
22. Tamura,M., Sasaki,Y., Koyama,R., Takeda,K., Idogawa,M. and Tokino,T. (2014) Forkhead transcription factor FOXF1 is a novel target gene of the p53 family and regulates cancer cell migration and invasiveness. *Oncogene*, 10.1038/onc.2013.427.
23. Milewski,D., Pradhan,A., Wang,X., Cai,Y., Le,T., Turpin,B., Kalinichenko,V. V. and Kalin,T. V. (2017) FoxF1 and FoxF2 transcription factors synergistically promote rhabdomyosarcoma carcinogenesis by repressing transcription of p21 Cip1 CDK inhibitor. *Oncogene*, 10.1038/onc.2016.254.
24. Ramos,A. and Camargo,F.D. (2012) The Hippo signaling pathway and stem cell biology. *Trends Cell Biol.*, 10.1016/j.tcb.2012.04.006.
25. Zhao,B., Ye,X., Yu,J., Li,L., Li,W., Li,S., Yu,J., Lin,J.D., Wang,C.Y., Chinnaiyan,A.M., *et al.* (2008) TEAD mediates YAP-dependent gene induction and growth control. *Genes Dev.*, 10.1101/gad.1664408.
26. Camargo,F.D., Gokhale,S., Johnnidis,J.B., Fu,D., Bell,G.W., Jaenisch,R. and Brummelkamp,T.R. (2007) YAP Increases Organ Size and Expands Undifferentiated Progenitor Cells. *Curr. Biol.*, 10.1016/j.cub.2007.10.039.
27. Zhou,D., Conrad,C., Xia,F., Park,J.S., Payer,B., Yin,Y., Lauwers,G.Y., Thasler,W., Lee,J.T., Avruch,J., *et al.* (2009) Mst1 and Mst2 Maintain Hepatocyte Quiescence and Suppress Hepatocellular Carcinoma Development through Inactivation of the YAP Oncogene. *Cancer Cell*, 10.1016/j.ccr.2009.09.026.
28. Benhamouche,S., Curto,M., Saotome,I., Gladden,A.B., Liu,C.H., Giovannini,M. and McClatchey,A.I. (2010) Nf2/Merlin controls progenitor homeostasis and tumorigenesis in the liver. *Genes Dev.*, 10.1101/gad.1938710.
29. Dong,J., Feldmann,G., Huang,J., Wu,S., Zhang,N., Comerford,S.A., Gayyed,M.F., Anders,R.A., Maitra,A. and Pan,D. (2007) Elucidation of a Universal Size-Control Mechanism in Drosophila and Mammals. *Cell*, 10.1016/j.cell.2007.07.019.





Addendum

English summary

Nederlandse samenvatting

Portfolio

Curriculum vitae

Publication list

Acknowledgement

Summary

The genetic information of a cell is held within genes in its DNA. Transcription of DNA into RNA is the first step, followed by translation of mRNA into proteins. Although, the vast majority of functions of the cells are carried out by proteins, DNA and mRNA control the “fate” of corresponding proteins. Interestingly, the genetic information required for protein (coding DNA sequence) production comprises an extremely small portion (around 2%) of the whole human genome sequence. It was thought that the remaining 98% of the human genome sequence was “junk DNA” without any biological function for a very long time. Discovery and characterisation of “junk DNA” that regulates the expression of genes challenged this “idea”. Until now, more and more studies have revealed that the so-called “junk DNA” has biological functions beyond protein-coding DNA. There are numerous functional “junk DNAs”, referred to as regulatory elements, in the human genome. The regulatory elements can be generally classified into two different groups, DNA elements (promoters, enhancers, and insulators) and RNA elements (lncRNAs, MicroRNA). Among them, enhancers and lncRNAs have been reported to play a critical role in the regulation of gene expression.

Cancer is a complicated “DNA disease” originating from “changes” in the DNA sequence, especially within the genes that control cell proliferation and survival. It is of note that the vast number of genetic variants associated with human diseases, especially cancer, reside in non-coding regions. Clarifying how the non-coding regions affect gene expression and contribute to the development of disease might have future implications in the diagnoses and treatment of those diseases, especially cancer. In this thesis, we described the functional identification of novel regulatory elements for OIS and YAP-mediated oncogenic growth.

Chapter 2 explored the understanding of lncRNAs function in RAS-induced senescence and addressed lncRNA-OIS1 as a new regulator in cellular senescence (OIS). We performed a functional enrichment screen using the shRNAs library to target the changed lncRNAs during OIS, showing that knockdown of lncRNA-OIS1 affects the activation of the nearby gene DPP4 on RAS induction. In addition, we identified that DPP4 is the target gene of lncRNA-OIS1 to regulate senescence, demonstrating that loss of DPP4 resulted in bypass of senescence. We reverted the bypass of senescence induced by the lncRNA-OIS1 knockdown through ectopic expression of DPP4. Thus, our findings suggest that DPP4 itself can be used as an additional senescence marker in the future.

In chapter 3, we identified that some OIS-induced regions (enhancers) are significantly enriched for the AP1 binding motif. A genome-wide functional screen focusing on the AP1 motif within these enhancers revealed that a novel AP1 associated enhancer, EnhA^{P1-OIS1}, regulated OIS through the target gene FOXF1. We provided the first evidence

indicating that FOXF1 is a potential tumour suppressor to regulate senescence, showing that FOXF1 regulates OIS in a p53 independent manner.

Chapter 4 focused on transcription factor-YAP-related enhancers, generating a new cell line by overexpressing the constitutively active YAP^(5SA) and AP1. We observed the oncogenic growth phenotype with accelerated cell proliferation and cellular morphological changes in this cell line. We successfully evaluated the efficiency of the CRISPR approach and performed the functional screen, identifying several novel enhancers required for YAP-mediated proliferation, providing evidence that YAP controls proliferation through different targets. We first predicted the target gene of one novel enhancer (enhancer^{Tram2}) is Tram2 (translocation associated membrane protein 2). More investigations need to be done to uncover the function of Tram2 in cancer.

Cellular senescence is a state of irreversible growth arrest which can be induced by different stimuli, including telomere shortening, DNA damage, oxidative stress or oncogenic activation. Chapter 2 and 3 focused on oncogene-induced senescence, presenting several novel regulators of OIS and discussed how their identification enables a better understanding of how tumour cells bypass intrinsic safety mechanisms. YAP is frequently activated in many tumours and it is the main factor in the Hippo pathway controlling cell proliferation, organ growth, cell death, and differentiation. Chapter 4 presented several potential targets that can be used for diagnoses and treatment for cancers.

In summary, this thesis investigated and characterised how the non-coding regions regulate gene expression based on different cellular systems, thereby contributing to the understanding of the “dark matters” in the human genome.

Samenvatting

De genetische informatie van een cel wordt in de genen in zijn DNA gehouden. Transcriptie van DNA naar RNA is de eerste stap, die gevolgd wordt door translatie van boodschapper-RNA (mRNA) in eiwitten. Hoewel de meeste functies van de cellen worden uitgevoerd door eiwitten, regelen het DNA en mRNA het “lot” van overeenkomstige eiwitten. Interessant is dat de genetische informatie vereist voor eiwit productie (de coderende DNA-sequentie) een extreem klein deel (ongeveer 2%) van de gehele humane genoomsequentie omvat. Er werd gedurende een zeer lange tijd aangenomen dat de rest 98% van de sequentie van het menselijk genoom “rommel-DNA” was zonder enige biologische functie. Ontdekking en karakterisering van ‘rommel-DNA’ dat de expressie van genen reguleert, daagde dit ‘idee’ uit. Tot nu toe lieten meer en meer onderzoeken zien dat het zogenaamde “rommel-DNA” een biologische functie heeft die verder gaat dan eiwit-coderend DNA. Er zijn talloze functionele stukken “rommel-DNA”, de regulerende elementen, in het menselijk genoom. De regulerende elementen kunnen in het algemeen worden geclassificeerd in twee verschillende groepen: DNA-elementen (promotors, enhancers en isolatoren) en RNA-elementen (lncRNA’s, MicroRNA). Onder hen werden enhancers en lncRNA’s veelvuldig beschreven in de literatuur vanwege de cruciale rol die ze spelen in de regulatie van genexpressie.

Kanker is een gecompliceerde “DNA-ziekte” die voortkomt uit “veranderingen” in de DNA-sequentie, vooral binnen de genen die de cel proliferatie en overleving reguleren. Het is belangrijk om op te merken dat het grote aantal genetische varianten geassocieerd met menselijke ziekten, met name kanker, voorkomt in niet-coderende regio’s. Verduidelijken hoe de niet-coderende regio’s de genexpressie beïnvloeden en bijdragen aan de ontwikkeling van ziekten zoals kanker, kan toekomstige implicaties hebben voor de diagnose en behandeling van die ziekte. In dit proefschrift beschrijven we de functionele identificatie van nieuwe regulatoire elementen voor oncogen geïnduceerde senescence en YAP-gemedieerde oncogene groei.

In hoofdstuk 2 hebben we de functie van lncRNA in RAS-geïnduceerde senescence onderzocht en het lncRNA-OIS1 geïdentificeerd als een nieuwe regulator in cellulaire senescence (OIS). We voerden een functionele verrijkings screen uit door gebruik te maken van shRNA’s om de lncRNA’s die in het proces van OIS een rol spelen, te targeten. We toonden aan dat knock-down van lncRNA-OIS1 invloed heeft op de activatie van het nabijgelegen gen DPP4 na RAS-inductie. En we hebben ook vastgesteld dat DPP4 het doelwit gen is van lncRNA-OIS1 om senescence te reguleren. We hebben aangetoond dat verlies van DPP4 resulteerde in bypass van senescence. We hebben de bypass van senescence, veroorzaakt door de knock-out van lncRNA-OIS1 teruggedraaid door ectopische expressie van DPP4. DPP4 zelf kan in de toekomst worden gebruikt als een extra marker voor senescence.

In hoofdstuk 3 hebben we enkele OIS-geïnduceerde regio's (enhancers) geïdentificeerd die significant verrijkt zijn voor het AP1-bindingsmotief. Daarom hebben we een genom-brede functionele screen uitgevoerd die gefocust is op het AP1-motief in deze enhancers. Hiermee hebben we een nieuwe AP1-geassocieerde enhancer, EnhAP1-OIS1, ontdekt die OIS reguleert via het doelwit gen FOXF1. We hebben het eerste bewijs geleverd dat aangeeft dat FOXF1 een potentiële tumorsuppressor is om senescence te reguleren. We hebben ook aangetoond dat FOXF1 OIS op een p53 onafhankelijke manier reguleert.

In hoofdstuk 4 hebben we ons gericht op enhancers die gereguleerd worden door een andere transcriptiefactor -YAP. We hebben een nieuwe cellijn gegenereerd door het constitutief actieve YAP^(5SA) en AP1 tot overexpressie te brengen. We observeerden het oncogene groeifotype met versnelde celproliferatie en cellulaire morfologische veranderingen in deze cellijn. We hebben met succes de efficiëntie van CRISPR-benadering geëvalueerd en een functionele enhancer screen uitgevoerd. We identificeerden verschillende nieuwe enhancers die allemaal nodig zijn voor YAP-gemedieerde proliferatie en het bewijs leveren dat YAP door verschillende doelen de proliferatie regelt. We voorspelden eerst dat het doelwit gen van een nieuwe enhancer (enhancerTram2) Tram2 is (translocatie-geassocieerd membraaneiwit 2). Meer onderzoek moet worden gedaan om de functie van Tram2 in kanker bloot te leggen.

Cellulaire senescence is een toestand van onomkeerbare groeistop die kan worden geïnduceerd door verschillende stimuli, waaronder telomeer verkorting, DNA-schade, oxidatieve stress of oncogene activering. Hoofdstuk 2 en 3 concentreerden zich op de door oncogen geïnduceerde senescence en presenteren verschillende nieuwe regulatoren van OIS en bespraken hoe hun identificatie ons in staat stelt beter te begrijpen hoe tumorcellen de intrinsieke veiligheidsmechanismen omzeilen. YAP wordt vaak geactiveerd in een groot aantal tumoren en het is de belangrijkste factor in Hippo pathway die celproliferatie, orgaangroei reguleert, en invloed uitoefent op celdood en differentiatie. Hoofdstuk 4 presenteert verschillende potentiële doelen die kunnen worden gebruikt voor diagnoses en behandeling van kankers.

Samenvattend, in dit proefschrift hebben we onderzocht en gekarakteriseerd hoe de niet-coderende regio's de genexpressie reguleren op basis van verschillende cellulaire systemen, wat heeft bijgedragen aan het begrip van de "dark matter" in ons genoom.

Portfolio

Name PhD student : Li Li
PhD period: 2013-2018
Name PhD supervisor: Prof. Reuven Agami

Course

- Experimental Oncology 2014
- Identification and analysis of RNA protein interactions 2014
- Epigenetics and non-coding RNA 2015
- Key methodologies in computational analyses and data handling 2016

Seminars and workshops

- Scientific Communication and Outreach workshop 2014
- Introduction to Project Management, the Scientific Approach and Ethics in Research 2014
- Project Management, Competence Mapping and Job Seeking 2017

Presentations at (inter)national conferences

- RNA train meeting in Copenhagen 2014
- RNA train meeting in Berlin 2014
- RNA train meeting in Italy 2015
- RNA train meeting in Basel 2016
- RNA train meeting in Prague 2017

Curriculum vitae

Li Li was born on February 9, 1988, in Yi Yang, Hunan, China. He received his high school diploma from the NO.1 middle school in Changsha, Hunan in 2006. In the same year, he started his study at Nanjing Agricultural University (Nanjing, China) and got his Bachelor's degree in Biotechnology from School of Life Science in 2010. In the following years, he continued his study at Beijing Normal University (Beijing, China) where he received his Master's degree in Biochemistry and Molecular Biology in 2013. In the same year, He was awarded PhD fellowship (CSC, China) and joined the group of Prof. Reuven Agami lab at the division of gene regulation at The Netherlands Cancer Institute in Amsterdam and worked as a PhD student to continue his scientific research. In 2014, he joined the RNA-train training network from European Marie Curie and completed the lncRNA project. All the studies presented in this thesis were performed in the Netherlands Cancer Institute under the supervision of Prof. Reuven Agami.

List of publications

Li,L., van Breugel,P.C., Loayza-Puch,F., Ugalde,A.P., Korkmaz,G., Messika-Gold,N., Han,R., Lopes,R., Barbera,E.P., Teunissen,H., et al. (2018) LncRNA-OIS1 regulates DPP4 activation to modulate senescence induced by RAS. *Nucleic Acids Research*, Vol. 46, No. 8 4213–4227.

Han,R *, **Li,L ***, Ugalde,A.P., Tal,A., Manber,Z., Barbera,E.P., Chiara,V.Della, Elkon,R. and Agami,R. (2018) Functional CRISPR screen identifies AP1-associated enhancer regulating FOXF1 to modulate oncogene-induced senescence. *Genome Biology* (2018) 19:118 (Co-first author)

Li,L, Alejandro P Ugalde, Zohar, Gozde Korkmaz, ly.momchev, Rui Lopes, Ran Elkon, Reuven Agami.(2018) A functional genetic screen identifies TRAM2 as a key target of YAP-mediated proliferation and oncogenesis. Manuscript in preparation

Acknowledgement

It has been 6 years since I first came to NKI. It feels like a dream, but so real, consist of exciting things, happiness, sadness, conflicts, pressures, difficulties, challenges. However, the guidance, encouragement, and support from many people have made me complete this extraordinary journey to PhD.

First of all, I would like to thank Reuven Agami for the privilege to work in your lab. I have learned a lot from you in many aspects, from designing experiments, doing experiments, analyzing data, thinking about results to writing papers. I have also benefited from you through your insightful guidance in science, your continuous support, and encouragement in career development. Thank you for trusting me and giving me the freedom to exploit new, sometimes crazy, ideas. Your enthusiasm, inspiration and wonderful sense of science have led me through the difficulties during my PhD and made my enjoyable life in NKI.

Ruiqi Han, I am very happy to meet you. We are friends more beyond the colleague. After so many collaborations and projects, we have finally succeeded in having a fruitful one! Anyway, I have learned a lot from the failed ones as well, mostly because of our extensive contact., It was a great pleasure to work with you in planning the experiments and discussing the results.

APU, I missed your home-made beer and bread since you have returned to Spain after finishing your postdoc here. I was very happy to work with you. Thank you for sharing your experience and answering my simple questions all the time when I came to this lab. I think our YAP story will be a really nice paper.

Fabricio, you are definitely a Chinese, not a Bolivians. Although I did not work with you, I have still learned a lot from you, such as your “can do” attitude and breadth of expertise. I like to talk to you because your helpful suggestions always gave me “hopes” and I have also learned other things from you apart from science. The way you face and deal with problems has impressed me so much.

I would like to thank the present (Gozde, Remco, Jane, Yuval, Abhi, Julien, Itamar, Behzad) and past (Boris, Pieter, Arie, Koos, Rui, Vittorio, Nicolas, Carlos, Veronica) members of the Agami lab for their input and criticism. Rani, thank you for the productive collaborations and your help to correct the manuscripts. Eric and lybo: I was very happy to guide you as my students. Your enthusiasm and dedication to work was a great help to me.

I was also fortunate to have collaborations outside of the lab, especially with the RNA train network. Thank all the RNA train members, we had really great time together to learn from each other and discuss the projects. We also enjoyed the time when we were together.

Fred, Heinz, Jacqueline: thank you for accepting being my PhD committee. Your suggestions and feedback during the PhD evaluation meetings always gave me the right direction to go.

I also want to thank the facilities in NKI especially Roel (deep seq), Martijn (FACS), Onno (Mass spectrometry). My projects will not move forward without your help.

Guido, Eva, Stefan, Wilbert, Jarno: thank you for accepting being my PhD defense committee.

Finally, I want to thank everyone who helped me during the past 6 years in NKI. I really appreciate all your support.

时光荏苒，岁月如梭。转眼间来到异国他乡荷兰已经6年，回首望去有太多的感触。如今“取完经，修成正果”方知“吃得苦中苦，方为人上人”这句话的深刻含义。这6年里，经历了太多，起起伏伏，但最终的结果是甜蜜的。

感谢在荷兰癌症研究所的其他中国兄弟姐妹们，崇导（孙崇），国泰（徐国泰），TAO（陈韬），女神（乔晓航），男神（孔祥俊），黄馨瑶，oba（韩瑞琦），孙建慧，存导（王存），王力勤，薛征，帅哥（金浩杰），朱燕韵，大庚（王耀庚），王玮，甘昌培，王静，李文龙，刘真，肖艳灵，张平，以及所有兄弟姐妹的家属们（排名不分先后，你们都很重要）。感谢你们的支持和帮助，和你们一起探讨科学是那么的受益匪浅。和你们畅谈人生是那么的有趣。和你们一起打球，玩狼人杀，打够级，吃火锅，旅游是那么的快乐，和你们在一起的快乐时光是我在异国他乡感受到最温暖的回忆。

感谢“CSC帮”的兄弟姐妹们，清哥（张志清），薛婷，于美辰，小杰（张永杰），小白（于良），小蜻蜓（周婷），蔡文静，亮亮（孙善亮）。感谢你们的帮助和支持，怀念和你们在一起的日子，各种八卦。怀念小杰的厨艺，怀念清哥酒后的样子。和你们在一起的日子让我感觉无比的温暖和开心。

罗晶晶，你是我老乡，也是我来荷兰的第一个朋友，还记得你第一次来我家里吃火锅，我们的战斗力是那么的强大，往后的日子里，每次我们吃火锅，都感叹战斗力大不如从前。我们很早就开始计划一起出去旅游，去冰岛，去徒步，去滑雪。因为吴虹怀Sunny，怀Simon，所有的计划都不得不搁浅，等二个拖油瓶稍微大一点，你，我，吴虹，我们三人一定要去实现之前的计划。

感谢我的初中班主任刘希兰老师，是您的严苛要求才让我没有被“班级千年老大”的现状冲昏头脑，不思进取。是您的指导和帮助，让我从永远的“全校千年老二”在最后中考的关键一战中，华丽涅槃重生成为“全校老大”。感谢您当年的用心良苦。

感谢我的高中班主任郭洪阳老师，陈建军老师，黄忠宇老师以及其他任课老师。高中三年的求学之路，是你们给予了关怀和帮助。

郭老师，您第一节英语课，一拐一瘸的拖着受伤的腿来给我们上课，说着一口流利的英式英语，让我印象尤为深刻。您让我敬畏，有种特别的威严感，但没有距离感，我特别喜欢您。我的英语底子是您一手打造的，相信应该没有给您丢脸。

陈老师，您在语文课上，声情并茂的讲解，让我领略了中华文化的博大精深，尤其喜欢上您的作文课，那是一种享受。高考的失利，让我倍受打击，虽然超出重点本科60多分，但离我预期的目标和预期的大学还有差距，是您给予了我肯定和鼓励，您说“高考不是你人生的终点，而是你人生的另一个起点”，您这句话让我没有选择复读。现在看来，一直一帆风顺并不是好事，偶尔的失利之后能够迎头赶上，是真正的智者所应该去做的，而我也一直在努力。

黄老师，我不得不说是您“误人子弟”将我带到“生物这个坑里”。生物相关专业曾经被网络标榜为“大学十大骗人专业榜首”。但我始终坚信，人类离不开生命科学。“母猪生九子，连母十个样”，这是您第一节生物课上说的让我最记忆犹新的一句话，相当的幽默，却又恰到好处的开启了我您在您课堂上的生物之旅，表型由遗传决定，受基因控制着。我不得不说您风趣幽默的教学方式让生物课是我打瞌睡概率为0的唯一一门课。我还记得上午最后一节生物课后，我总是会“耽误”您去吃饭的时间，拖着您问各种奇怪的问题，算习题册上各种疾病遗传概率的题目。您总是百般耐心的为我讲解，孜孜不倦的陪着我算概率，有时候我自己没算晕，却把您给绕晕了。您从来不反感，永远都是那么热心的帮助我，我想这也是为什么我能成为“生物学”博士的关键原因吧。

南京农业大学是我将自己的“生物学想法”付诸实践的第一个战场，感谢班主任老师朱云枝，您给了我很多的帮助和指导。大宝老师（许承保），您教会了我很多在课堂上学不到的东西，如何做人，如何做事，感谢您对我的支持和帮助。王卉老师，是您给了我机会让我做自己的项目（SRT），让我将自己的想法去真正实践的第一人。您给了我很多指导和帮助。

北京师范大学是我进一步深造的第二战场。感谢我的导师魏群，向本琼。感谢我的师姐佟丽。

魏老师，在我保送硕士研究生时，您向我伸出了有力的一只手并且拉了我一把，感谢您给我机会在您的实验室攻读硕士，您对待科研的态度深深影响了我，

不仅仅在科研上，您全力支持我。在生活中，您更像亲人对我有着无微不至的关怀和照顾。即便毕业这么多年了，您还是一直默默关注着我，支持着我。我很荣幸能成为您的学生，也希望将来您能因为我感到骄傲。向老师，感谢您对我三年研究生的帮助和指导，您给了我莫大的鼓励和支持。

佟姐，三年的研究生生活，与您打交道很多，您帮魏老师管理着实验室的日常，您像我们的大管家，但我觉得您更像我们的姐姐。感谢您给予我的帮助和支持，在我实验遇到困难的时候，您给我指点迷津。在我生活遇到困难的时候，您更是挺身而出，设身处地为我着想，帮助我渡过难关。从您身上，我也学到了许多做人做事的道理。

感谢我硕士期间的师兄王新禹，张文，岑举人，苏振义，程金波。同窗李翔，李雁青，徐澜，还有其他师兄师姐师弟师妹。感谢你们给予我的帮助和支持，和你们在一起的日子很开心。

感谢我的岳父母，谢谢你们给予我的支持与帮助，在我工作学习与生活压力很大的时候，来荷兰帮我照顾小孩和家庭，为我分担了许多。你们健康快乐是我的心愿。

感谢我的好哥们，杜坚坚，陈鑫等等。每次回国度假，和你们一起聚会玩耍是我享受度假最重要的环节。感谢你们对我的支持和鼓励。

感谢我的亲戚们，每次回国，都感受到整个大家族的温暖，和谐幸福。科哥，伟哥，凌哥，妹姐，冬哥，做你们的老弟，很幸福。感谢外婆儿时的陪伴，您陪着我的那几年，是我童年最美好的回忆。

感谢我的父母，感恩你们生我养我，从小到大给我无尽的关怀，支持和鼓励。感谢你们为我无私的奉献一切。你们开心快乐，身体健康是我最大的心愿。

感谢我的妻子，吴虹。你默默的支持和宽容陪伴着我最终完成我的博士学业。感谢你操持着家里的一切，让我安心的工作，虽然我平日里不说，但我知道你为这个家付出了很多。你承担了大部分的家务杂事，虽然我有时会吐槽你家务做得不干净，然后亲自上阵，虽然我有时会吐槽你做菜不好吃，然后亲自下厨，但我由衷的感谢你替我承担了许多，让我专注自己的学业。不管我博士期间发表过多少篇文章，我最自豪的是我俩一起发表的2篇nature，你是第一作者，我是通讯作者，第一篇是2014年7月26日出生的“李荷萱-Sunny”，第二篇是2018年4月9日出生的“李沐暄-Simon”。感谢你给我带来了二位天使一样的宝宝。一起养育他们，陪伴他们成长是我们共同的责任，但让你们幸福快乐的生活，让Sunny和Simon健康快乐的成长，是我这一生奋斗的目标。

感恩我生命中出现的所有人，感谢你们对我的帮助和支持。

